

Past and present ocean dynamics in the western subtropical Atlantic

Dissertation
zur Erlangung des Doktorgrades
der Naturwissenschaften im Fachbereich
Geowissenschaften
der Universität Hamburg

vorgelegt von
Tanja Carolin Mildner
aus Cuxhaven
Hamburg

2013

Als Dissertation angenommen vom Fachbereich
Geowissenschaften der Universität Hamburg
Auf Grund der Gutachten von
Prof. Dr. Carsten Eden und Prof. Dr. Dirk Nürnberg
Hamurg, den 04.07.2013

Prof. Dr. Christian Betzler
Leiter des Fachbereichs Geowissenschaften

Contents

Zusammenfassung	vi
Abstract	viii
Abbreviations	x
1 Introduction	1
1.1 Motivation	1
1.2 The ocean circulation system in the Gulf of Mexico and adjacent seas . . .	4
1.3 The Earth's energy budget	7
1.4 Climate fluctuations during the last glacial-interglacial cycle	7
1.4.1 Milankovitch cycles	8
1.4.2 Heinrich events	10
1.4.3 Dansgaard-Oeschger events	10
1.5 The past and the present ocean circulation in the North Atlantic	11
1.6 The role of the present and the glacial wind system over the North Atlantic with special focus on the Caribbean	13
1.7 Sea level fluctuations during the last glacial period	15
1.8 Observations in the Gulf of Mexico and its connections to the glacial envi- ronment	19
1.9 The present and the past Gulf Stream separation latitude	20
1.10 Thesis outline	22
2 Revisiting the relationship between Loop Current rings and Florida Cur- rent transport variability	27
2.1 Abstract	28
2.2 Introduction	28
2.3 Model and data	30
2.4 Results	31
2.4.1 Mechanism	35
2.5 Discussion	37
3 Impact of Last Glacial Maximum wind stress and lowered sea level dur- ing the deglaciation on the Loop Current in the Gulf of Mexico	40

3.1	Abstract	41
3.2	Introduction	41
3.3	Modeling approach	45
3.4	Model results	49
3.4.1	CONTROL simulation analysis	49
3.4.2	Sea level experiments	53
3.4.3	Wind stress experiments	54
3.4.4	Combining lowered sea level and LGM wind stress forcing	58
3.5	Discussion	59
3.6	Summary	62
4	The Gulf Stream position during the LGM	64
4.1	Abstract	65
4.2	Introduction	65
4.3	Experimental design	67
4.4	Results	70
4.4.1	Influence of sea level and glacial wind stress forcing	71
4.5	Summary and conclusions	75
5	Conclusions and outlook	79
6	Appendix	85
6.1	The model	85
6.2	Model configuration for paleoclimate experiments	87
6.2.1	Sea level experiments	87
6.2.2	Wind stress experiments	89
	List of Figures	95
	List of Tables	96

Zusammenfassung

In der vorliegenden Doktorarbeit werden die physikalischen Prozesse betrachtet, die für die Variabilität des Loop Current im Golf von Mexiko verantwortlich sind, sowie deren Verbindung zur Karibik und zur Florida Straße. Das Ziel ist es, zum Verständnis der Ozeandynamik im westlichen Nordatlantik beizutragen, insbesondere in der bedeutenden Übergangsphase seit dem letzten glazialen Maximum bis ins Holozän während der letzten 25000 Jahre. Es wird ein kombinierter Ansatz verfolgt, in welchem Modelle mit hoher räumlicher Auflösung, Beobachtungen aus der heutigen Zeit und aus Proxyanalysen für die Vergangenheit helfen konnten, die räumliche und zeitliche Auflösung der Veränderungen der Loop Current Dynamik zu untersuchen und die relativen Beiträge der unterschiedlichen externen Einflussfaktoren zu verstehen. Diese Arbeit umfasst drei, in sich abgeschlossene Teile:

Der erste Teil dieser Arbeit adressiert den Einfluß der atmosphärischen und internen Ozeanvariabilität auf den Loop Current und den damit zusammenhängenden Florida Straßen Transport auf zwischenjährlichen bis dekadischen Zeitskalen. Es konnte ein klarer Zusammenhang zwischen den verschiedenen Stadien während eines Ablösungszyklus des Loop Current in den Golf von Mexiko und den Minima im Volumentransport der Florida Straße gefunden werden, sowohl in Modellstudien als auch in den Beobachtungen. Es konnte gezeigt werden, dass Volumenänderungen im Florida Straßen Transport einen signifikanten Einfluss auf die Variabilität auf zwischenjährlichen bis dekadischen Zeitskalen haben. Unterschiede (und zeitliche Veränderungen) zwischen der Ablösungsperiode eines Eddies und dem saisonalen Zyklus der Florida Straße auf zwischenjährlicher bis dekadischer Variabilität führen zu einer zwischenjährlichen bis dekadischen Schwebungsperiode, die einen großen Anteil der Variabilität im Volumentransport der Florida Straße in den Modellsimulationen erklärt. Dieser übersteigt sogar die Variabilität im Windantrieb auf den betrachteten Zeitskalen. Auch wenn zusätzliche Ereignisse den Ablösungsprozess unterstützen könnten, wird hier angenommen, dass der Volumentransport der Florida Straße hauptsächlich von interner Dynamik angetrieben wird.

Der zweite Teil konzentriert sich auf den Einfluss der Loop Current Eddy-Ablösung auf den Wärmehaushalt des Golf von Mexiko bei unterschiedlichen Meeresspiegelständen und unterschiedlichem Windantrieb. Die Modellsimulationen deuten darauf hin, dass sich keine Eddies während des letzten glazialen Maximums abgelöst haben, welches durch einen wesentlich tieferen Meeresspiegel und eine veränderte Topographie in der Yucatan Straße gekennzeichnet war. Während der letzten Deglaziation nach Ende des letzten Glazials gab

es einen sukzessiven Anstieg der Eddie-Häufigkeit, einhergehend mit einer kontinuierlichen Erwärmung des Golf von Mexiko. Unterstützt wird dies von paleo-ozeanographischen Proxy-daten, die einen kontinuierlichen Anstieg der Oberflächentemperatur im nördlichen Golf von Mexiko dokumentieren. Obwohl nicht viel über die atmosphärische Zirkulation des letzten glazialen Maximums bekannt ist, wird eine Intensivierung der atmosphärischen Zirkulation zu dieser Zeit mit einer Verschiebung der innertropischen Konvergenzzone nach Süden angenommen. Als Konsequenz bewirken die glazialen Winde eine Verstärkung im Volumentransport des Subtropenwirbels und damit eine Verstärkung des Volumentransports durch die Florida Straße und durch die Yucatan Straße. Je größer der Transport ist, desto weniger Eddies lösen sich ab. Beobachtungen aus paleo-ozeanographischen Rekonstruktionen sind hier nicht eindeutig. Obwohl die atmosphärische Zirkulation wegen des größeren meridionalen Temperaturgradienten während des letzten glazialen Maximums stärker war, so zeigen Studien von Proxydaten teils einen stärkeren, teils aber auch einen schwächeren Transport in der Florida Straße während des letzten glazialen Maximums.

Abschließend wird im dritten Kapitel dieser Arbeit die Position des Golfstroms während des letzten glazialen Maximums diskutiert. Während das Absenken des Meeresspiegels im Modell keine wesentlichen Unterschiede in der großräumigen Zirkulation im Nordatlantik bewirkt, sieht man sehr wohl eine starke Veränderung, wenn der Windstress des letzten glazialen Maximums in das Modell implementiert wird. Die Unterschiede in der atmosphärischen Zirkulation des letzten glazialen Maximums bewirken neben einer geographischen Ausdehnung des nördlichen Rezirkulationswirbels eine südwärtige Verschiebung der Orte, an denen die Rotation des Windstress verschwindet. Das 'Ekman pumping' wird ebenfalls verstärkt und es kommt zu einer Verschiebung des Golfstroms. Der Subtropenwirbel ist jedoch schwächer ausgeprägt als heute. Belege aus Paleo-Beobachtungen sind nur eingeschränkt vorhanden wegen der hohen Variabilität und Stärke des Stromsystems in dieser Region, die einen guten und ungestörten Erhalt der Sedimente verhindern. In Übereinstimmung mit den Ergebnissen dieser Studie gibt es Paleo-Beobachtungen, die eine Verschiebung der Polarfront zeigen und dies auf die großen kontinentalen Eisschilde sowie auf die Veränderungen der atmosphärischen Zirkulation zurückführen. Andere Beobachtungen zeigen jedoch nur geringe Veränderungen der Position des Golfstroms während des letzten glazialen Maximums, was den simulierten Ergebnissen mit Änderungen im Windantrieb widerspricht. Abschließend kann man sagen, dass der Ablösungsmechanismus des Golfstroms von der Küste von vielen unterschiedlichen Faktoren abhängt und deshalb kann es auch eine Kombination aus Faktoren sein, die mit der atmosphärischen Zirkulation zusammen einen Einfluss ausüben können.

Abstract

The main physical processes responsible for the past and present Loop Current variability in the Gulf of Mexico and its interconnection with both, the Caribbean Sea and the Florida Straits are investigated in this PhD thesis. The aim is to contribute to the understanding of ocean dynamics in the western part of the North Atlantic across the prominent transition from the Last Glacial Maximum to the Holocene during the last 25 kyr (kilo years). A combined approach using high resolution models, present day observations and paleo-proxies has helped to explore the past and the present spatial and temporal changes of Loop Current dynamics and to understand the relative contributions of different external forcing factors. This PhD thesis consists of three research papers:

The first part of this thesis addresses the influence of atmospheric and internal ocean variability on the Loop Current and the associated Florida Straits transport on inter-annual to decadal scales. A clear relationship is found between different stages within a ring shedding cycle of the Loop Current in the Gulf of Mexico and transport minima in the Florida Current transport, both in observations and in model simulations. It is demonstrated that transport changes in Florida Straits have a significant influence on the transport variability on monthly to decadal time scales. Differences (and changes) between the ring shedding period and seasonal cycle lead to an interannual to decadal beat frequency, which explains large parts of the variability of the Florida Current transport in the model simulations, even exceeding atmospheric forcing variability on the considered time scales. Although additional trigger events might support the ring shedding process, the Florida Straits transport is influenced mainly by internal dynamics.

The second part focuses on the influence of the Loop Current eddy shedding on the heat budget of the Gulf of Mexico at changing sea levels, different wind stress forcings and topographic effects. The model simulations imply that the process of eddy shedding was most likely absent during the Last Glacial Maximum at lowered sea level and modified Yucatan Strait topography. Subsequently, eddy shedding increases gradually across the deglaciation thereby warming the Gulf of Mexico. In support, paleoceanographic proxy data reveal a continuous sea surface temperature increase in the northern Gulf. Although little is known about the glacial atmosphere, a strengthened atmospheric circulation is assumed for the LGM with a shift in the ITCZ position towards the south. As a consequence, glacial wind stress causes enhanced Sverdrup transport within the Subtropical Gyre thus leading to a strengthened Florida Straits and Yucatan Strait through-flow. Eddy shedding decreases the stronger the transport is. Paleoceanographic proxy data are ambiguous in this respect. Although atmospheric circulation was stronger during the Last Glacial

Maximum due to the enhanced meridional temperature gradients, paleoceanographic reconstructions reveal both, negative and positive sign in Florida Straits transport for the Last Glacial Maximum.

Finally, in the third part of this thesis the glacial position of the Gulf Stream is discussed. While the lowered sea level by itself does not lead to significant changes in the current system of the North Atlantic, the combination with glacial wind stress forcing does. The changes in the glacial atmospheric circulation leads to the geographical expansion of the northern recirculation gyre towards the south with a subsequent increase in the Ekman pumping within the gyre. Therefore, the line of zero wind stress curl and the Gulf Stream are shifted southwards. The subtropical gyre, hence, is weaker during the LGM. Paleoevidence is unfortunately scarce mainly due to the highly variable and strong current regime in this region preventing a good conservation of sediment records. Nevertheless, paleoceanographic proxy reconstructions reveal a shift of the polar front due to the large continental ice sheets and the changes in wind supporting the results of this study. Other paleo-observations thus suggests only a slight shift of the present Gulf Stream position during the LGM which contradicts the simulated response to changes in wind forcing. Overall, the separation process off the coast itself is very sensitive to a variety of factors and therefore, a combined effect together with the influence of the atmospheric circulation is also conceivable.

Abbreviations

AADW	<u>A</u>nt<u>A</u>rctic <u>D</u>eep <u>W</u>ater
AAIW	<u>A</u>nt<u>A</u>rctic <u>I</u>ntermediate <u>W</u>ater
AMOC	<u>A</u>tlantic <u>M</u>eridional <u>O</u>verturning <u>C</u>irculation
APF	<u>A</u>ntarctic <u>P</u>olar <u>F</u>ront
AVISO	<u>A</u>rchiving, <u>V</u>alidation and <u>I</u>nterpretation of <u>S</u>atellite <u>O</u>ceanographic data
CCR	<u>C</u>old <u>C</u>ore <u>R</u>ing
CDW	<u>C</u>ircumpolar <u>D</u>eep <u>W</u>ater
CLIVAR	<u>C</u>LIimate <u>V</u>ariability <u>A</u>nd <u>P</u>redictability
DWBC	<u>D</u>eep <u>W</u>estern <u>B</u>oundary <u>C</u>urrent
ERS-1	<u>E</u>uropean <u>R</u>emote-Sensing <u>S</u>atellite
FLAME	<u>F</u>amily of <u>L</u>inked <u>A</u>tlantic <u>M</u>odel <u>E</u>xperiments
FC	<u>F</u>lorida <u>C</u>urrent
GNAIW	<u>G</u>lacial <u>N</u>orth <u>A</u>tlantic <u>I</u>ntermediate <u>W</u>ater
GoM	<u>G</u>ulf of <u>M</u>exico
H1	<u>H</u>einrich Event <u>1</u>
IPCC	<u>I</u>ntergovernmental <u>P</u>anel on <u>C</u>limate <u>C</u>hange
ITCZ	<u>I</u>nter<u>T</u>ropical <u>C</u>onvergence <u>Z</u>one
LC	<u>L</u>oop <u>C</u>urrent
LGM	<u>L</u>ast <u>G</u>lacial <u>M</u>aximum
MIS	<u>M</u>arine <u>I</u>sotope <u>S</u>tage
MOC	<u>M</u>eridional <u>O</u>verturning <u>C</u>irculation
MOCHA	<u>M</u>eridional <u>O</u>verturning <u>C</u>irculation and <u>H</u>eatflux <u>A</u>rray
NADW	<u>N</u>orth <u>A</u>tlantic <u>D</u>eep <u>W</u>ater
NGRIP	<u>N</u>orth <u>G</u>reenland <u>I</u>ce core <u>P</u>roject
NOAA	<u>N</u>ational <u>O</u>ceanic and <u>A</u>tmospheric <u>A</u>dmistration
NRG	<u>N</u>orthern <u>R</u>ecirculation <u>G</u>yre
OGCM	<u>O</u>cean <u>G</u>eneral <u>C</u>irculation <u>M</u>odel
PMIP	<u>P</u>aleoclimate <u>M</u>odelling <u>I</u>ntercomparison <u>P</u>roject
SSS	<u>S</u>ea <u>S</u>urface <u>S</u>alinity
SST	<u>S</u>ea <u>S</u>urface <u>T</u>emperature

STACS	S ub T ropical A tlantic C limate S tudies
THC	T hermo H aline C irculation
TOPEX	Ocean T OPography E Xperiment
WCR	W arm C ore R ing
XBT	E Xpendabel B athy T hermograph
YC	Y ucatan C urrent
YD	Y ounger D ryas

1 Introduction

1.1 Motivation

The transport of heat by ocean currents from the equatorial regions to the high latitudes is a critical component in the global climate system. Ocean general circulation models (OGCMs) are powerful tools for understanding and predicting climate and climate change on regional and global scales. Reconstructions of important climate periods such as the Last Glacial Maximum (LGM), the Younger Dryas (YD)¹ cold event and the present interglacial provide the opportunity to test the ability of OGCMs to simulate extreme changes in climate and to improve our understanding of the mechanisms of climate change. In particular, high resolution models can reveal meso-scale processes such as meso-scale eddies that may play an important role in regional oceanic heat transport (i.e. in the Gulf of Mexico). The reliability of future climate projections depends strongly on our understanding of the underlying driving mechanisms for climate change (Marotzke, 2000, and references therein). For this, it is essential to validate models against observations and climate proxy reconstructions. The large number of available proxy data allows us to constrain and compare them to the model results. A proxy is a measured variable (e.g. isotope ratios) used to infer the value of a variable of interest in the climate research state, such as ocean temperature or salinity. Proxy reconstructions from marine sediment cores or corals can then be compared to model results allowing for the validation of model results.

The diagram of the global overturning circulation in Figure 1.1 displays surface flow in the ocean and deep bottom currents (Richardson, 2008) and is a revised figure of the IPCC report of 2001² now including gradients of water mass density transformations. Further, schematic anticyclonic eddies are illustrated, demonstrating that in some parts of the Atlantic the overturning circulation consists of large, translating and coherent eddies. The general circulation implies that the warm upper layers of water in the North Atlantic are cooled and transferred to the cold, fresh and dense waters at high latitudes at a rate

¹The Younger Dryas was named after the alpine-tundra wildflower *Dryas octopetala*, which was common in Germany and Scandinavia during this time.

²http://www.grida.no/climate/ipcc_tar/slides/04.18.htm, Fig. 4-2 of the “Climate Change-2001 Synthesis Report”

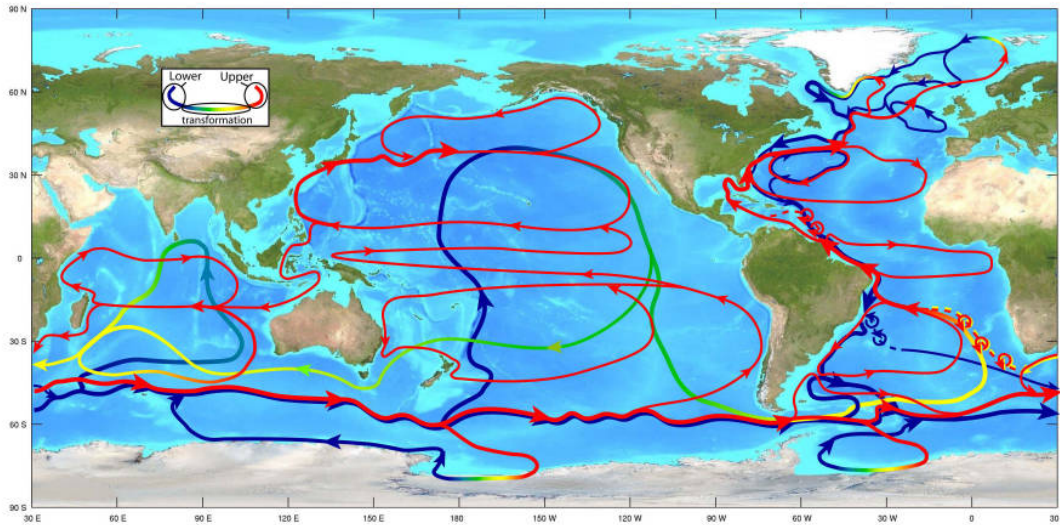


Figure 1.1: Schematic diagram of the global meridional overturning circulation. Recirculation loops are implemented by Lumpkin (2007). Shown are shallow surface currents (red), deep bottom currents (blue) and currents between surface and the deep ocean which are displayed by a gradient from red to blue. The Loop Current in the Gulf of Mexico belongs to the strongest surface currents feeding the Gulf Stream. Adapted from Richardson (2008).

of 15 to 20 x 10⁶ m³/s (Gordon, 1986; Döös, 1995), forming North Atlantic Deep Water (NADW). The NADW flows southward as a Deep Western Boundary Current (DWBC) in the North Atlantic, crossing the South Atlantic, continuing into the Indian Ocean and finally into the Pacific Ocean. In the Pacific, the deep water masses are transformed mostly by diapycnal mixing processes into warmer upper layer waters that split and flow back into the Indian Ocean returning to the Atlantic Ocean passing around Cape Horn. The cold water route, where sub-antarctic water is transported from the Pacific to the Atlantic Ocean within the Drake Passage, is of minor importance for the warm water route transport (~25%). The path of the warm water return flow leads from the Pacific to the Indian Ocean through the Indonesian Seas. These waters are then advected from the Indian Ocean, through the Mozambique Channel, entering the South Atlantic by a branch of the Agulhas Current. Finally the upper waters are advected northward to the subtropical gyre of the South Atlantic (Gordon, 1986).

The wind driven upwelling in the Southern Ocean brings Circumpolar Deep Water (CDW) to the surface within the zone of the Antarctic Polar Front (APF). The APF is a region of strong currents with high horizontal gradients in density, temperature and salinity and marks the location where Antarctic surface waters moving northward are transformed to sub-antarctic waters (Moore et al., 1999, and references therein). Part of the water masses of the CDW loses buoyancy and eventually forms Antarctic Deep

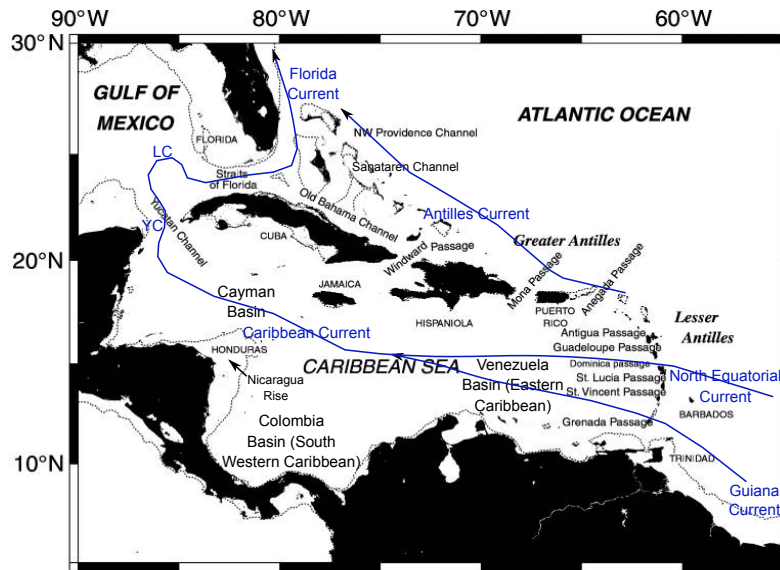


Figure 1.2: Map of the Caribbean Sea and the main passages between the Atlantic Ocean and the Caribbean Sea. Displayed in blue and simplified are the main surface currents including the Florida Current, the LC = Loop Current, the YC = Yucatan Current, the Caribbean Current, the North Equatorial Current, the Guiana Current and the Antilles Current. Figure modified after (Johns et al., 2002).

Water (AADW). The other upwelled water masses move northward under the forcing of the prevailing westerly winds. The driving mechanisms of the Wind-driven upwelling and vertical mixing are contributing to driving the Meridional Overturning Circulation ((MOC); Kuhlbrodt et al., 2007).

The current circulation system in the Gulf of Mexico (GoM) and adjacent ocean basins, also shown in Fig. 1.2, plays an important role because it features large water mass transports flowing through the Yucatan Channel as the Loop Current (LC) and exiting the GoM through the Straits of Florida as the Florida Current (FC). The LC and the FC are of major importance for past and present climates because of the large amounts of heat and freshwater they transport northward. The Florida Current is a component of the western boundary current system of the North Atlantic subtropical gyre. In addition to being a component of this wind-driven gyre, it is also a pathway for the warm water return flow of the Atlantic Meridional Overturning Circulation (AMOC) which is important in the context of climate change. These circulation systems are highly variable and sensitive to various changes that occurred in the past (e.g. the shift of the Intertropical Convergence Zone (ITCZ) (Peterson et al., 2000, and references therein)) and at present (e.g. the possible slowdown of the North Atlantic gyre (Quadfasel, 2005, and references therein)). The ITCZ is a region close to the equator and marks the boundary where the northern and the southern trade winds converge (see Chapter 1.6 for more information).

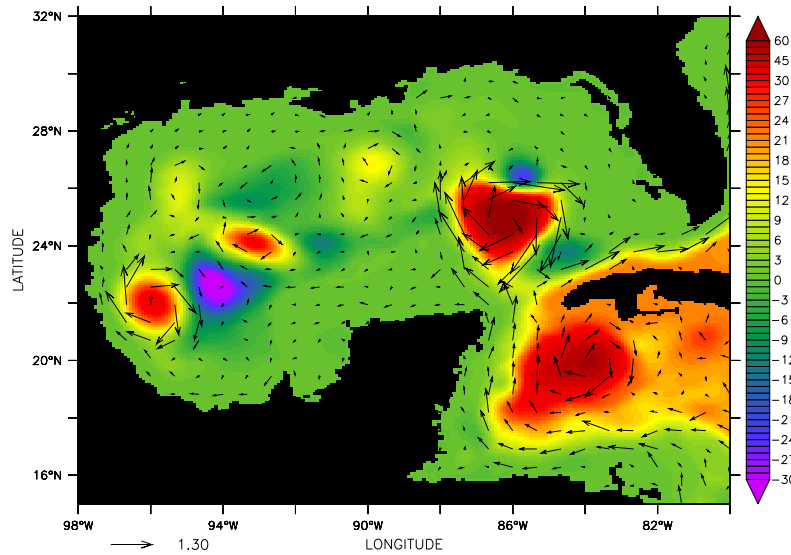


Figure 1.3: Snapshot of barotropic streamfunction in the Gulf of Mexico in Sv (colors) from the $1/12^\circ$ model (from June). The positive values indicate transports that can be associated with elevated SSH. Negative values show the cyclonic eddies and are associated with depressions. The velocity/current speed is displayed by the vectors (in cm/s).

Moreover, the ocean circulation in the Gulf of Mexico is important to the oil and gas industry, especially since the 2010 Deepwater Horizon oil spill incident. A proper understanding of ocean currents in this region is crucial to understand the transport pathways of the oil and its remnants.

1.2 The ocean circulation system in the Gulf of Mexico and adjacent seas

The circulation system in the Caribbean (see Fig. 1.2) is strongly influenced by the North Brazil Current which feeds the Guiana and the Antilles Current. The Guiana Current enters the Caribbean together with the North Equatorial Current through the Lesser Antilles, flowing as the Caribbean Current towards the Yucatan Channel where it becomes the Yucatan Current (YC). This current connects the Caribbean Sea with the Gulf of Mexico, where the Loop Current is located. During most times of the year, the Loop Current forms a loop in the GoM north of the Yucatan Channel and turns into the Florida Current bending again to the North and continuing between Florida and the Bahama Islands becoming eventually the Gulf Stream. The Loop Current occasionally forms a complete eddy that separates from the main current and travels to the northern/northwestern flank of the Gulf, influencing the Florida Straits outflow. A sketch of this eddy shedding process is displayed in Fig. 1.3 showing the barotropic streamfunction

(colors) overlain by the current speed in cm/s. The anticyclonic and cyclonic eddies are important for the heat and salt budget of the Gulf.

The Florida Current between Florida and the Bahamas has been investigated and observed since the 1980's when the Subtropical Atlantic Climate Studies (STACS) program was initiated by the National Oceanic and Atmospheric Administration (NOAA) (Molinari et al., 1985) followed by submarine cable measurements (Larsen et al., 1985). Since 2004 the monitoring with a mooring array became an essential part of the 'Rapid Climate Change/Meridional Overturning Circulation and Heatflux Array' (RAPID/MOCHA) program which was implemented to understand the flow compensation associated with the MOC at 26°N (Kanzow et al., 2007). The first measurements of the Florida Current revealed a mean transport of 30 Sv (1 Sv = 10^6 m³/s) with a 34 Sv maximum in summer and a 25 Sv minimum in early winter (Niiler et al., 1973). The annual cycle was investigated by several authors (Schott et al., 1988; Schmitz et al., 1991; Larsen, 1992; Baringer et al., 2001), but modern transport estimates from submarine cable data confirmed that the FC does not have an annual cycle. Combining the inflow from the Antilles island and the Caribbean Sea passages, Johns et al. (2002) calculate a 'combined' Florida Current transport of ~30 Sv. The small contributions of river runoff and the atmospheric water balance in the Gulf are only minor contributions to the transport in the Florida Straits (L. Czeschel, pers. comm.).

The Yucatan Current between Florida and Cuba was analyzed by Hamilton and Lee (2005) from December 1990 to November 1991. They found a mean transport of ~25 Sv. This observation agrees well with the estimated 23.8 Sv of Sheinbaum et al. (2002) during the CANEK³ program which started in late 1996 and ended in mid 2001. During this program shipboard Acoustic Doppler Current Profiler (ADCP) and CTD (conductivity, temperature, depth) measurements were applied. A current meter mooring array was also deployed to monitor the transport changes in the Yucatan Channel. The transport estimates revealed a lower transport in the Florida Straits than reported in other studies (see above). The missing ~ 8 Sv are suggested to pass through the Old Bahama Channel, north of Cuba and through the passages between the Bahama Islands (Baringer et al., 2001), but estimates by Atkinson et al. (1995) of 1.9 Sv for the Old Bahama Channel and of 2-3 Sv in the North West Providence Channel by Leaman et al. (1995) are not sufficient to compensate for the missing outflow. A possible higher contribution from the Santaren Channel of 6.6 Sv was also suggested by Atkinson et al. (1995).

The Loop Current is the most prominent surface circulation feature in the GoM and can

³named after an important Mayan character in the Mexican literature

extend as far to the north as the Mississippi river delta or the continental shelf (Wiseman et al., 1988). It sheds anticyclonic (clockwise) eddies on an irregular basis at intervals of 6 and 11 months (Sturges et al., 2000) into the GoM. The shedding itself is a long process that can take up to several months. Leben (2005) found separation periods ranging from 3 to 18 months, illustrating the high variability of the current system. The formation of cold cyclones that form around the shedding eddy during the separation period was also observed and analyzed by Fratantoni et al. (1998) and Schmitz (2005). Moreover, the LC position is extremely variable depending on many different controlling factors including the topography or the inflow from the YC.

Since the 1970's, observations from satellite infrared data were analyzed to understand the shedding behavior, although 3-4 months per year of the flow field could not be interpreted because of the uniform, warm surface temperatures in summer (Vukovich and Maul, 1985). In 1992 the topographic observations improved due to the use of multi-satellite sampling techniques by altimeters aboard the TOPEX/Poseidon, ERS-1 and ERS-2 satellites. These measurements are still collected today (Sturges et al., 2000) allowing for a better reliability of the data and thus leading to a continuous record of sea surface height (SSH) data.

In summary, the Yucatan Channel and the Florida Straits transport variability and the mechanism of the LC eddy shedding are current research topics, and yet highly controversial and debated in observational and modeling studies. The mechanism of the ring shedding (e.g. when it occurs or what the final separation process determines) is not completely understood because of the complex and chaotic behavior of the LC. Coherencies between the Loop Current retraction and extension and the seasonal migrations of the ITCZ are assumed to play a role in its variability (Johns et al., 2002; Poore et al, 2004). The mechanism controlling the ring separation frequency is still under debate but is often related to the mass and/or vorticity flux through Yucatan Channel (e.g. Pichevin et al., 1997; Candela et al., 2002) which is partly controlled by the local wind (Chang and Oey, 2010, 2012). Bearing in mind that the LC is assumed to be chaotic, a forcing by biannual wind is not conceivable. The apparent non-existing annual cycle in FC transport calculated from conductivity measurements of a submarine cable at 27°N supports this theory. Impacts due to changes in the MOC, with a maximum inflow to the southern Caribbean in summer and a minimum in fall (Johns et al., 2002) are also unlikely for the same reason. Romanou et al. (2004) proposed the baroclinic transfer of eddy potential to eddy kinetic energy as the main mechanism for eddy shedding.

High-resolution models show a strong correlation between eddy shedding and minimum

transport in the Yucatan Channel (Lin et al., 2010) and in the Florida Straits. The strong non-linear shedding mechanism is not yet determined though, many attempts have been made to connect the LC intrusion into the GoM and eddy shedding with the transport and flow structure of the YC (e.g. Sturges et al., 2000; Bunge et al., 2002; Sheinbaum et al., 2002; Candela et al., 2003; Leben, 2005). However, the variability in the LC system, including the FC and the YC, and the associated eddy shedding remains elusive. The main purpose of this study is to determine the main driving mechanisms that control the LC variability in the past and in the present.

1.3 The Earth's energy budget

The Earth receives most of its energy from the sun. Energy from the Earth can either be reflected or emitted back into space. Earth's albedo affects the amount of solar energy that is reflected back to space. The albedo of the planet can change according to Earth's surface conditions and changes in cloud cover. The Earth's temperature rises if the amount of energy received is higher than the amount that is emitted. Nevertheless, it is assumed that the present Earth-ocean-atmosphere system is in balance. This balance can be modified by greenhouse gas concentrations in the troposphere and water vapor causing increased reflection and heat radiation back to Earth leading to a warming (Colling, 2001). The oceans play an important role in this context because its heat capacity is 1000 times larger than that of the atmosphere (Bindoff et al., 2007), resulting in much slower heating and cooling compared to the atmosphere. Redistribution of heat between low and high latitudes is carried out by winds and the ocean circulation. Especially in the tropics where heat gain of the ocean is greatest, changes in the energetic balance play a crucial role with impacts on the atmospheric and ocean circulation system. These variations can have an impact on the ocean currents therefore leading to significant climate changes (Webb et al., 1997). The amount of heat stored in the ocean therefore, plays a crucial role in controlling Earth's climate, and influences in particular variations on seasonal to decadal time scales with regard to currents, heat and freshwater content and stratification.

1.4 Climate fluctuations during the last glacial-interglacial cycle

During ice ages, a substantial volume of fresh water was stored in large continental ice sheets that covered parts of Northern Europe and large parts of North America. Results from ice core records like the North Greenland Ice Core Project (NGRIP) covering the last 123 kyr (Andersen et al., 2004) and Antarctica (Vostok) covering the last 420 kyr including

the four past glacial cycles (Petit et al., 1999) hold information about the atmospheric gas concentrations of past climates. These ice cores contain enclosed gas bubbles and are therefore of major interest for climate scientists. Fig. 1.4 displays the variations in climate for the last 800 kyr.

1.4.1 Milankovitch cycles

Some events that affected changes in the past climate system are well known or can be reconstructed with great confidence including the Milankovitch cycles (Hays et al., 1976, and references therein). A dramatic and frequent shift in Earth's climate occurred over the last million years, with Earth's climate alternating between ice ages (glacials) and warmer periods (interglacials) known as Milankovitch cycles. These glaciation cycles occurred on periods near 23, 41 and 100 kyr (1 kyr = 1000 years). The direction of the axial tilt of the Earth has a 19-23 kyr cycle (precession), the variation in the Earth's amplitude of the axial tilt has a 41 kyr cycle (obliquity) and the main orbital eccentricity has a 100 kyr cycle.

These cycles modify the latitudinal and seasonal distribution of solar radiation reaching the Earth's surface and hence the energy it receives from the sun. The quasi-periodic cycles agree to a good extent with the climatic variations shown in Figure 1.4. Temperatures estimated from stable isotope analyses are shown in Fig. 1.4 **a** and **c**, atmospheric CO₂ in Fig. 1.4 **b** and the chemical information from e.g. ash layers of volcanic eruptions can be calculated from sediment reflectance and is displayed in Fig. 1.4 **d**. The 41 kyr cycle is associated with an insolation increase (poleward) in both hemispheres, while the 23 kyr cycle dominates insolation changes at low and mid latitudes (Fairbanks, 1989).

Atmospheric CO₂ varied between 180 and 300 ppm (parts per million) over the glacial and interglacial cycles of the last ~700 kyr (Jansen et al., 2007; Sigman et al., 2010) with an estimated concentration of 190 ppm for the LGM (Bouttes et al., 2011). Terrestrial changes cannot explain the low glacial values of the atmospheric CO₂ concentration though, because terrestrial storage of carbon was also low at the Last Glacial Maximum due to low global biosphere productivity. Atmospheric CO₂ is mainly governed by the interplay between air-sea gas exchange, ocean circulation, marine biological activity, ocean-sediment interactions, and seawater carbonate chemistry during the last glacial/deglacial period (Jansen et al., 2007).

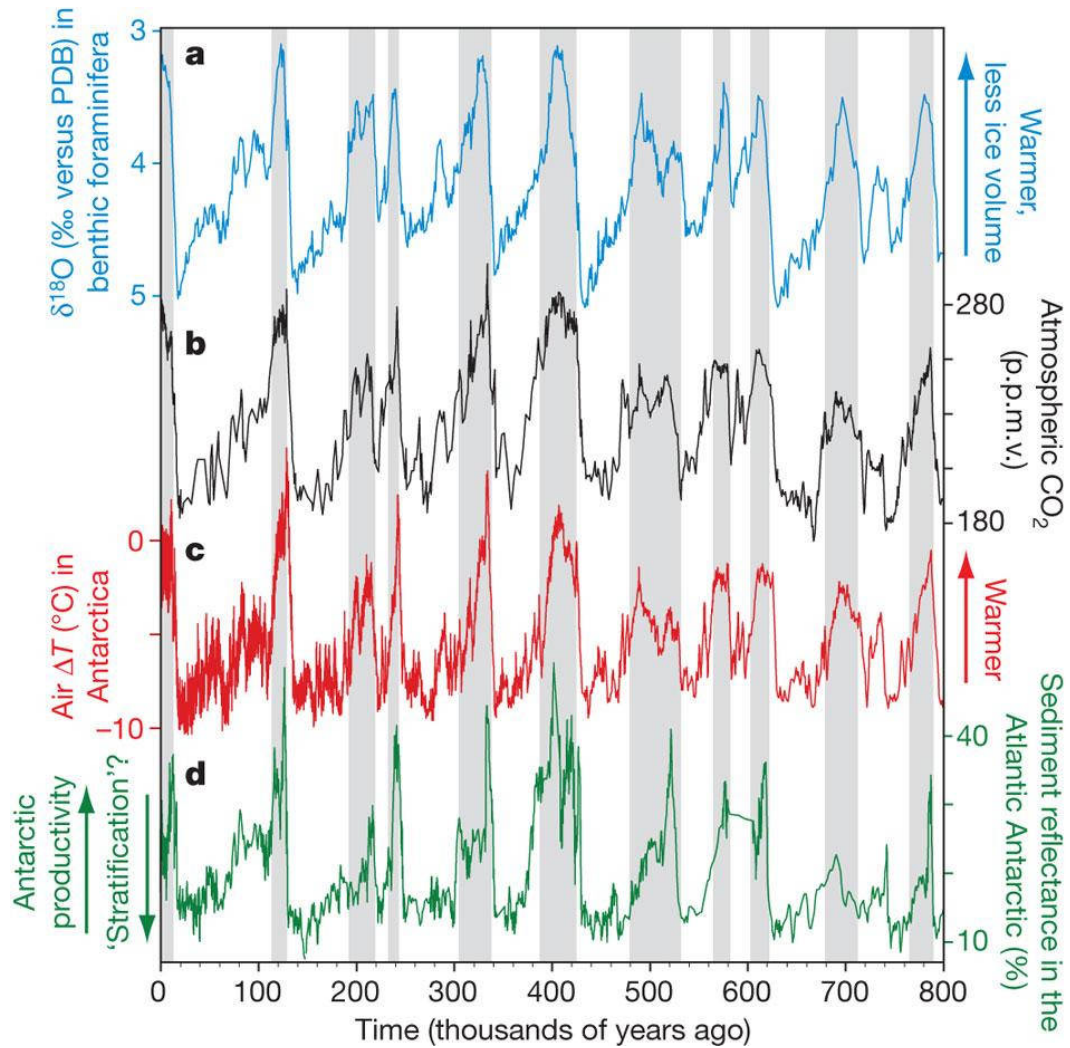


Figure 1.4: Variations in climate over the last 800 kyr BP (before present). Fig. 1.4 a) shows a compilation of benthic foraminiferal $\delta^{18}\text{O}$ records revealing changes in continental glaciations and deep ocean temperature, 1.4 b) atmospheric CO_2 reconstructed from Antarctic ice cores. In 1.4 c) the Antarctic air temperature derived from the deuterium content of an Antarctic ice core is displayed and in 1.4 d) the sediment reflectance of the Antarctic sediment core ODP 1094 revealing the export of biogenic material out of the upper ocean layers. Grey shaded are warm intervals (interglacials). Figure from Sigman et al. (2010).

1.4.2 Heinrich events

The last glacial cycle marking the transition to the Holocene was not homogeneous. Prominent cold-deglacial events like Heinrich events⁴ (Figure 1.5) and warm-deglacial rapid climate fluctuations like the Dansgaard-Øeschger (D-O) events (the Bølling-Allerød is the latest of these events) occurred.

Heinrich events are characterized by layers in eastern and northern Atlantic sediments with high ratios of ice rafted debris and occurred at intervals of roughly 10 kyr. These sudden inputs are the result of debris released during melting of massive icebergs into the North Atlantic that may stem from surges along the eastern margin of the Laurentide ice sheet, thereby reducing the circulation (Heinrich, 1988; Broecker et al., 1991). A contribution of other ice sheets during these events mostly based on Sr-Nd isotope signals of ice-rafted debris (Bard et al., 2000; Grousset et al., 2000) is discussed. The input of freshwater from the melting icebergs is a possible mechanism for the shutdown of the MOC. A freshening of the North Atlantic ocean, with a decrease in the density of the surface waters could have suppressed the formation of NADW formation. When the MOC is shut down, heat transport between the hemispheres is strongly disturbed, leading to an interhemispheric see-saw effect (Broecker et al, 1985; Stocker, 1998; Seidov et al., 2001). The see-saw effect is characterized by a contemporaneous warming in some regions of the Southern Hemisphere due to the reduction in NADW. The decreased meridional heat transport from the south leads to a cooling in the Northern Hemisphere (Clark et al., 2002).

1.4.3 Dansgaard-Oeschger events

Dansgaard-Oeschger events are characterized by an abrupt warming (up to 10°C temperature rise within a few decades) during cold glacial conditions and occurred about 25 times during the last glacial period (see Figure 1.5, not all events are shown). Sixteen of these events between 25 kyr and 60 kyr occurred on average every 2000 years. These events are reflected by a warming in the North and cooling in the Southern Ocean due to the enhanced northward transport of heat (Bond et al., 1993). A possible freshwater feedback on the MOC (slow-down) with greenhouse gas concentrations in the atmosphere that deviate from the present levels is conceivable and has been analyzed in a model study by Clark et al. (2002). D-O events can last between 10 and 100 years and are followed by

⁴Heinrich events are named after the German oceanographer Hartmut Heinrich (* March, 5th 1952); H. Heinrich: Origin and consequences of cyclic ice rafting in the northeast Atlantic Ocean during the past 130,000 years, 1988.

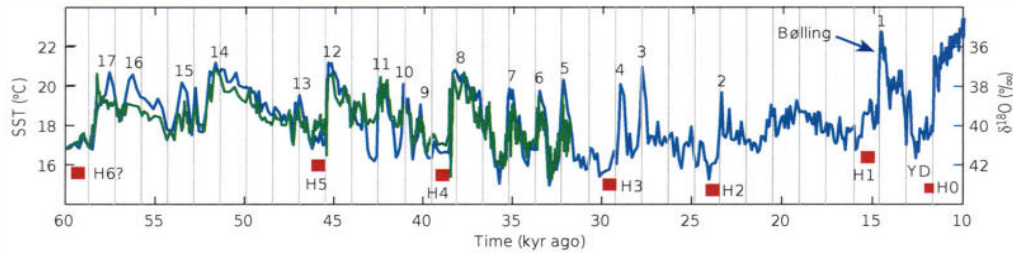


Figure 1.5: SST reconstruction from Greenland ice and from ocean sediments. The green line displays the proxy data from the Atlantic (Sachs et al., 1999), the blue line displays data from GISP2 (Greenland). Several Dansgaard-Oeschger events are indicated with numbers, Heinrich events are indicated by red squares. The thin lines displays intervals of 1470 kyr pointing to a tendency of periodic re-occurrence of the Dansgaard-Oeschger events. Figure from Rahmstorf (2002).

a slow cooling over approximately 1000 years back to glacial conditions (Gornitz et al., 2009).

The mechanisms behind the timing and the amplitude of the D-O events are still not understood but a possible coupling between the Scandinavian ice sheets, the ocean and the atmosphere was assumed by Bond et al. (1993).

1.5 The past and the present ocean circulation in the North Atlantic

The present surface circulation in the North Atlantic with major currents is shown in Fig. 1.6. The circulation in the Atlantic is part of the global thermohaline circulation consisting of the zonal currents (wind-driven) and the primarily (thermohaline) meridional flows that involve the transformation of warm to cold water at high latitudes. The transport of heat from the equator to the poles is mostly accounted for by the atmosphere but also by ocean currents (Talley et al., 2011). Warm tropical surface waters are transported northwards within the strong western boundary current (the Gulf Stream) which is part of the wind-driven North Atlantic subtropical gyre. North of $\sim 40^\circ\text{N}$ there are subpolar and polar current systems, tropical currents systems can be found at low latitudes south of $\sim 20^\circ\text{N}$. The equatorial current system is located in the vicinity of the equator.

In the subtropical North Atlantic the AMOC dominates the meridional heat flux while in subpolar latitudes and in the subtropical South Atlantic the gyre circulations are more important. The AMOC can be monitored by measuring arrays that span over the entire North Atlantic e.g. at 26.5°N or 43°N . The entire water column can be observed on a daily basis improving the understanding of AMOC variability in terms of density and bottom pressure variability. The zonally integrated geostrophic flow in combination with

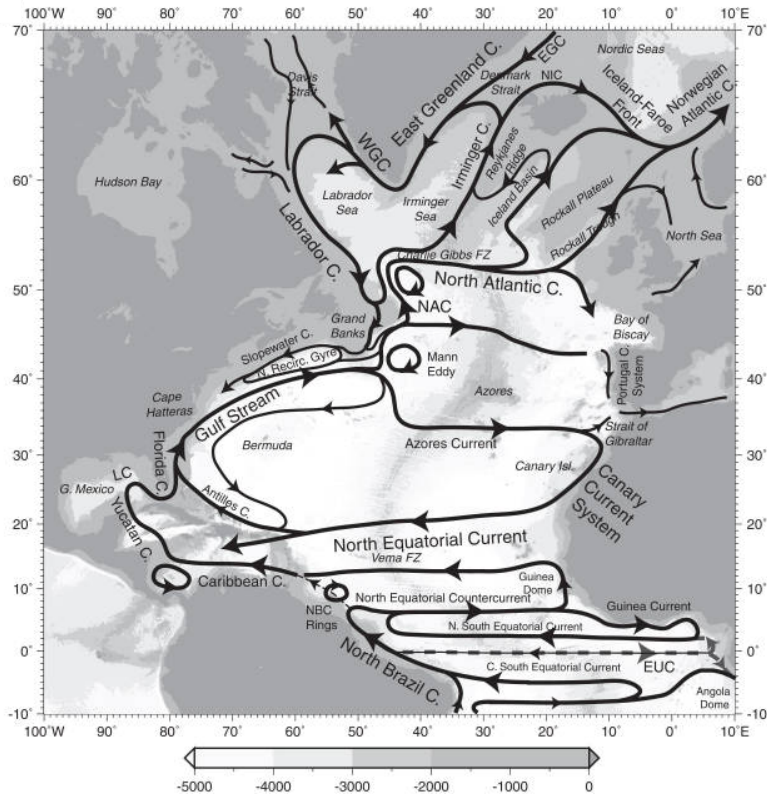


Figure 1.6: Surface circulation scheme of the North Atlantic Ocean from Talley et al. (2011).

temperature and salinity measurements can be carried out over the complete array. Wind driven surface variability is derived from QuickScat satellite observations to complete the survey (Cunningham et al., 2010).

Due to the fact that paleo evidence is scarce, only little is known about the North Atlantic ocean circulation during the LGM. Nevertheless, the prevalent paradigm is that the LGM circulation was weaker than today. Lynch-Stieglitz et al. (1999) concluded that the geostrophic shear in Florida Straits was diminished, reflecting a reduced gradient of North Atlantic thermohaline circulation during the LGM. Nevertheless, it is neither yet clear whether the MOC was reduced (Lippold et al, 2012, and references therein) nor if the Florida Straits transport was reduced. Assuming the glacial periods were characterized by stronger winds than the non-glacial periods, the proposed reduction is hard to justify. The higher radiocarbon ages compared to the present found in foraminifera shells by Broecker et al. (1991) could also be interpreted as an increase in mass circulation due to the enhanced input of southern hemisphere water into the North Atlantic (Wunsch, 2003). In contrast to these findings there are studies by LeGrand et al. (1995) and Yu et al. (1996) who support the hypothesis of an unchanged or increased North Atlantic circulation which is more conceivable regarding the stronger wind system. The higher

dust deposits in marine sediment cores during these times (Grousset et al., 1998) support this theory.

For the LGM, models show a large discrepancy in simulating the Atlantic deep circulation (Oka et al., 2012). The abyssal circulation is thermohaline and wind-driven with a major influence from tidal forcing. The lowered sea level during the LGM may have lead to a decrease in shelf areas and therefore to a possible increase in the deep ocean mixing. In addition, stronger winds and the thermohaline forcing could have contributed to an increase in the vertical mixing and with it to the strength of the AMOC (Munk et al., 1998).

Ocean models are critical tools in the reconstruction of LGM conditions due to their capability of implementing varying boundary conditions. A model study by Oka et al. (2012) showed a weakening of the AMOC when freshwater fluxes are increased, but a strengthening when heat fluxes are applied. The authors further conclude that there is a thermal threshold controlling the AMOC and already slight changes in surface cooling or wind stress changes can lead to very different responses of the AMOC. Additional sensitivity experiments contribute to the understanding of the ocean circulation changes in the past and in the present and are also a major focus of this thesis. Nevertheless, also models are set up with boundary conditions and assumptions that can have totally different effects on the ocean circulation and have to be set up and analyzed carefully.

1.6 The role of the present and the glacial wind system over the North Atlantic with special focus on the Caribbean

Climate in the tropical North Atlantic is mainly controlled by variations in the strength of the trade winds, the position of the ITCZ, and SSTs. The ITCZ controls the hydrological cycle over the tropics and changes position following the seasonal cycle of insolation. The present maximum southern position occurs in January, whereas the northernmost position is reached in July (Fig. 1.7).

The atmospheric circulation has the potential to influence local/regional and large scale ocean circulation. Little is known about wind stress over the North Atlantic during the LGM, but the large air temperature oscillations reconstructed from Greenland ice cores imply massive reorganizations of the atmosphere/ocean system during this time period (Bond et al., 1993). A southward shift of the ITCZ during the LGM is assumed, caused by the large continental ice sheets in the Northern Hemisphere (Chiang et al., 2005). The subsequent cooling of the Northern Hemisphere is likely accompanied with a modification

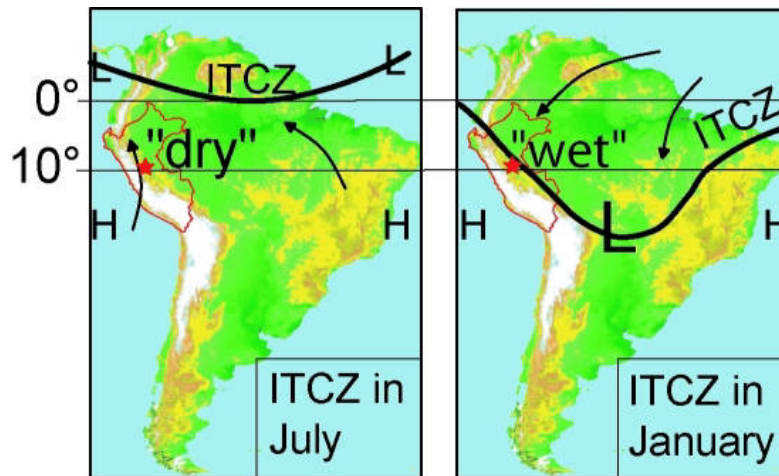


Figure 1.7: Mean position of the recent ITCZ (Robinson et al., 1999) shown for July (left) and January (right). During boreal summer the ITCZ is in its northernmost position while in austral summer it is shifted to its southernmost position below 10°S.

of the westerly winds (Slowey et al., 1995). Stronger winds during the LGM over tropical west Africa are also proposed by Grousset et al. (1998) analyzing stable Sr-Nd isotopes in Saharan sediments. The position of the ITCZ in the eastern equatorial Pacific during the last 30 kyr has been reconstructed by Koutavas et al. (2005) using measurements of oxygen isotopic composition (^{18}O) and magnesium/calcium ratios (Mg/Ca) in planktonic foraminifera from deep-sea sediment cores. The ratio of the heavier oxygen isotope ^{18}O to the lighter oxygen isotope ^{16}O is used to estimate temperatures of the surrounding water of the time where e.g. a foraminifer grew. ^{16}O preferentially evaporates first from sea water leaving an ocean enriched in ^{18}O in the tropics. Alterations in global patterns of evaporation and precipitation due to changes in climate can therefore change the ^{18}O ratio. Mg/Ca is a paleo proxy for deriving SSTs in planktonic foraminifera but can also be used for estimating paleo bottom water temperatures. The advantage of combining ^{18}O and Mg/Ca is to isolate the record of the $\delta^{18}\text{O}_{\text{water}}$. Changes in precipitation and evaporation can then be reconstructed but also changes in the continental ice volume (e.g. Lea et al., 2000). As an indicator of the ITCZ front/boundary e.g. Koutavas et al. (2005) use the intensity of the Atlantic equatorial cold tongue, which is seasonally appearing. They suggest that during the LGM a weaker cold-tongue ITCZ front prevailed, indicating a more southerly ITCZ at that time. The position can further be inferred from the color or the mineralogy of the marine sediments from Cariaco Basin (located north of the Venezuelan coast) revealing the rainfall intensity (Peterson et al., 2000; Haug et al., 2001; Lea et al., 2003; Wang et al., 2004). Results from foraminiferal Mg/Ca ratios and the

gray-scale records by Lea et al. (2003) seem to be in phase, corroborating their estimation of the glacial/deglacial ITCZ position. There are also indications that the ITCZ shifted due to changes in the interhemispheric temperature contrast found in model experiments by Broccoli et al. (2006).

The influence of glacial winds on the subtropical gyre in the North Atlantic with its influence on the transport through the Caribbean Sea is a major focus of this thesis with regard to the possible influence on the Loop Current eddy shedding in the Gulf of Mexico and the possible successive consequences. The GoM as part of the gyre circulation of the subtropical North Atlantic, and hence the eddy shedding process, can be influenced by the wind stress due to the connection of the GoM with the Caribbean Sea. A stronger subtropical gyre will influence also the Gulf because the water masses need to be recirculated in the gyre and enter therefore the Caribbean between the Lesser Antilles Islands due to mass balance.

1.7 Sea level fluctuations during the last glacial period

Global climate fluctuation like the Heinrich events or the Dansgaard-Oeschger events over the last glacial cycle have led to changes in the oceanic and the atmospheric circulation. These fluctuations in the past climate have been reconstructed from a large number of paleo proxies, revealing the order of magnitude such climate impacts can have. In the geological past, periods of lowered sea level (see Figure 1.8) are linked to significant changes in the global ice volume, and consequently the oceanic and atmospheric circulation patterns. These sea level fluctuations occurred during the glacial periods as a result of the periodic changes in Earth's axis rotation and orbit around the sun. The changes in ice volume associated with it can either be inferred from geological mapping or from marine oxygen isotope reconstructions (Fairbanks, 1989; Sidall et al., 2003). A lowered sea level can influence the ocean dynamics in ocean basins with extended shelf areas like the Gulf of Mexico, due to a narrowing of e.g. the Yucatan Channel or the Florida Straits leading to variations in the throughflow.

The Last Glacial Maximum

The last glacial maximum marks the peak of the last glacial period ranging from 26.5 kyr until 19-20 kyr (Peltier, 1994; Clark et al., 2009). At the height of the LGM, when ice sheets were at their maximum extension (see Fig. 1.9 for a reconstruction of the northern hemisphere ice sheets obtained from relative sea level history and a variety of geomorpho-

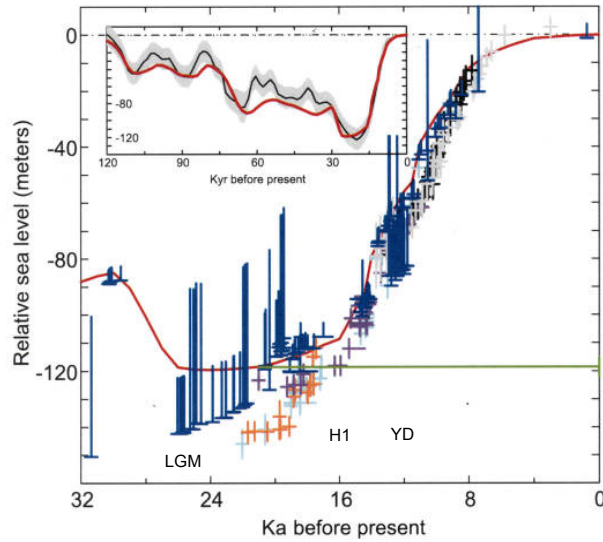


Figure 1.8: Sea level history estimates from Barbados coral records (blue symbols), prediction with ICE-5G(VM2) model and values from Lambeck et al. (2002) (cyan) for Barbados, Bonaparte Gulf (orange), Huon Peninsula (grey), Tahiti (purple) for the Sunda Shelf (black). Light green transparent bars mark the LGM at 26 kyr, the H1 event at ~16 kyr and the YD at ~12 kyr. Small figure shows the sea level reconstruction (black line) and its error (grey surrounding) by Waelbroeck et al. (2002) for the last 120 kyr derived from oxygen isotope measurements, red line displays the prediction by the ICE-5G model. Figure modified after (Peltier et al., 2006).

logical and modern geodetic constraints), the global mean sea level was approximately 120 m lower than today because large amounts of water were bound in huge continental ice sheets (Fairbanks, 1989; Waelbroeck et al., 2002; Wright et al., 2009). Nevertheless, also minimum subpolar SST (Bard et al., 2000) and colder air temperatures over Greenland (Grootes et al., 1993) occurred during H1 and hence suggest that the LGM should not be viewed simply as a climatic extreme event everywhere on the globe (McManus et al., 2004). An interesting aspect of the topography change, or rather a change in the coast line during these times of lowered sea level, is the dynamical impact on the circulation in the GoM, in particular on the changes in the regional depth-averaged circulation, changes in the LC and its associated eddy shedding. A possible alteration in the circulation most likely affects the heat budget in the Gulf, thus influencing paleo-records from this region and associated ocean basins e.g. the Caribbean.

The Younger Dryas

The Younger Dryas was a cold and short geological period between approximately 12.9 and 11.5 kyr (Edwards et al., 1993; Carlson et al., 2007). During the YD, climate fluctuations led to large changes in the continental ice volume and a lowered sea level (Fig. 1.8)

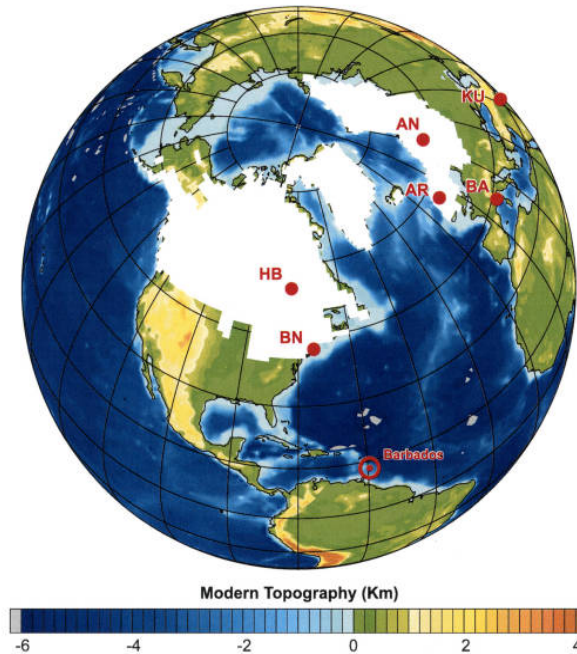


Figure 1.9: Locations of relative sea-level records and the northern hemisphere continental ice sheets at the Last Glacial Maximum from Peltier et al. (2006)

of ~ 70 m (Fairbanks, 1989; Waelbroeck et al., 2002).

A disintegration of the North American ice sheets is discussed as the initiating event for the onset of the YD cold period, eventually followed by the onset of runoff from glacial lakes like Lake Agassiz (see Fig. 1.10, (Peltier, 1994)). The large amount of freshwater discharge associated with it may have sustained the effects due to a decrease in the oceanic surface water density in the North Atlantic hence leading to a slowdown of the AMOC (Clark et al, 1999; Carlson et al., 2007) or an interruption of NADW formation (Barker et al., 2009; Schmidt et al., 2011). The freshwater might have caused a reduced surface-to-deepwater transformation with a decrease in the northward flow from tropical surface waters, and hence a reduction in northward heat transport from the southern hemisphere.

Nevertheless, the forcing of the AMOC reduction is not yet resolved (Carlson et al., 2010). Modeling studies suggest, that low ^{14}C content in the deep ocean indicates a weak conveyor belt. Although ^{14}C concentration is highest in the early Younger Dryas and declines gradually, an additional mechanism which lowers the ^{14}C during this period of possibly reduced deep-water formation is assumed by Hughen et al. (1998). An increase in North Atlantic Intermediate Water (NAIW) and a possible export to other ocean basins could have led to an increased uptake of atmospheric CO_2 by the ocean. An increase in the convection in the Southern Ocean is also assumed as a possible sink for atmospheric CO_2 .

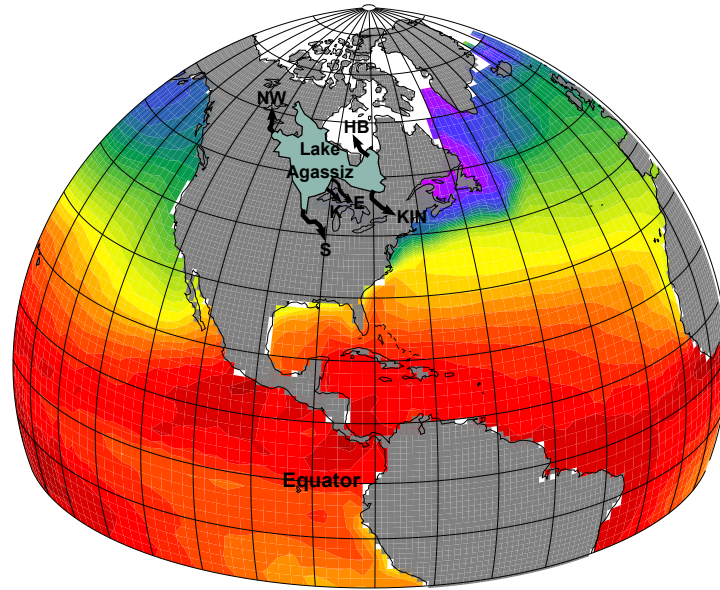


Figure 1.10: Map of total area covered by Lake Agassiz during its 5 kyr history (Leverington et al., 2003). Arrows and letters show the main routes of overflow; NW=northwestern outlet, S=southern outlet to the Gulf of Mexico via the Minnesota and Mississippi river valleys, K=eastern outlets through Thunder Bay area, E=eastern outlets through Nipigon basin, KIN=Kinojvis outlet, HB=Hudson Bay route of final drainage. Colors are sea surface temperatures from Levitus (red = warm, blue = cold).

The routing of glacial Lake Agassiz, which was located in the middle of the northern part of North America and fed by glacial meltwater is not yet clear (Clark et al., 2001; Broecker, 2006). Nevertheless, wherever the freshwater originated from - the underlying mechanism forcing these waters to flow into the Atlantic at the onset of the YD remains elusive. Speculations about meteorites (Fireston et al., 2007; Bunch et al., 2012) still circulate, but are not confirmed (Mayewski et al., 1993). Large volcanic eruptions were proposed by Bay et al. (2006) as another mechanism for Pleistocene climate variability.

The Holocene

The period of the Holocene started at around 12 kyr following the YD cold period. Remnants of glacial ice sheets were still present in northeastern North America and Scandinavia in the early Holocene (Peltier, 1994). The post Younger Dryas sea-level rise appears to have been rapid and uniform until 9 kyr years ago at a rate of about 15 mm/year (Lambeck et al., 2002). They interpret their combined data set as a linear, but still rapid, rising sea-level after the Younger Dryas. At around 7 kyr the sea level approached present day level (Peltier, 1994).

As mentioned earlier, greenhouse gas concentrations have an influence on the energy

budget of the Earth and are associated with temperature changes. Atmospheric CO₂ concentrations increased from about 180 ppm at the LGM to 265 ppm in the early Holocene (~12 kyr (Monnin et al., 2001)) and increased even further to a concentration of ~280 ppm in the pre-industrial (Ruddimann et al., 2011). At present, the CO₂ measured at Mouna Loa, Hawaii is at a level of ~400 ppm (<http://www.esrl.noaa.gov/gmd/ccgg/trends/>). Insolation changes dominate the climate forcing during the Holocene. In the early Holocene, warming occurred in northern and southern high latitudes and is attributed to the enhanced tilt compared to present day (Berger, 1978). The steep CO₂ increase since the 19th century is most likely anthropogenically influenced (Keeling et al., 1989).

1.8 Observations in the Gulf of Mexico and its connections to the glacial environment

Instrumental records of global temperature exist since the 1850s (Brohan et al., 2006). However, climate proxies provide useful information about climatic conditions because they yield preserved physical characteristics. These proxies are thus of high importance for understanding past climates and mechanisms that led to the large changes in past climate regimes found in the paleo records. Proxies can be derived from ocean and lake sediments, corals, pollen, tree-rings and ice cores because they yield chemical elements e.g. certain isotopes that were produced and build into e.g. foraminifera shells or corals under different climatic conditions. During the time of growth of a proxy or deposition they have influenced the genesis of a proxy (e.g. the growth rate or deposition character) and can give useful information when undisturbed. After deposition the proxies can lose important information due to bioturbation (information loss due to benthic organisms reworking the marine sediment) and compaction in marine sediments (sediment is losing porosity due to the effect of loading) or solubility (e.g. shells can dissolve in the ocean due to an increase of the pH caused by the uptake of anthropogenic carbon dioxide) and therefore they would not be suitable for precise climate reconstructions anymore. Due to the unknown extent of the impact such alterations can have respectively the magnitude of errors, proxies need to be analyzed with caution. Problems can further arise by the applied sampling method or during the physical interpretation e.g. transferring core depth into age etc. (Huybers et al., 2010).

Besides the high importance of the variable Loop Current, the Gulfs' hydrography is also influenced by the freshwater discharge of the Mississippi River. The Mississippi River is one of the largest drainage systems (~3800 km; <http://ga.water.usgs.gov/edu/>

[riversofworld.html](#) 08.04.2013) in North America beginning as a small stream flowing from lake Itasca in the northern USA down to Mississippi and Louisiana with an annual discharge of $13500 \text{ m}^3 \text{ s}^{-1}$ (Morey et al., 2003). It became of major importance in the past during glacial periods when the melting of the North American ice sheets occurred. These major important hydrographic features exert a combined influence on sea surface temperature (SST) and sea surface salinity (SSS) in the Gulf of Mexico. During the LGM, the sea surface salinity in the GoM was significantly reduced. A number of studies in the GoM (e.g. Aharon, 2003; Flower et al., 2004; Hill et al., 2006) found negative ^{18}O excursions during the deglacial leading to the assumption of so called 'super flood events' and also model studies by Kim et al. (2002) assume a threefold increase of Mississippi discharge. The reconstructed SSS and SST in the northern GoM and in the Caribbean ideally reflect the temporal dynamics of the hydrological system and show an enhanced gradient between these areas especially during cold phases. In addition to the increased Mississippi discharge, Nürnberg et al. (2008) point to the connection of the development of the Atlantic Warmpool and the position of the ITCZ (Fig. 1.7) also influencing the hydrology of this region. They also propose that the cooling and freshening in the northern GoM is a combination of the less established Loop Current with a strengthened Mississippi discharge and a more southerly position of the ITCZ. This could explain the differences in sea surface temperature and salinity derived from combined Mg/Ca and stable isotope analyses on planktonic foraminifera that are found in the paleorecords between the Caribbean and the Gulf of Mexico, showing higher temperatures for the Cariaco Basin in the Caribbean (Nürnberg et al., 2008; Schmidt et al., 2011). The deglacial temperature increase in the north eastern GoM calculated from $\text{SST}_{\text{Mg/Ca}}$ of 6.5°C is linked to the northward propagation of the ITCZ in combination with the northward shift of the Atlantic Warmpool due to the waning ice cover over North America (see also Chapter 1.6).

1.9 The present and the past Gulf Stream separation latitude

Nowadays, the Gulf Stream system (see Fig. 1.11) extends into the North Atlantic up to approximately 50°W (Rasmussen et al., 2012; Talley et al., 2011), where it splits into four different branches: the North Atlantic Current and the Azores Current, a southern recirculation gyre and a northern recirculation gyre (Schmitz, 1996). Observations by current meters reveal a transport of 29-31 Sv (Schott et al., 1988; Leaman et al., 1995), submarine cable measurements estimate approximately 29-33 Sv (Baringer et al., 2001) and geostrophic estimates reveal transports between 28-30 Sv (Schmitz et al., 1968). Spe-

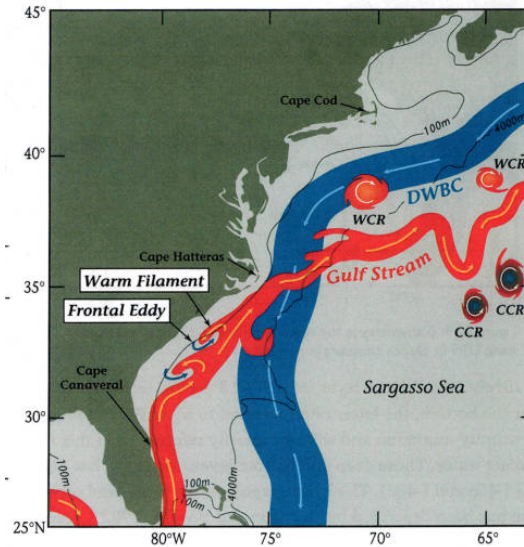


Figure 1.11: Major currents in the westernmost North Atlantic from Schmitz (1996). Displayed is the DWBC (Deep Western Boundary Current) in blue, the Gulf Stream in red and typical features accompanying the GS like warm core rings (WCR) and cold core rings (CCR).

cial features of the Gulf Stream are the warm core rings evolving on the northern side of the current and the cold core rings that evolve in the south and pinch off from the main current. The position of the Gulf Stream can be estimated with a good accuracy from satellite images (e.g Minobe et al., 2008). It flows parallel to the North American coast as a western boundary current until it turns east near Cape Hatteras passing the New England Seamount chain. The boundary between the North Atlantic subtropical and subpolar gyre is the line, where no convergence or divergence of water in the directly wind-forced surface layer of the ocean occurs (line of zero Ekman pumping/line of zero wind stress curl (see Stommel, 1948; Munk, 1950)). This line is referred to as a mark for the boundary between the Gulf Stream and the North Atlantic Current system in ocean general circulation theories (Keffer et al., 1988).

Modeling the strongly meandering Gulf Stream is still a challenge. Early simulations of numerical OGCMs often failed in simulating the separation latitude off the coast at Cape Hatteras and could not reproduce the volume transport correctly (Dengg et al., 1996). The improvement in modeling the GS separation was achieved by a resolution refinement ($1/10^\circ$ and higher). Using finer grids allows for processes like meso-scale baroclinic instabilities and the first baroclinic Rossby radius of deformation can be resolved (Smith et al., 2000; Bryan et al., 2007). Increasing the resolution also led to larger Reynolds numbers due to the possibility of implementing smaller viscosities (Dengg et al., 1996).

Observations are available from Expendable Bathythermograph (XBT) surveys, buoy and ship observations, moorings and infrared and altimeter satellite data providing a basis for statistical analyses of the GS position. Some of the observations though are not available at high resolution (Niiler et al., 2003) and are only useful to obtain the current main axis position. The validation of high resolution OGCMs by comparing them to satellite data is difficult because precise computations of the ocean mean dynamic topography are not available due to the lack of an accurate geoid on the meso-scale (Chassignet et al., 2008). Nevertheless, OGCM results were analyzed in the past regarding due to their high sensitivity of different subgrid scale parameterizations (Bryan et al., 2007). Best results were obtained when the viscosity operator is prescribed as a combination of the Laplacian (harmonic) and the biharmonic operators (Chassignet et al., 2001). Recapitulating, numerical models of at least $1/10^\circ$ resolution provide a common basis and are capable of simulating today's Gulf Stream position. Nevertheless, the separation from the coast is very sensitive to a variety of factors like representation of topography, DWBC strength, subpolar gyre strength and water mass properties and subgrid meso-scale parameterization (Munk, 1950; Haidvogel et al., 1992; Dengg et al., 1996; Bryan et al., 2007, and references therein).

Only little is known from observations for the glacial Gulf Stream position because it is a challenge to recover marine sediment cores that contain undisturbed glacial sediment due to the strong current regime. Nevertheless, studies of the LGM emphasized that wind stress plays an important role for the changes in the North Atlantic circulation system. A cooling of the northern hemisphere and the changes in the atmospheric circulation system are assumed to be accompanied by a southward shift of the polar front during the LGM. A southward shift of the currents in the North Atlantic due to this shift has been found in the paleo-records by Ruddiman et al. (1981). However, the present and the past Gulf Stream position were analyzed in a study by Matsumoto et al. (2003). Their reconstruction of today's Gulf Stream axis using planktonic foraminifera yielded satisfying results so they extended their study to the LGM with the conclusion that the glacial GS had almost the same position compared to the present. This motivates further research as undertaken in Chapter 4 to test the response of the Gulf Stream circulation system to a stronger wind field as prevalent in the LGM.

1.10 Thesis outline

This dissertation contains three chapters each addressing an independent research question written in the style of journal publications. Each chapter can be read self-contained and

includes an introduction, experimental set up (design), results, and discussion section.

The main objective of this thesis is to understand the regional climate variability in the Gulf of Mexico in both the past and in the present. Numerical ocean circulation models and observations are used to investigate the main physical processes responsible for the Loop Current variability and its interconnection with the Caribbean Sea on glacial-interglacial timescales. The influence of the Loop Current eddy shedding on the heat budget of the GoM at changing sea levels and different wind stress forcings as well as topographic effects are studied based on high resolution model results. In particular, this research comprises (1) the use of a three-dimensional OGCM to simulate deglacial ocean circulation, ocean dynamics and variability in the Caribbean, the Gulf of Mexico and the Florida Straits assessing the models behavior, and (2) the analyses of observational data (such as stable isotope analyses for e.g. temperature and current reconstruction in marine sediment cores, current observations (e.g. submarine cable data at 27°N) and sea surface height from satellite observations (e.g. AVISO) and with a validation/comparison to the model results. A three dimensional high resolution OGCM is used instead of a fully coupled climate model because ocean dynamics can evolve more efficient than in fully coupled models with a large number of parameterizations and prescriptions, sometimes even flux adjustments, to allow for a better stability of the respective model. OGCMs are therefore considered to be more realistic. It is further computationally much less expensive allowing for more experiments.

Manuscript No. 1 presents a study of the mechanism of the Loop Current variability. Models are compared at different resolutions to sea surface height (SSH) satellite data (AVISO) and to Florida Straits cable transport data. The influence of different boundary conditions as well as different surface forcings in MIT (model with no slip conditions and free surface) and FLAME (model with free slip conditions and rigid lid) are investigated focusing in particular on today's LC dynamics. It is suggested that internal variability may play a significant role in Florida Current transport variability on monthly to decadal time scales and that the position of the Loop Current eddy plays an important role.

Therefore, the following question is addressed in the first manuscript:

1. What causes the interannual to decadal variability in the Florida Straits/Yucatan Channel transport?

In manuscript No. 2 the Loop Current variability and its influence on the hydrology in the Gulf of Mexico during the last deglaciation is investigated. Here the different setups of the FLAME model experiments are described in detail. Moreover, changes on the

circulation due to different sea levels are analyzed as well as due to different wind stress anomalies, in order to separately evaluate the role of sea level and wind stress. The wind stress anomalies were calculated using PMIP 2 (Paleoclimate Modelling Intercomparison Project 2) wind stress data and compared to the CONTROL experiment (present day conditions) and to proxy data from marine sediment cores by e.g. Nürnberg et al. (2008) and Schmidt et al. (2004).

These sensitivity experiments complete the understanding of the variability of the ocean circulation in the Caribbean, the Straits of Florida, in the Gulf of Mexico and in the Gulf Stream area during the last ~ 26 kyr.

The questions addressed in manuscript 2 are as follows:

1. How did the ocean circulation change in the Gulf of Mexico and adjacent seas during the transition from glacial to interglacial times?
2. How does the process of Loop Current eddy shedding affect
 - a) the heat budget of the GoM?
 - b) the salt budget of the GoM?
 - b) the surface circulation pattern of the GoM?
3. What causes the eddy shedding and why does it change through time?

Some experiments of manuscript 2 are further investigated and compared to model studies using high resolution model experiments of the FLAME model in manuscript 3. Due to the well known bias of low resolution models to accurately represent the position of the present Gulf Stream axis, experiments with the high resolution model were performed and analyzed. Bearing in mind, that only little is known about the Gulf Stream position during the LGM, model experiments can help to improve the understanding of processes that could have led to a southward shift of the current system in the North Atlantic. As processes and mechanisms are still controversially debated, manuscript 3 investigates the Gulf Stream separation in more detail, addressing the following questions:

1. Where was the Gulf Stream separation latitude located during the LGM?
2. If a southward shift in separation latitude occurred, what are the possible causes?

Finally, major findings of this thesis are summarized in Chapter 5, also addressing future research topics related to this thesis.

Chapter 2 has been submitted to *Palaeoceanography*⁵. Chapter 3 has been submitted to *Journal of Geophysical Research*⁶ and Chapter 4 is in preparation for submission⁷.

⁵Mildner, T. C., Eden, C. and Nürnberg, D.: Impact of Last Glacial Maximum wind stress and reduced sea level during the deglaciation on the Loop Current in the Gulf of Mexico, *Paleoceanography*, submitted.

⁶Mildner, T. C., Eden, C. and Czeschel, L.: Florida Straits transport variability driven by Loop Current eddy shedding, *JGR*, submitted.

⁷Mildner, T. C., Eden, C., Czeschel, L. and Nürnberg, D.: The Gulf Stream position during the LGM, *GRL*, in preparation

2 Revisiting the relationship between Loop Current rings and Florida Current transport variability

T. C. Mildner¹, C. Eden¹ and L. Czeschel¹

This chapter is under review in the 'Journal of Geophysical Research - Oceans'.

¹ KlimaCampus, Institut für Meereskunde, Bundesstr. 53, 20146 Hamburg, Germany.

2.1 Abstract

It is suggested that internal variability plays a significant role in Florida Current (FC) transport variability on monthly to decadal time scales. A clear relationship is found between different stages within a ring shedding cycle of the Loop Current (LC) in the Gulf of Mexico and minima in the FC transport, both in observations and in meso-scale eddy-permitting ocean model simulations. Differences (and changes) between the ring shedding period and seasonal cycle lead to an interannual to decadal beat frequency, which explains large parts of the variability of the FC transport in the model simulations, even exceeding atmospheric forcing variability on the considered time scales. Model simulations without ring shedding produce significantly less variability in FC transport. Simulations without interannual variability in the surface forcing show almost as large (or even larger) interannual FC transport changes as without forcing variability.

2.2 Introduction

In this study the Loop Current variability in relation to a reduced Yucatan and Florida Straits transport at times, where the LC is about to shed a ring, is investigated. Fig. 2.1 shows the observed monthly mean time series of FC transport from 1982 to 2005, based on cable voltage measurements between Florida and the Bahamas (Baringer et al., 2001).

Experiment	mean FC transport	σ monthly	σ annual
Cable	32.07	2.52	1.17
LOW	23.93	3.05	1.26
LOW-ncep	24.23	3.39	1.58
LOW-noeddy-ncep	28.90	1.30	0.62
HI	20.38	2.38	1.08
HI-ncep	22.39	2.29	0.81

Table 2.1: Mean volume transports between Florida and the Bahamas (79.2°W; 25.5°N) in the observations and the model experiments and standard deviations of the monthly and annual means. All values are given in Sv.

The mean transport calculated from these measurements is close to 32 Sv (1 Sv = 10⁶ m³/s). Already a subjective visual inspection of the FC transport time series indicates significant variability on time scales from months to decades. A statistical analysis (Peng et al., 2009; Meinen et al., 2010) indicates a slightly red spectrum with no significant maxima or minima. In particular, no clear seasonal cycle can be found, hence the mean seasonal cycles calculated from different periods of the time series differ substantially

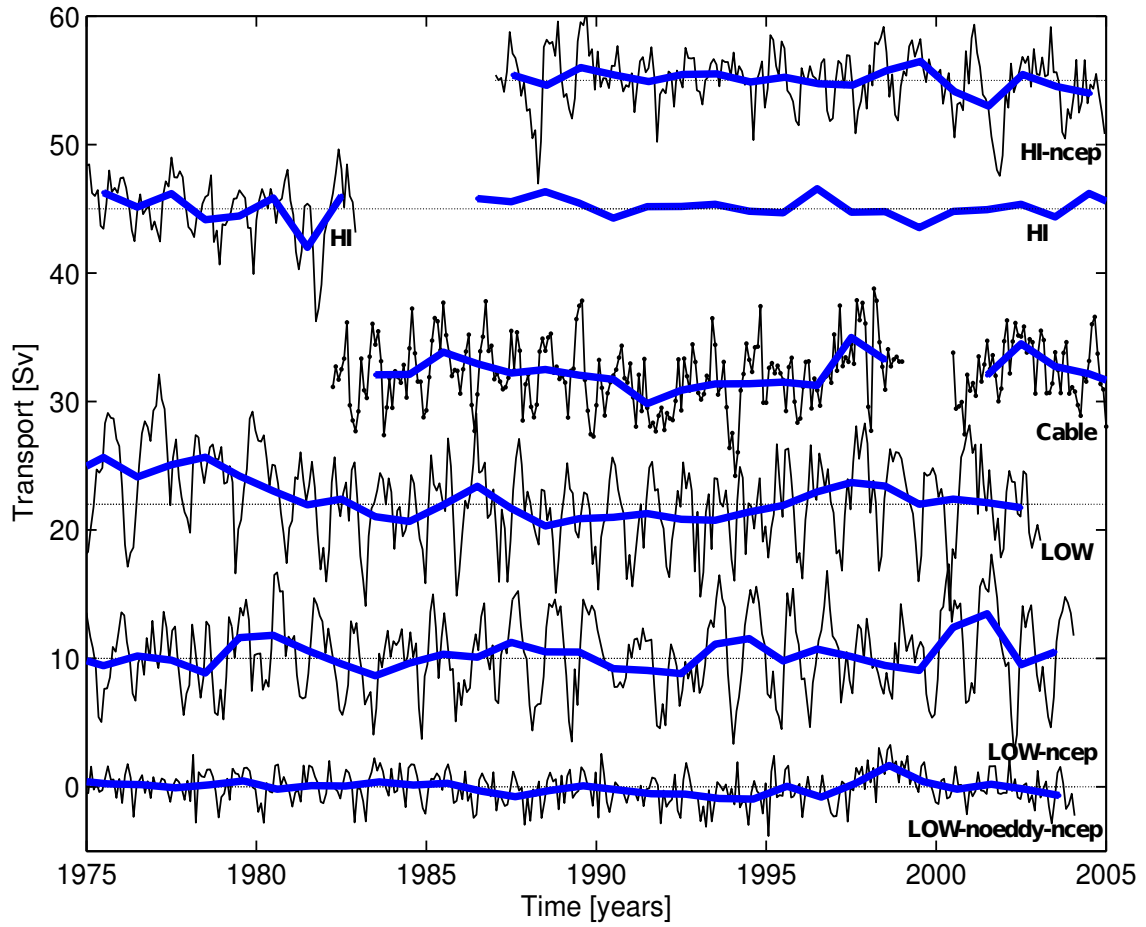


Figure 2.1: Time series of volume transport between Florida and the Bahamas (79.2°W at 25.5°N) from observations (Cable) and model simulations (HI, HI-ncep, LOW, LOW-ncep, LOW-noeddy-ncep). Blue lines denote annual averages, black lines monthly averages. Note that except for Cable, arbitrary mean transports have been added to the time series in order to shift them vertically. The dashed black lines denote zero means for each experiment, respectively. Mean transports in the model simulations are listed in Table 2.1.

(Baringer et al., 2001; Sturges et al., 2005; Meinen et al., 2010). In fact, the systematic seasonal cycle related to the atmospheric forcing – essentially given by the wind forcing – was shown by Czeschel et al. (2011) using an adjoint model approach to be much smaller than the observed variability of the FC transport.

Moreover, the observed FC transport shows significant interannual to decadal variations. These changes have been related to atmospheric forcing on corresponding time scales, in particular to the North Atlantic Oscillation (e.g. Baringer et al., 2001; Meinen et al., 2010). DiNezio et al. (2009) also suggest that a substantial fraction of the Florida Current transport variability at periods of 3 to 12 years might be driven by low-frequency variability in wind stress curl over the North Atlantic. On the other hand, Atkinson et al. (2010) find that variability on timescales >60 days cannot be significantly connected to the North Atlantic wind field. Meinen et al. (2010) find that the long-term relationship is only sporadic, e.g. it does not hold for the period 1970 to 2000.

In this study, we argue that a large part of the interannual to decadal fluctuations in FC transport is internally driven by the seemingly chaotic behavior of the Loop Current ring shedding in the Gulf of Mexico. Although clearly of fundamental importance, the dynamics and mechanism leading to a shedding of a ring from the Loop Current is still not fully understood yet. Recent studies suggest that the Loop Current system may behave with some regularity forced by the biannually-varying trade winds [e.g. Chang and Oey (2012)]. However in the following we consider the Loop Current variability and the ring shedding process as internally driven, while the precise understanding of the ring shedding process is beyond the scope of our study

Using a regional model of the western subtropical North Atlantic, Lin et al. (2009) demonstrated that ring shedding of the Loop Current is related to transport minima through Yucatan Channel and Florida Straits. A substantial fraction of the FC transport variability driven by internal ocean dynamics in a model simulation was also reported by Atkinson et al. (2010). In this study we find similar to Lin et al. (2009) a relationship between ring-shedding and FC transport changes in a variety of model simulations and demonstrate its significance for interannual to decadal variability of FC transport.

2.3 Model and data

We are using monthly mean Sea Surface Height (SSH) satellite altimeter observations (AVISO, <http://www.aviso.oceanobs.com>) and estimates of monthly mean FC transports based on cable voltage measurements between Florida and the Bahamas (Baringer et al.,

2001). In addition, we are discussing meso-scale eddy-permitting numerical models simulations, at high ($1/12^\circ \cos \phi$, where ϕ denotes latitude) and low resolution ($1/3^\circ \cos \phi$). All models are members of the Family of Linked Atlantic Model Experiments, covering the North Atlantic from 20°S to 70°N with 45 vertical levels. The regional models are described in detail in e.g. Eden and Böning (2002) and in Eden and Dietze (2009). The high-resolution regional model experiments are either climatologically forced using a Haney-type formulation by Barnier et al. (1995) (experiment HI), or monthly mean anomalies of wind stress, surface heat flux and friction velocity for the mixed layer closure are added to the climatological forcing (HI-ncep). The surface forcing anomalies are taken from the NCEP/NCAR reanalysis data (Kalnay et al., 1996) for the period 1988 - 2005 (note that, although observations to 2012 are available, we do not expect the model versus observations comparison to change significantly neither qualitatively nor quantitatively after 2005).

While in HI the scheme for vertical diffusivity by Gaspar et al. (1990) is used, in HI-ncep the scheme by Kraus and Turner (1967) and also additionally isopycnal diffusivity is used. These small differences in the model configuration are assumed as minor without significant impact on the model results discussed here. The low resolution models (LOW and LOW-ncep) use the forcing as in HI and HI-ncep and are identical otherwise. All models permit meso-scale eddy activity, except for an additional simulation at $1/3^\circ \cos \phi$ resolution (LOW-noeddy-ncep) in which we inhibit this variability by adding eddy-driven velocities to the tracer advection following Gent and McWilliams (1990) with an isopycnal thickness diffusivity of $2000 \text{ m}^2/\text{s}$ and harmonic instead of biharmonic friction. Consequently, meso-scale eddy activity including Loop Current ring shedding is suppressed in LOW-noeddy-ncep. LOW-ncep and LOW-noeddy-ncep are integrated from 1975 to 2005. All model simulations shown here are preceded by a 10 year long spinup integration, in order to reach a quasi-dynamical equilibrium.

2.4 Results

Fig. 2.2 shows (negative) correlations of monthly mean SSH anomalies from the AVISO satellite data and observed FC transport variability (1992-2010) at different lags (data available from www.aoml.noaa.gov/phod/floridacurrent/).

At negative lags (Fig. 2.2a-d), i.e. before a minimum in FC transport, the Loop Current begins to extend more and more into the Gulf of Mexico and after the separation (which occurs between lag 0 (Fig. 2.2e) and lag 1 (Fig. 2.2f)) the ring heads towards

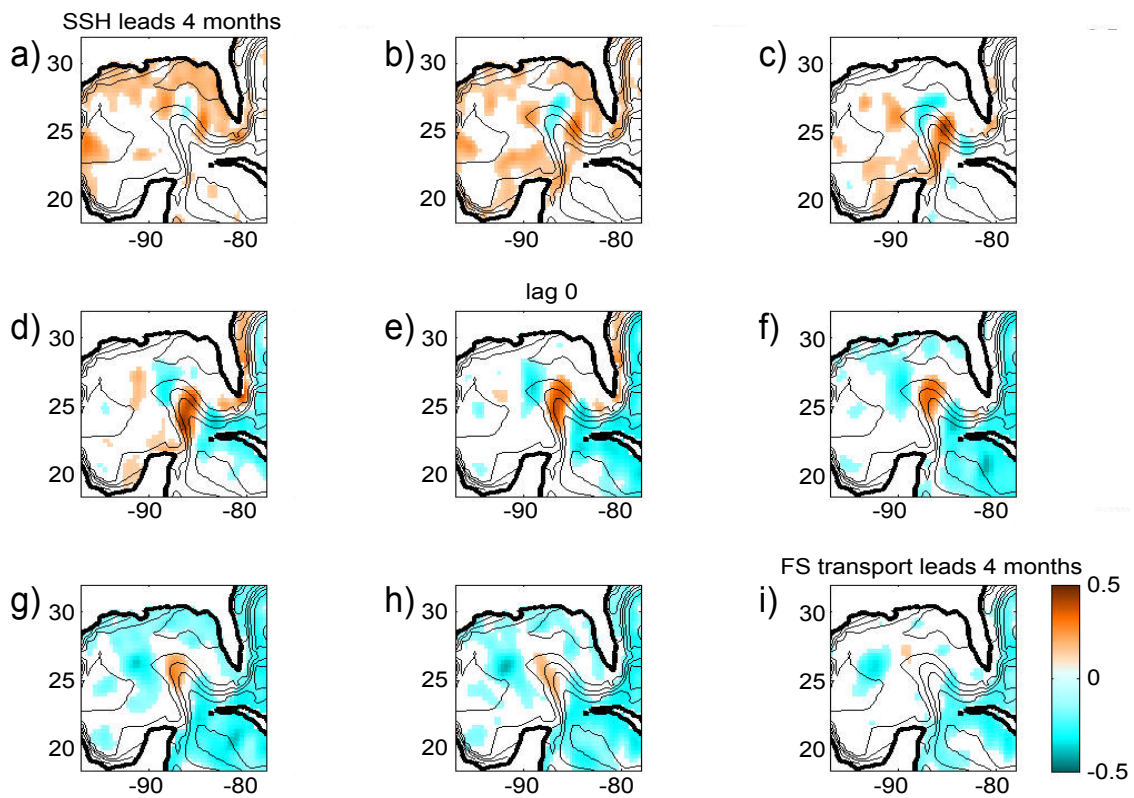


Figure 2.2: Lagged (negative) correlation of observed monthly mean SSH and FC transport anomalies (1992-2010). Note that negative correlation coefficients are shown to indicate the relation between positive SSH anomalies and FC transport minima. Correlations are shaded only when they are significantly different from zero with a likelihood of 95%. Also shown is the mean SSH taken from Niiler et al. (2003) as thin lines (contour distance of 10 cm) and the coastlines as thick lines.

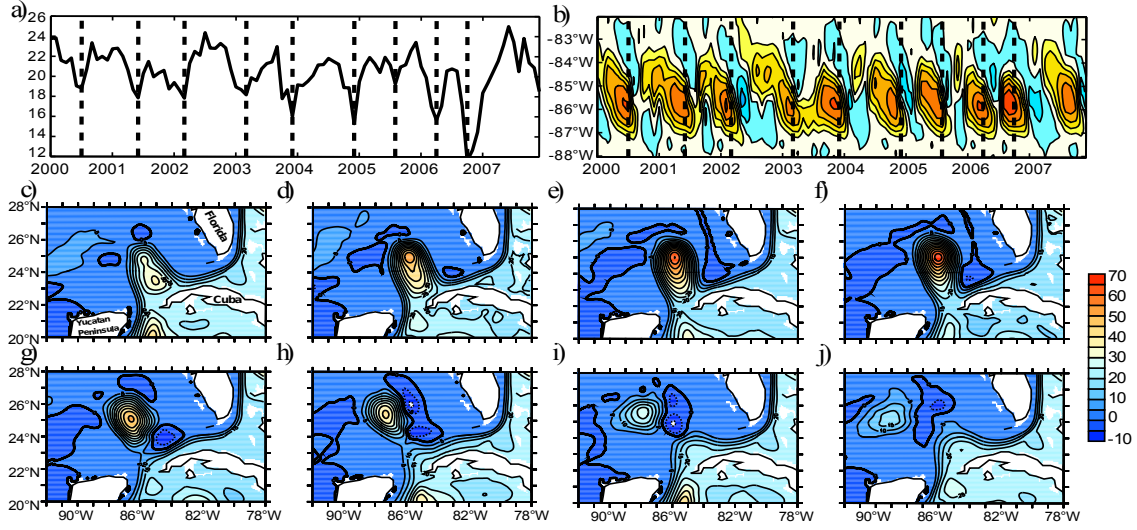


Figure 2.3: a) Transport between Florida and Bahamas at 25.5°N in HI (in Sv). b) Monthly mean volume transport (in Sv) in HI at 24°N in the Gulf of Mexico. c)-j) Composites of monthly mean streamfunction (in Sv) and FC transport minima as indicated in a) and b) by solid dashed lines in HI for lags -3 to 0 (c-f) and lags 1 to 4 months (g-j, FC leads). In the 8 year long time series, we found 9 minima of FC transport and corresponding ring shedding. Contour interval is 5 Sv.

the north/north-west (Fig. 2.2f-i). Note that the colors only display lags and leads where the correlation is above the significance level (i.e. significantly different from zero at the 95% level). Also shown (as contour lines) in the figure is the mean sea level (Niiler et al., 2003). At lag 0 (Fig. 2.2e), there is a significant correlation of about 0.3 between FC transport minima and reduced SSH gradient across the Florida Straits, in agreement to reduced local surface geostrophic flow measured by the satellite altimeter. In addition, however, significant correlations of similar or larger magnitudes show up within the Loop Current ring shedding region: A positive SSH anomaly in this region is related to FC transport minima and indicates an ongoing ring shedding. Even larger correlations in the ring shedding region can be seen when SSH leads the FC transport by one month (Fig. 2.2d). This points to a possible blocking situation in the Yucatan Channel before the LC ring detaches from the main current (as discussed below). Further, a westward propagation of the positive SSH anomaly in the ring shedding region at lag zero, can be seen going from lags where SSH leads to zero lag (Fig. 2.2a-e), and to lags where the FC transports leads (Fig. 2.2f-i). This propagation is also indicative of a ring shedding process. The observations thus suggest a relation between ring shedding and FC transport variability, as previously noted by Lin et al. (2010). The relation can be seen more clearly in the model simulations: Fig. 2.3c-j show composites of monthly mean streamfunction of the depth-integrated flow leading (c-f) and lagging (g-j) the FC transport minima in an 8 year long time series (shown in Fig. 2.3a+b) of the high-resolution model simulation HI.

Altogether 9 minima were identified in the FC transport – indicated by the dashed vertical lines in Fig. 3a and b – which are all related to a ring shedding process. Further, the composite of the streamfunction shows a similar shedding and westward propagation as indicated in Fig. 2.1. In HI-ncep we also find transport minima in FC whenever a ring is about to shed from the Loop Current (not shown).

The ring shedding process in the model simulations HI and HI-ncep shares many features with the observed ring shedding (Leben, 2005; Sturges et al., 2000), insofar that it is irregular with periods of individual shedding events between 6 and about 17 months with a mean period close to 12 months. On the other hand, ring shedding in LOW has a mean period of 13 month and appears too regular. The reason might be the missing smaller scale cyclonic eddy activity, which often surrounds the ring and might influence its shedding (Schmitz, 2005). These smaller scale eddies are largely unresolved in LOW but present in HI, which might therefore be more realistic compared to observations in its more chaotic ring shedding process.

A further model bias is given by the too low mean FC transport compared to observations (about 32 Sv, Table 2.1). A trend can be seen in the FC transport during the spinup phase of each of the models, showing higher transports in the first years of the model simulations (not shown). Mean FC transports after the spinup phase are 23.93 and 24.23 Sv for experiments LOW and LOW-ncep, respectively, while in HI and HI-ncep we find even lower values of 20.38 and 22.39 Sv, respectively. Smith et al. (2000) also report a FC transport of only 24.9 Sv in their regional eddy-permitting model. This low bias has not been resolved in more recent global versions of that model (A. Griesel, pers. comm), and thus appears to be a common problem of basin-wide eddy-permitting models. Note that the strength of the mean MOC (Meridional Overturning Circulation) in HI and LOW is in the range of standard model solutions (Eden and Böning, 2002; Smith et al., 2000) and also to what observations suggest (Xu et al., 2012). Further, the interannual variability of the mid-latitude MOC in HI-ncep and LOW-ncep is also in the range of previous model solutions. Sensitivity experiments with LOW and HI using different topography (i.e. changes in depth and width of Windward Passage, etc.), different surface and lateral boundary formulations, and different wind stress products do not show any improvement of the Florida Currents’ low bias in Sv transport. However, we assume here that the low bias in the simulated FC transport does not affect significantly the FC transport variability in the model simulations, which is the focus of the present study.

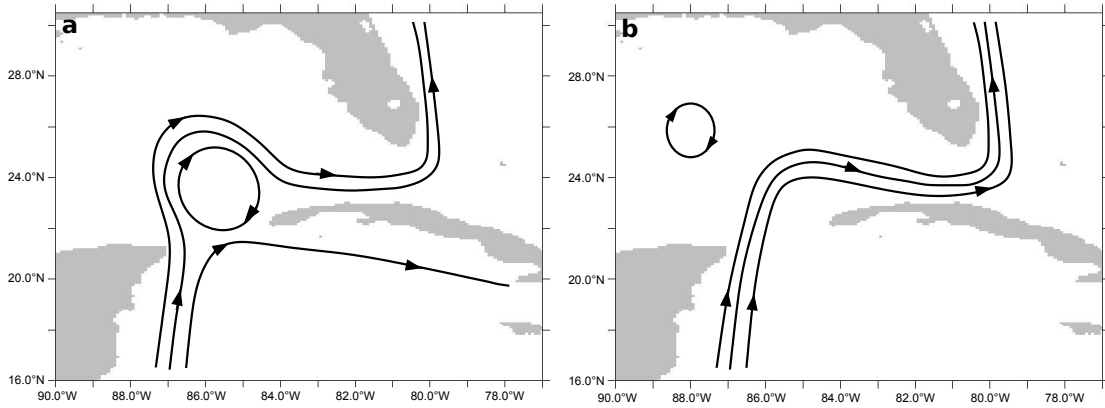


Figure 2.4: Two stages of LC ring shedding cycle. (a) shows a blocking situation in Yucatan Strait. (b) release of blocking together with ring shedding

2.4.1 Mechanism

Loop Current rings are characterized by positive SSH anomalies, i.e. the Loop Current loses volume after detachment of a ring, which might explain the minimum of the FC transport. However a typical ring with a radius of 300 km and a SSH anomaly of 30 cm would result in a negative transport anomaly of only 0.1 Sv for 10 days, i.e. much less than the FC transport anomalies found in the models. Furthermore all model experiments discussed here use a rigid lid formulation and the mechanism described above is absent in these experiments. A companion experiment using a free-surface formulation shows nearly identical results (not shown) so that the loss of volume by the Loop Current rings can not explain the accompanied transport minima of $\sim 4\text{-}8$ Sv in the FC transport (Fig. 3a).

We here suggest a simple mechanism following the idea of atmospheric blocking. The basic mechanism is sketched schematically in Fig. 2.4 showing the streamlines before (a) and after (b) a ring sheds from the Loop Current.

In a) a strong coherent ring is embedded within the Loop Current forcing the streamlines to go round it. As this blocking takes place in the relatively narrow Yucatan Strait some of the transport is forced to flow south of Cuba. The signal of the resulting transport minimum in Yucatan Strait is then propagating through the Florida Straits by fast barotropic waves leading to a high correlation between Yucatan Strait and FC transport. The situation changes when the Loop current expands further northwards which is typically the case during a ring shedding process, such that the embedded coherent ring no longer blocks the inflow into the Gulf of Mexico. A northward intrusion of the Loop Current into the Gulf of Mexico is usually accompanied by a ring shedding (Fig. 2.4b) but the exact timing of the shedding is not critical for the observed increase in the transport

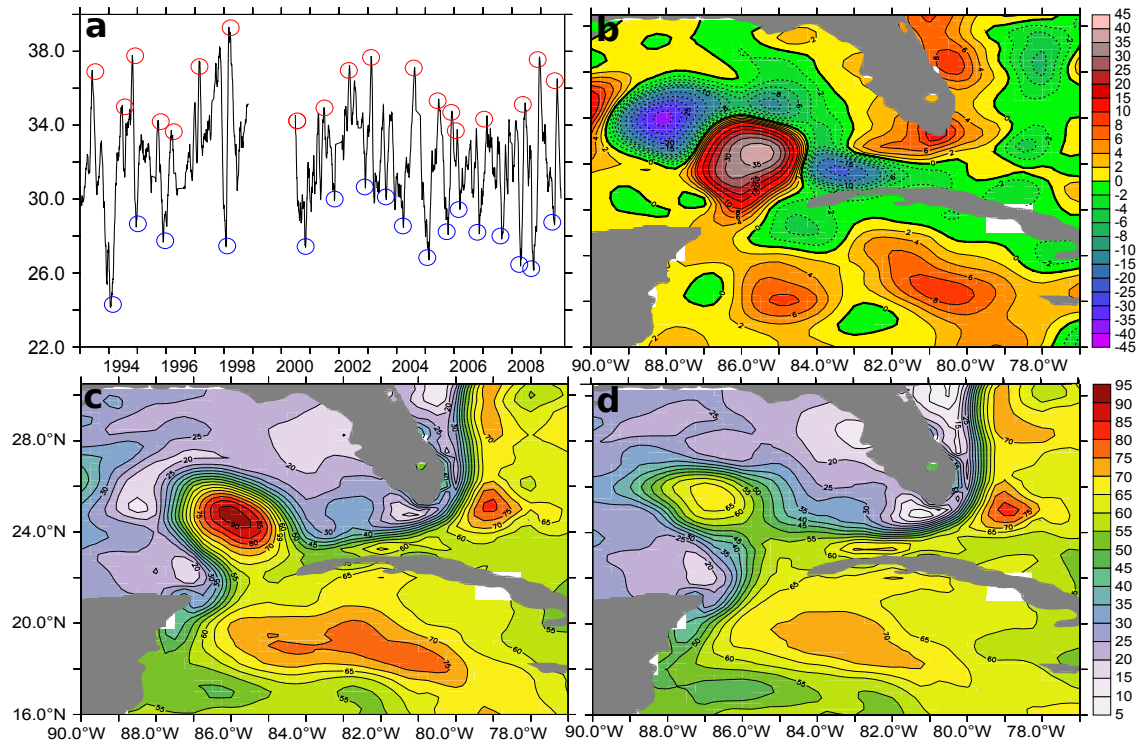


Figure 2.5: a) Maxima (red circles) and minima (blue circles) in Florida Straits cable derived transport in Sv, b) a composite of SSH (in cm) derived from AVISO satellite data for all the marked minima minus maxima in Florida Straits cable derived transport, c) composite of all minima in the cable transport (blocking situation shortly before a ring is shed), and d) composite of all maxima in the cable transport (after or during a ring detachment).

through the Yucatan and Florida Straits, since the ring might reattach again to the Loop Current.

The described mechanism is apparently evident in all our model runs (see e.g. Fig. 2.3(c-f) for the blocked and Fig. 2.3(g-j) for the unblocked throughflow). Observations further support our hypothesis: Fig. 2.5a shows the 15-day running mean filtered FC transport (in Sv) derived from the cable measurements.

Marked are the maxima (red circles) and minima (blue circles) in the transport. Fig. 2.5c and d show composites of the SSH from weekly AVISO satellite data calculated for minima and maxima in the cable transport, respectively. Fig. 2.5c represents the blocking situation with a strong anti-cyclonic ring just north of Yucatan Strait leading to southward flow on the eastern side of Yucatan Strait. Fig. 2.5d shows the situation where the ring has cleared the way and moved to the north/west. The maximum values in the FC transport are usually reached when the ring has shed from the Loop Current, but often the ring is still attached or is reattaching again to the Loop Current. Fig. 2.5b gives

the difference between both situations. The corresponding geostrophic surface currents show a southward anomaly east of Florida and in the Yucatan Strait, indicating reduced transport. In the Caribbean south of Cuba we have anomalous eastward flow similar to the blocking situation sketched in Fig. 2.4a.

2.5 Discussion

In agreement to Lin et al. (2009), we found a clear relation between the Loop Current evolution and FC transport minima both in model solutions and observations. They suggest a bottom form drag mechanism to explain this relation, i.e. the density and resulting bottom pressure anomalies during the Loop Current evolution act in concert with the variable bottom topography between Cuba and Florida to reduce the FC transport. Here we suggest a simpler mechanism focusing on the pronounced minima seen in the FC transport: A coherent ring just north of the relatively narrow Yucatan Strait and embedded in the Loop Current partly blocks the inflow into the Gulf of Mexico. The blocking situation occasionally holds up for several months (see Fig. 2.3) causing an anomalous FC transport. The low transport through the Yucatan Strait might be partly compensated by a counter clock-wise flow around Cuba and an increased flow through the Old Bahama Channel (Lin et al., 2009).

As the Loop Current grows and intrudes further into the Gulf of Mexico the embedded ring moves to the north and releases the blocking. The transport through Yucatan and Florida Straits increases whereas the ring is perhaps still attached to the Loop Current but is now more likely to shed. On the other hand, the actual ring detachment and a possible reattachment modulates the transport through the straits only slightly compared to the blocking mechanism. The mechanism controlling the ring separation frequency is still under debate but is often related to the mass and/or vorticity flux through Yucatan Strait (e.g. Pichevin et al., 1997; Candela et al., 2002) which is partly controlled by the local wind (Chang and Oey, 2010, 2012). Here we want to point out that the development of the ring itself has a feedback on the mass and vorticity flux through the Yucatan Strait. Additionally there might be trigger events supporting the ring shedding process. Sturges et al. (2010) find a pulse of increased FC transport approximately 20 days before ring separation. Oey and Chang (2011) state that several model studies show that such a downstream trigger is not necessary for a ring to separate and hold the view that more cautious investigations are necessary.

The internally driven ring shedding leads to interannual changes in FC transport because

it is irregular but has a mean period close to but not identical to the seasonal cycle, which can be seen both in the observations and the eddying model simulations. Adding seasonal cycle and the mean period of ring shedding leads to a beat period of the FC transport changes on interannual to decadal scale (a ring shedding period of e.g. 11, 10 or 9 months would generate a beat period of 11, 5, or 3 years, respectively). The idea of the beat frequency was first postulated by Sturges et al. (2000). They speculated that a lack of power at 12 months might be caused by a beat-frequency effect and that the power at a lower frequency modulates the power at the annual period.

Experiment HI shown in Fig. 2.1 and 2.3 is climatologically forced, which means that the atmospheric forcing is the same in each year (but monthly varying), such that any kind of variability in the FC transport, except for the seasonal cycle, is driven by internal ocean dynamics, i.e. the ring shedding. The beat period leads to considerable interannual to decadal variation in the FC transport with magnitudes on the order of the variability in the cable data (see also Tab. 2.1). Fig. 2.1 also shows the monthly mean FC transport times series in LOW and LOW-ncep. In LOW-ncep interannual variability is not much larger compared to the climatologically forced experiment LOW: standard deviation of annual (monthly) means of FC transport are 1.26 Sv (3.05) and 1.58 Sv (3.39) in LOW and LOW-ncep, respectively (Tab. 2.1). In LOW and LOW-ncep fluctuations are too regular due to the missing smaller scale cyclonic eddy activity during eddy-shedding. However, in HI, and HI-ncep fluctuations are irregular and in much better agreement with observations. Annual (monthly) mean standard deviations are here of similar magnitude – in fact even higher – in HI compared to HI-ncep. The higher variability in HI might be related to the small differences in vertical and lateral mixing parameterizations between the model setups, or to exceptionally high variability in HI simply for statistical reasons. We conclude that most of the interannual variability in FC transport in the eddying models LOW-ncep and HI-ncep can be caused by internal dynamics of the ocean, related to the ring shedding. Adding interannual changes in the surface forcing, lead to an increase of only 10% of the total FC transport variability in LOW-ncep compared to LOW.

On the other hand, the relative amount of atmospherically forced variability in FC transport can also be quantified using the simulation LOW-noeddy-ncep, showing indeed much smaller interannual variability. Note, however, that westward propagating eddies from the interior, which might also influence western boundary currents (Kanzow et al., 2009), are also missing in LOW-noeddy-ncep. The standard deviation in LOW-noeddy-ncep of annual (monthly) means of 0.62 Sv (1.30), amounts to only 39% of the variability in the eddying model LOW-ncep.

Based on our model simulations, AVISO satellite observations and FC cable derived transport, we attribute the variability in FC transport changes to a large extent to internal variability, i.e. to the ring shedding, and not to the direct effect of interannually changing surface forcing. On the other hand, possible important events which trigger or delay ring shedding (Sturges et al., 2010; Chang and Oey, 2010) can be attributed to surface forcing and might explain the previously reported correlations between wind stress and FC transport (Baringer et al., 2001; DiNezio et al., 2009; Peng et al., 2009). However, this correlation shows up only sporadically as shown by Meinen et al. (2010).

In the models we found a very close relation between ring shedding and FC transport changes. In contrast, the correlations between observed monthly mean SSH anomalies and cable transport data in Fig. 2.2 although significant are lower, i.e. at maximum only 0.4. It appears that it is either not possible to transfer the model results to the real ocean because of missing processes or model biases, or the noise in the observational estimates hampers the statistical analysis. We are not able to answer this question, but note that the correlation between FC transport and SSH gradients from the Bahama Islands to Florida, i.e. the geostrophic relation, is even weaker than the correlation with ring shedding. A detailed discussion about the difficulties of obtaining transport estimates from satellite SSH data over sloping topography near the boundaries is given in Kanzow et al. (2009). Note also that variance on sub-monthly time scales dominates FC transport variance (Meinen et al., 2010), which is not present in the model simulations which are driven by monthly mean surface forcing. We assume that variability at time scales shorter than a month does not affect the seasonal to interannual variability.

3 Impact of Last Glacial Maximum wind stress and lowered sea level during the deglaciation on the Loop Current in the Gulf of Mexico

T. C. Mildner¹, C. Eden¹ and D. Nürnberg²

This chapter is under review in the AGU Journal 'Paleoceanography'.

¹ KlimaCampus, Institut für Meereskunde, Bundesstr. 53, 20146 Hamburg, Germany.

² GEOMAR Helmholtz Centre for Ocean Research Kiel, Wischhofstr. 1-3, 24148 Kiel, Germany.

3.1 Abstract

The role of wind stress and sea level changes across the deglaciation and their impact on transports and on the eddy-shedding dynamics of the Loop Current in the Gulf of Mexico are discussed. We use an eddy-permitting regional model of the North Atlantic, driven by changes in wind stress as given by the PMIP 2 database and at different scenarios of lowered sea level. Last Glacial Maximum (LGM) wind stress leads to a stronger Yucatan Channel and Florida Straits transport, due to the equatorward shift of the Intertropical Convergence Zone, a stronger meridional gradient in zonal wind above the Subtropical Gyre and thus, to an increase in the Sverdrup transport of the Subtropical Gyre in the North Atlantic. The lowered sea level during the LGM tends to reduce eddy-shedding, which comes along with a reduced oceanic heat transport into the Gulf of Mexico. Increased transport between Cuba and Florida and Yucatan Strait transport also tend to decrease eddy shedding. According to our results we propose that during LGM, the Loop Current eddy-shedding was most likely absent and heat transport into the Gulf of Mexico reduced.

3.2 Introduction

Ocean heat transport from the equatorial regions to high latitudes is a critical component to the global climate system. The current circulation system in the Gulf of Mexico features large transports flowing through the Yucatan Channel (YC) as the Yucatan Current. Most prominent in the Atlantic Ocean, in this respect, is the Yucatan Current flowing northward into the Gulf of Mexico and changing into the Florida Current (FC). When bending eastward, meso-scale eddies shed on an irregular basis into the Gulf transporting oceanic heat into the northern Gulf as the Loop Current (LC). This circulation system is the initial part of the large-scale western boundary current system of the North Atlantic. In addition to being a component of the wind-driven gyre, the LC is also a component of the pathway for the warm-water return flow of the global meridional overturning circulation (MOC).

Motivation to model the dynamics of the circulation in the Gulf of Mexico during the last 25 kyr are the paleorecords of high salinity and temperature variability differing between the Gulf and the Caribbean. Fig. 3.1 shows the sea surface temperatures (SST)

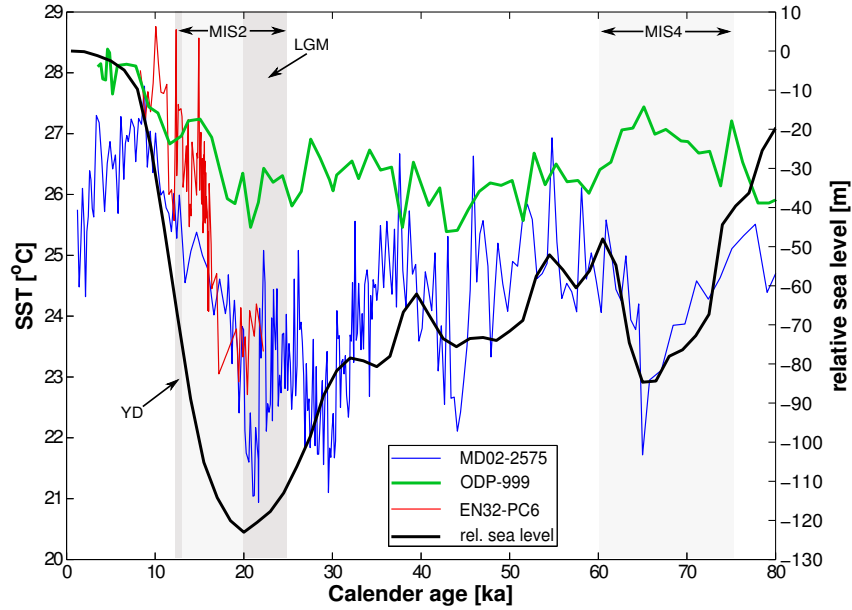


Figure 3.1: Sea surface temperatures reconstructed from marine sediment core MD02-2575 (blue) from De Soto Canyon (Nürnberg et al., 2008), EN32-PC6 (red) from Orca Basin (Flower et al., 2004) and from ODP-999 (green) from Columbia Basin (Schmidt et al., 2004) (see also Fig. 3.2 for core locations) overlain by the relative sea level curve after Waelbroeck et al. (2002) for the last 80 kyr. Grey shaded are the even marine isotope stages (MIS) representing cold glacial periods and in dark grey the Younger Dryas (YD) and the Last Glacial Maximum (LGM).

reconstructed for the last 80 kyr from marine sediment cores at different locations in the Gulf and in the Caribbean Sea: MD02-2575 (Nürnberg et al., 2008) from the De Soto Canyon (north-east Gulf), EN32-PC6 (Flower et al., 2004) from Orca Basin (northern Gulf) and ODP Site 999 (Schmidt et al., 2004) from the Columbia Basin. For comparison the relative sea level curve of Waelbroeck et al. (2002) is shown. Positions of the sediment cores are indicated in Fig. 3.2. The reconstructed SST within the Gulf (De Soto Canyon and Orca Basin) shows much larger variability and a much larger increase during the deglaciation than the Caribbean SST record (ODP Site 999). It is likely that the large variability is related to changes in the circulation system of the Gulf of Mexico. We here hypothesize that Loop Current eddy-shedding in YC plays a dominant role in influencing SST and sea surface salinity (SSS) patterns in the Gulf of Mexico. At times of high (low) eddy-shedding, the heat and freshwater transports into the central Gulf of Mexico were enhanced (lowered), which might explain the large changes in surface ocean properties in the Gulf during the deglaciation.

The YC has been monitored since the 1970's. Transport estimates by Schlitz (PhD thesis, 1973) range from 23 Sverdrup ($1 \text{ Sv} = 10^6 \text{ m}^3/\text{s}$) to 33 Sv (Ochoa et al., 2001), while Johns et al. (2002) report a transport of 28.5 Sv. During the CANEK program, moorings

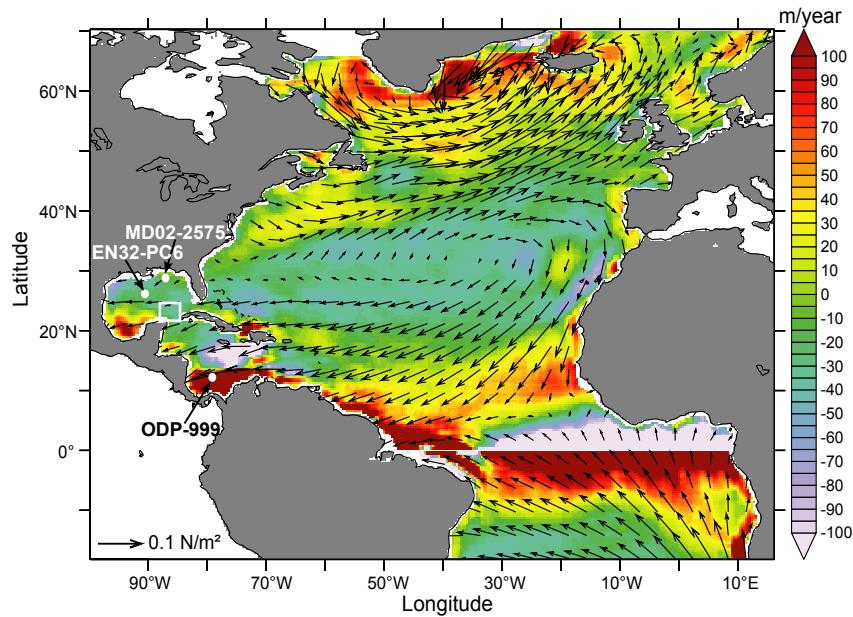


Figure 3.2: Wind stress for CONTROL (arrows, in N/m^2) and Ekman transport in m/year (see legend). Positive values denote Ekman suction, while negative values denote Ekman pumping. Note that the Ekman transport cannot be calculated within $\sim 5^\circ$ of the equator. Also shown are the marine sediment core locations mentioned in Fig. 3.1. The white square marks the area considered for the velocity calculations shown in Fig. 3.5.

with Acoustic Doppler Current Profilers (ADCPs) and thermometers were deployed across the YC from 1999 to 2001 revealing a mean transport of 23.1 Sv (Candela et al., 2003). Between May 2001 and May 2006 Rousset and Beal (2010) used ADCPs for transport estimates of the Yucatan Current. They found a mean transport between 28.2 Sv and 33.6 Sv.

The FC has been monitored since the late 1960s and almost continuously since the early 1980s. The transport measured in mooring arrays by Schott et al. (1988) revealed a mean transport of 30.5 Sv, while transport calculated from marine cable measurements exhibits a long term mean transport of 32.3 Sv (Baringer et al., 2001). Mean Florida Straits (FS) transport calculated from transects from the 1960s by Schmitz Jr and Richardson (1968) are in the range of the cable derived mean transport.

The modern LC connecting the Caribbean with the Gulf of Mexico and Florida Straits has been in the focus of various studies (e.g. Chérubin et al., 2006; Nof and Pichevin, 2001; Sturges, 1992) but not much is known about its behavior during the past, in particular during cool climate stages when sea level was drastically lower than today. Today, the LC sheds meso-scale eddies on an irregular basis and with an anticyclonic pattern (warm core rings (WCR)). The separation is defined as the final detachment of a ring-like eddy

shed from the LC with no later reattachment. These WCR can have diameters ranging between ~ 100 up to 300 km (Vukovich and Maul, 1985) and a depth signature of up to 1,000 m. The average diameter is ~ 180 km (Elliott, 1982; Hamilton et al, 2002). These eddies propagate westwards at speeds of $\sim 2 - 5$ km day $^{-1}$ (Coats, 1992; Elliott, 1982) and supply heat to the inner part of the Gulf. Hamilton and Lee (2005) found similar zonal propagation speed ranging from 3 to 6 km day $^{-1}$ whereas their swirl velocities amount to 100 – 150 cm/s. The formation of cold core cyclones in the surrounding area of the separating LC ring is also observed and was described by (e.g. Cochrane, 1972; Vukovich and Maul, 1985; Chérubin et al., 2006). Eddy-separation periods are highly variable ranging between 3 and 18 months (Leben, 2005). The average shedding period in observations is 11 months. Although the seasonal dependence is not clear, observations from satellite data combined with *in situ* and ship measurements between 1974 and 2010 by Chang and Oey (2012) show a high frequency of ring separation in March while during December no separation of rings was observed.

Being part of the basin-scale gyre circulation of the subtropical North Atlantic, the circulation system in the Gulf of Mexico including the eddy-shedding process is governed by the wind stress over the North Atlantic. Little is known about wind stress changes during the LGM, but the large air temperature oscillations first observed in the oxygen isotopic composition ($\delta^{18}\text{O}$) of Greenland ice cores reflect massive reorganizations of the atmosphere/ocean system during the last glacial period (Bond et al., 1993). Climate in the tropical North Atlantic is mainly controlled by variations in the strength of the trade winds, the position of the Intertropical Convergence Zone (ITCZ), and sea surface temperatures.

The ITCZ marks the boundary where north and south trade winds confluence. It regulates the hydrological cycle over the tropical continents and interacts tightly with the tropical oceans. The north-south position of the ITCZ nowadays has its northern maximum position in January while it reaches its southernmost position in July. A southward displacement of the ITCZ and the Polar Front during the LGM is attributed to the large continental ice sheet induced cooling of the Northern Hemisphere going along with modifications in the westerly wind field. Evidence for the southward shift of the Polar Front can be found in Kuhlemann et al. (2008). The variability of the ITCZ during the past 30 kyr was estimated by using oxygen isotope and foraminiferal Mg/Ca paleothermometry techniques by (Koutavas et al., 2005). As an indicator for the front of the ITCZ the authors use the intensity of the cold tongue, which is seasonally appearing in the equatorial Atlantic. They suggest that during the LGM a weaker cold tongue-ITCZ front prevailed, indicating a more southerly ITCZ at that time. The position can further be

inferred either from the color or the mineralogy of the marine sediments from Cariaco Basin to reconstruct the rainfall intensity (Haug et al., 2001; Lea et al., 2003; Peterson et al., 2000; Wang et al., 2004). Results from foraminiferal Mg/Ca ratios and the gray-scale records by (Lea et al., 2003) seem to be in phase corroborating their estimation of the glacial/deglacial ITCZ position. There are also indications that the ITCZ shifted due to changes in the interhemispheric temperature contrast found in model experiments by Broccoli et al. (2006).

The key questions we want to address in this paper are as follows:

1. How did the oceanic circulation change in the Gulf of Mexico and adjacent seas during the transition from glacial to interglacial times?
2. How does the process of Loop Current eddy shedding affect the heat and salt budget and the surface circulation pattern of the Gulf?
3. What causes eddy shedding and why does it change through time?

In the following our modeling experiments will be described in detail including experiments at different sea level stands followed by experiments including glacial wind stress anomalies, and finally by experiments with a combination of lowered sea level and wind stress anomalies. The model results will be discussed in view of observational and modeling studies.

3.3 Modeling approach

We use an eddy-permitting ocean general circulation model of the Atlantic Ocean (FLAME, <http://www.ifm.zmaw.de/mitarbeiter/prof-dr-carsten-eden/numerical-models>) to assess the impact of sea level change on the dynamics of the Gulf of Mexico upper ocean circulation. The model is based on a revised version of Geophysical Fluid Dynamics Laboratory (GFDL) Modular Ocean Model 2 (MOM2; (Pacanowski, 1995)) and has been used to address various topics (e.g. Dengler et al., 2004; Eden et al., 2004). To resolve meso-scale processes such as the eddy-shedding in the Gulf of Mexico the model version used in the present study is based on a configuration for the Atlantic Ocean from 20°S to 70°N and 16°E to 100°W with 45 vertical levels (10 m thick at the surface increasing to 250 m starting from 2,300 m below sea level to the maximum depth of 5,500 m/bottom) and with a spatial resolution of $1/3^\circ \cos \phi$. All model experiments are forced using a Haney-type heat flux condition as given by Barnier et al. (1995). Atmospheric forcing is taken identical to the present day reference simulation also given by Barnier et al. (1995) and a restoring

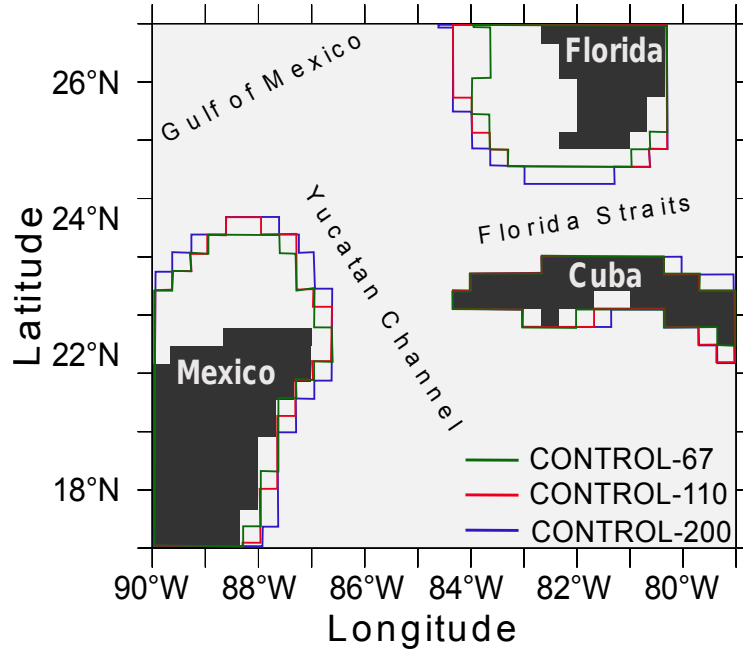


Figure 3.3: Topography changes for different sea level experiments compared to CONTROL (landmasses in black). The blue line marks the coastline for a lowered sea level by 200 m (CONTROL-200). The red line is for lowered sea level by 110 m (CONTROL-110). The CONTROL-67 scenario (green) implies a lowered sea level by 67 m. CONTROL-24 has the same coast line as CONTROL.

boundary condition for sea surface salinity, using the Antonov et al. (1998) climatology, which serves also as initial condition. Northern and southern margins of the domain are formulated as open boundaries after Stevens (1991). The temperature and salinity climatology are taken from Levitus and Boyer (1998). For further model details see the control run (prognostic) in Eden et al. (2004).

In a first set of experiments, we re-configure our CONTROL experiment of the FLAME model with different sea levels corresponding to the cold-glacial period LGM (approximately 21,000 yr BP (before present) and cold-deglacial period Younger Dryas (YD; lasted approximately 1300 years between 12,800 yr and 11,500 yr BP). For the period of the LGM the sea level was lowered by 110 m (CONTROL-110), for the YD it was lowered by 67 m (CONTROL-67), for the late Holocene it was lowered by 24 m (CONTROL-24), respectively, according to observational estimates from Barbados, the North Atlantic and New Jersey by Fairbanks (1989); Waelbroeck et al. (2002); Wright et al. (2009). In addition, a sensitivity test was performed by lowering the sea level by 200 m (CONTROL-200).

We have reduced the sea level in the model by eliminating the first 2, 6, 9 and 13 levels of the original vertical grid of 45 levels of the model, respectively (see also Fig. 3.3, shown are the different land marks for different sea level experiments). In all experiments we

allow for a dynamical quasi-steady equilibrium of the basin-wide circulation, which the model reaches after approximately 50 model years. Note that due to the restricted length of the integrations, the simulations are not in equilibrium with the thermohaline surface forcing and the water mass characteristics prescribed at the open boundaries. Further, we note that we do not have changed the thermohaline forcing in the model, i.e. it represents current climate. Therefore we do not aim to realistically simulate the response of the thermohaline circulation in our model simulation, but to focus on the response of the wind-driven, quasi-geostrophically balanced regional circulation in the Gulf of Mexico to the changes in sea level and wind stress.

We have performed experiments with LGM wind stress taken from the PMIP2 database (LGM-wind experiments). Available to us are results from the HadCM (HadCM3M2) (Gordon et al., 2000), CCSM (the National Center for Atmospheric Research CCSM3 model) (Otto-Bliesner et al., 2006), FGOALS (FGOALS-1.0g) (Yu et al., 2002), MIROC (the CCSR/NIES/FRCGC MIROC3.2.2 (medres)) (Hasumi and Emori, 2004) and the ECBILT (ECBilt/Louvain-la-Neuve CLIO intermediate complexity) (de Vries and Weber, 2005) model. All models in PMIP2 use the same boundary conditions namely ICE-5G (ice sheet) and topography described among others in L  n   et al. (2009) and online accessible from <http://www.pmip2.lsce.ipsl.fr>. They provide large continental ice sheets over North America and northern Eurasia. Forcings for PMIP2 models differ from present day insolation due to a difference in the Earth's orbit. Derived from the Greenland and Antarctic ice core records they included the changes in atmospheric carbon dioxide (185 ppmv - parts per million by volume) concentration, methane (350 ppbv - parts per billion by volume) and nitrous oxide (200 ppbv). Also these models are fully coupled atmosphere-ocean-ice models. We calculated anomalies of monthly mean wind stress from steady state model solutions for 21 kyr simulations minus present day control simulations of each PMIP model mentioned above and added this anomaly to our monthly varying forcing of CONTROL to create a new forcing for each experiment (altogether five with LGM-wind). These experiments can also be found in Tab. 3.1 named as follows: HadCM-wind, CCSM-wind, FGOALS-wind, MIROC-wind and ECBILT-wind.

As a further experiment we combined the wind stress anomalies with the lowered sea level. These experiments can be found in Tab. 3.1 named as follows: HadCM-wind-110, CCSM-wind-110, FGOALS-wind-110, MIROC-wind-110 and ECBILT-wind-110.

Model-experiment	forcing sea level -24m	forcing: sea level -67 m	forcing: sea level -110 m	forcing sea level -200 m	forcing: LGM wind anomalies	Eddy-shedding period [month] 1930 – 50	FS transport [Sv]	surface heat flux [PW]
ECBILT-wind	-	-	-	-	✓	9.3	20.83	-0.027
HadCM-wind	-	-	-	-	✓	-	31.44	-0.020
FGOALS-wind	-	-	-	-	✓	14.6	25.09	-0.029
MIROC-wind	-	-	-	-	✓	14.3	26.01	-0.032
CCSM-wind	-	-	-	-	✓	-	31.86	-0.026
ECBILT-wind-110	-	-	✓	-	✓	12.6	17.79	-0.018
HadCM-wind-110	-	-	✓	-	✓	-	30.48	-0.014
FGOALS-wind-110	-	-	✓	-	✓	-	23.11	-0.016
MIROC-wind-110	-	-	✓	-	✓	-	24.52	-0.018
CCSM-wind-110	-	-	✓	-	✓	-	31.09	-0.017
CONTROL	-	-	-	-	-	13.2	23.32	-0.025
CONTROL-24	✓	-	-	-	-	17.1	23.16	-0.016
CONTROL-67	-	✓	-	-	-	18.3	20.95	-0.020
CONTROL-110	-	-	✓	-	-	46.1	20.16	-0.016
CONTROL-200	-	-	-	✓	-	-	17.98	-0.010

Table 3.1: List of experiments and forcings applied and the calculated eddy shedding periods, and Florida and Yucatan Channel water mass, heat and salt transports. The Florida Straits fluxes were calculated for the area 23.17° and 24.39°N at 81.83°W (between Cuba and Florida) whereas Yucatan Channel fluxes were calculated between 87.17° and 84.5°W at 21.94°N in CONTROL. For the experiments at lowered sea level, the transports were calculated considering new coastlines due to the exposed shelf areas (see Fig. 3.3). The values are mean transports for 20 model years (1930 – 1950). The surface heat flux is calculated from 3 years of daily averages and reveals the amount of heat being delivered to the atmosphere. Higher negative values denote a higher amount of heat delivered to the atmosphere.

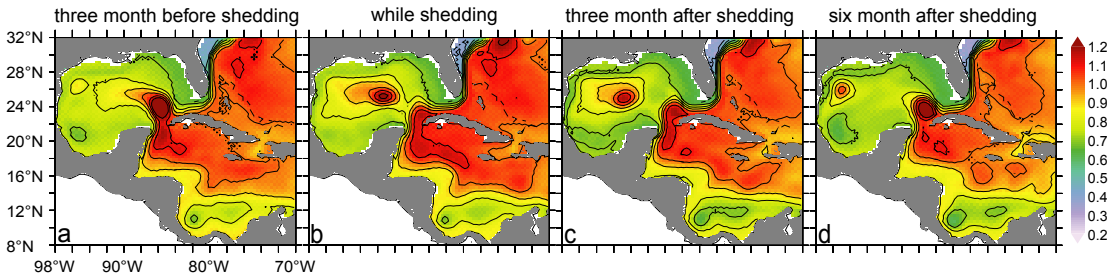


Figure 3.4: Eddy separation process in CONTROL shown by sea surface elevation depicted as composite from 20 years simulation (18 events in total) in meters; contour lines are 0.8 – 1.2 meters with 10 cm interval.

3.4 Model results

3.4.1 CONTROL simulation analysis

In CONTROL we find a FC transport of 23.32 Sv calculated for the last 20 model years, which is low compared to observations. A detailed debate of this issue can be found in the discussion section. Nonetheless, we assume that the low bias in the simulated FC transport does not affect significantly the FC transport variability in the model simulations, which is the focus of the present study. Note that the goal of this study is not to reproduce the absolute transport through the straits but rather to capture the sensitivity of the transport to the different sea level and wind stress conditions during the YD and the LGM.

Fig. 3.4 shows a mean eddy shedding event in CONTROL as a composite of the surface pressure that was averaged over the 20 year period after 30 years of integration time. A composite is here the average of 18 eddy shedding events in total, showing the characteristic situation in the Gulf of Mexico and adjacent ocean basins. Fig. 3.4a shows the composite three months before a shedding event. The LC eddy has already almost completely developed north of the YC. Fig. 3.4b shows the situation directly after the detachment from the LC. In Fig. 3.4c the composite three months after shedding is displayed. The eddy has already propagated half way towards the western boundary of the Gulf. Six months after the eddy has separated from the main current, it is degraded to a small anticyclone with lower surface elevation than three months after shedding (Fig. 3.4d). The next eddy has already developed in the area of the LC. Note that the detachment can take months though, until a complete new separation will be completed. Just before the complete separation in every shedding event we often observe a small cyclone in the east of the LC possibly supporting the shedding process. This small cyclone fosters the detachment with its westward movement in the area, where the connection to the main current is getting weaker with the shedding progress. However, these features

are not visible in the composites due to averaging over the 18 events. These so called 'Tortugas cyclones' were also found by Vukovich and Maul (1985), in hydrographic data and current meter moorings, as well as in satellite infrared data by Leben (2005) and by Oey et al. (2005), who found these features in both model results and observations from radiometry.

The mean shedding period \bar{T}_{shed} averaged for the last twenty model years are given in Tab. 3.1, while Fig. 3.5. shows the mean absolute velocities in YC as a time series over the same period. Since a local minimum in speed occurs whenever an eddy is shed, Fig. 3.5 shows the individual eddy shedding events. However, to detect eddy shedding in an objective manner, we are using the criteria of the breaking of the 0.8 m contour in sea surface deviation. Based on this criteria, the shedding period in CONTROL (Fig. 3.5a) varies from 10.3 to 15.5 months and has a mean period of 13.2 (Tab. 3.1), which is in good agreement with observations by Leben (2005) and by Vukovich (1995).

Heat transport into the Gulf of Mexico and the eddy shedding are related: Fig. 3.6a shows a time series of eddies as they propagate from east to west within the Gulf of Mexico. Shown is the speed for CONTROL at 100 m water depth averaged between 23°–27°N. The black line in Fig. 3.6b shows the amount of heat that remains between YC (see also section A in Fig. 3.7) and FS (see also section B in Fig. 3.7). This amount can either be transported into the western part of the Gulf heating the water or it can be released to the atmosphere. The red line in Fig. 3.6b displays the amount of heat that crosses the meridional section in the middle of the Gulf displayed also as red section in Fig. 7. The heat transport divergence through YC and FS is calculated for a 3-year mean (0.015 PW on average) using daily averages of the model variables as

$$\begin{aligned}
 T_{FS-YC} = & \rho_0 \bar{c}_{p,0} \int_{23.17^\circ N}^{24.39^\circ N} \int_{-5000m}^{0m} T u dy dz \\
 & - \rho_0 \bar{c}_{p,0} \int_{84.5^\circ W}^{87.17^\circ W} \int_{-5000m}^{0m} T v dx dz.
 \end{aligned} \tag{3.1}$$

where ρ_0 is a reference density and $\bar{c}_{p,0}$ a mean heat capacity of seawater at constant pressure. Note that T_{FS-YC} denotes the advective heat transport into the Gulf and balances in steady state the surface heat flux over the Gulf (if one neglects diffusive heat transports in the model). For FS it is calculated at 81.83°W, for YC at 21.94°N. Whenever we find an eddy separating from the main current, we can also detect that a higher amount of heat, than under normal circumstances, is transported with this separating anticyclone towards the west. Fig. 3.7 also shows the annual mean surface heat flux which is obviously greatest in the western boundary current in the North Atlantic but concerning the Gulf we

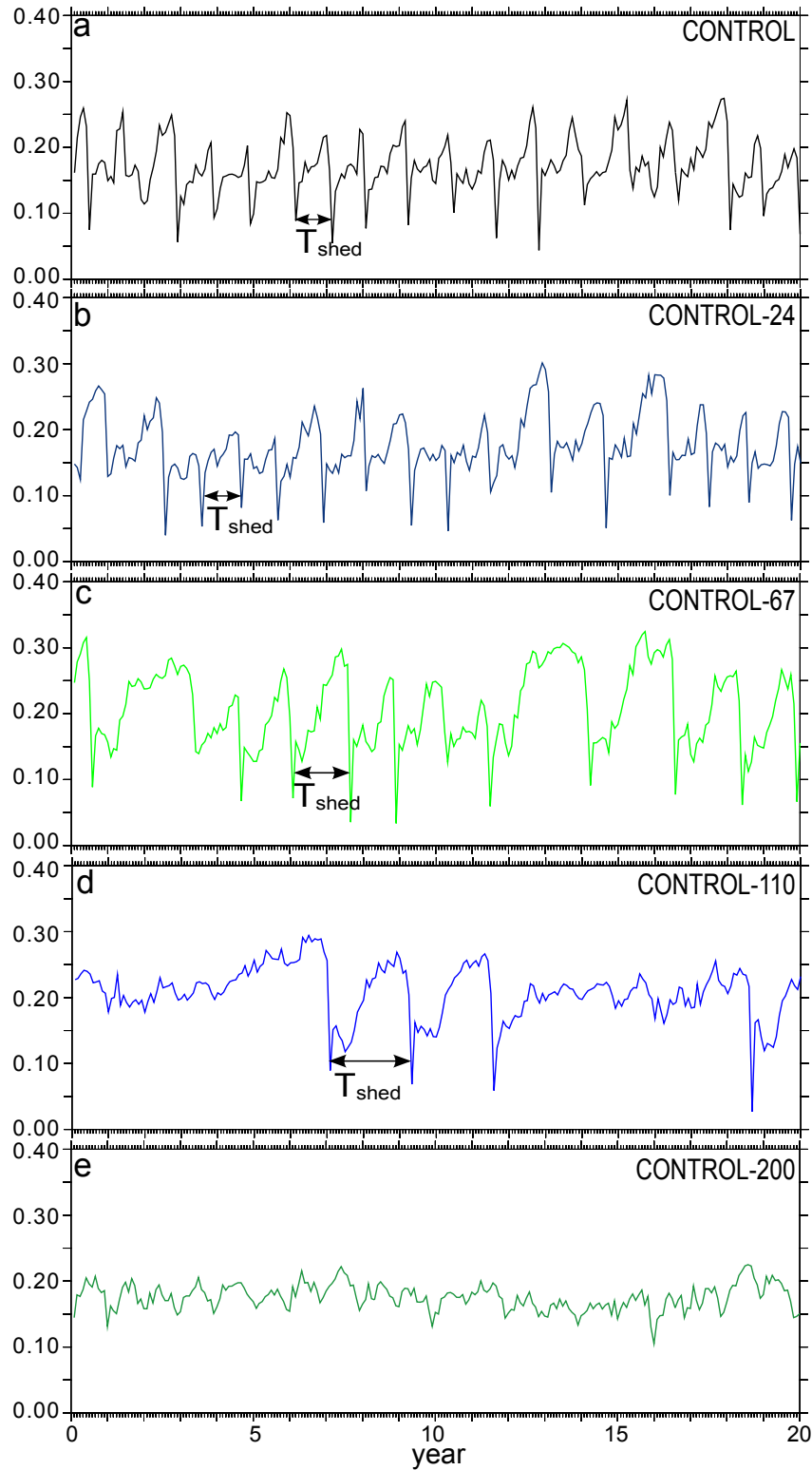


Figure 3.5: Transect of velocities averaged between 22°N and 24°N and between 87°W and 84°W (see white square in Fig. 3.2) in m/s through Yucatan Channel for 20 model years at 200 m water depth. Shown are the experiments for lowered sea level and CONTROL (description of the experiments can be found in the text). Note the increase in eddy shedding across the deglaciation derived from these experiments. \bar{T}_{shed} is the shedding period of the LC from one eddy detachment until the next.

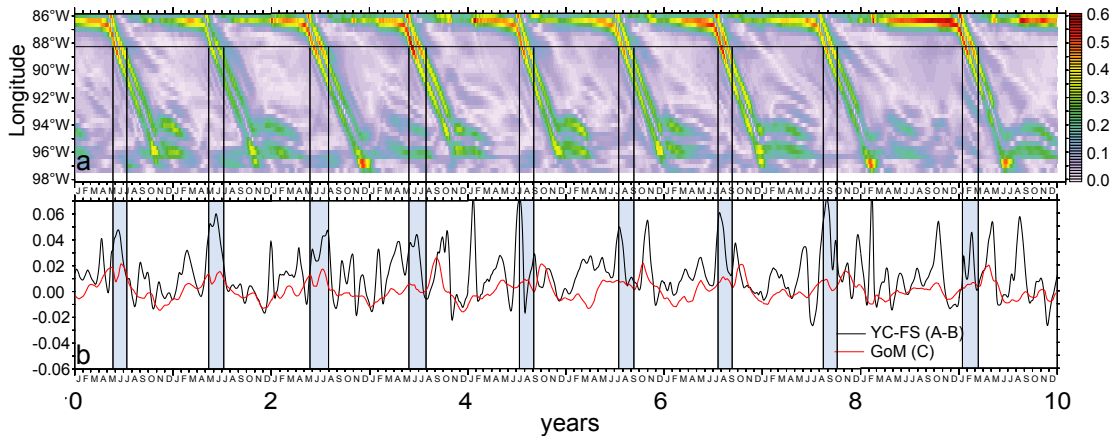


Figure 3.6: **a** presents a time series of speed (m/s) calculated from 10 years of daily averages at 100 m water depth averaged between 23°- 27°N; **b** reveals two time series of heat transport in PW across section A-B (black line) and C (red line) calculated for the same time period; both figures show data of CONTROL.

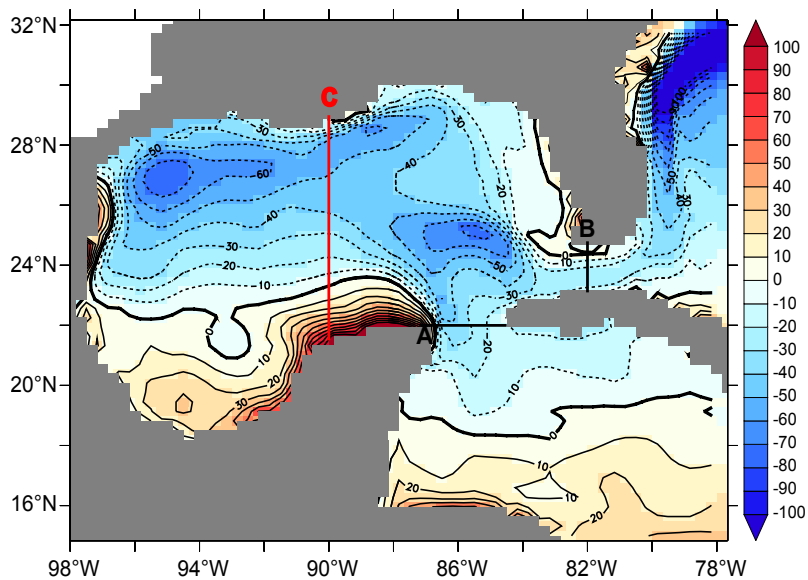


Figure 3.7: Annual mean surface heat flux in W/m^2 calculated from 10 years of daily averages from CONTROL.

find the highest annual mean surface heat flux in the region where eddy shedding occurs and also in the region where the eddies of the LC dissipate. Negative values denote here the transport into the atmosphere, while positive values show the flux into the ocean.

3.4.2 Sea level experiments

Next, we describe the changes in the circulation in the Gulf and the eddy-shedding at lowered sea level. Fig. 3.3 shows the topographic changes for all experiments with varying sea level. The most prominent changes obviously occur when lowering the sea level by 67 m (CONTROL-67). This entails a reduction of the YC profile by 7.5% in area compared to CONTROL and by 10.2% in FS. In CONTROL-110 the profile changes are most striking along the west Florida shelf region while smaller differences occur around Cuba and Mexico. The YC is reduced in area by 12% compared to CONTROL and by 15% in FS. For our sensitivity experiment CONTROL-200, the most dominant changes are on the southern shelf of Florida and to a smaller extent around Campeche Bank. The YC is reduced by 20.5% in area while the FS profile was 26.8% smaller than in our reference experiment CONTROL.

Over the twenty-year period, the transport through YC and FS is reduced by 0.7% in CONTROL-24 and by 10.2% in CONTROL-67 compared to CONTROL due to the lowered sea level. The transport in CONTROL-110 is further reduced by 3.4%. We find the lowest mean transport in CONTROL-200. In this sensitivity experiment, YC transport is reduced by 23% compared to CONTROL. The reductions in transport follow closely the profile reductions of FS and YC and the wind stress forcing and the resulting wind-driven Sverdrup transport remain the same in all experiments. It follows that an increasing part of the wind-driven Sverdrup transport recirculates east of the Caribbean Sea in the experiments with reduced sea level.

Furthermore, the reduced sea level comes along with reduced eddy-shedding: Fig. 3.5b simulating the late Holocene shows already an extended shedding period compared to CONTROL, while Fig. 3.5c indicates that the shedding period for the Younger Dryas in CONTROL-67 becomes also longer but also less regular (18.3 months on average, Tab. 3.1). The range of the individual shedding period is also more variable ranging from 14.8 up to 31.7 months. CONTROL-110 (Fig. 3.5d), simulating the low sea level during LGM, shows even more decreased eddy-shedding. An eddy in this experiment is shed every 46.1st month on average. Also note that the shedding becomes even more intermittent than in CONTROL and CONTROL-67 with even longer shedding intervals (Tab. 3.1).

The shedding period is highly variable and lies between 26.5 and 84.1 months. For a lowered sea level by 200 m (CONTROL-200, Fig. 3.5e), no eddies are shed anymore over the complete simulated period (50 years in total).

Lowering the sea level leads to a reduction in heat transport between YC and FS: Younger Dryas sea level conditions (CONTROL-67) lead to a reduction in heat transport into the Gulf by approximately 30%, while LGM sea level conditions (CONTROL-110) reduce the heat transport by 46%. We observe the most extreme difference in heat transport in CONTROL-200, where the reduction is 80%. Although the heat fluxes in the Gulf and the relative changes in heat transport between FS and YS are not balanced completely, heat content changes and surface heat flux (Tab. 3.1) show the same trend. The lower the sea level the smaller the heat transport into the Gulf going along with a reduction in surface heat flux from the Gulf. The imbalance is to a large extent related to the heat storage, while diffusive heat transports contribute to a lesser extent.

3.4.3 Wind stress experiments

Changes in wind stress during glacial periods also have the potential to influence transports through the Caribbean Sea, YC and FS and thus, might have affected eddy-shedding and heat transport into the Gulf of Mexico. We describe experiments with changes in wind stress (LGM-wind hereafter) according to the PMIP2 model ensemble for the LGM scenario as described above, to see if changes in wind stress support or counteract the sea level changes. Fig. 3.2 shows the present-day wind stress vector $\boldsymbol{\tau}$ in CONTROL. Also shown is the Ekman pumping velocity, $w_E = \mathbf{k} \times \nabla \cdot \boldsymbol{\tau} / f$. Note that positive values of w_E denote Ekman suction, while negative values denote Ekman pumping. The negative values in the center of the subtropical gyre generate southward volume transport – the Sverdrup transport – which is compensated at the western boundaries by northward flow, and thus in part by the circulation system in the Caribbean Sea. Changes in wind stress during the LGM can increase or decrease this way the amount of YC and FS transports.

From Fig. 3.2 it becomes obvious that the Ekman pumping and Sverdrup transport in the Subtropical Gyre of the North Atlantic is governed to a large extent by the meridional gradient of the zonal wind stress τ_x , and it is reasonable to assume that this holds also during the LGM. Fig. 3.8 shows the zonally averaged τ_x from the LGM-wind experiments and from CONTROL. In most experiments with LGM wind forcing, τ_x is strengthened compared to CONTROL. Only in CCSM-wind we find a decrease in zonal wind between 30°N and 60°N of 20%. In addition to the increase, we see a southward shift of τ_x , which is

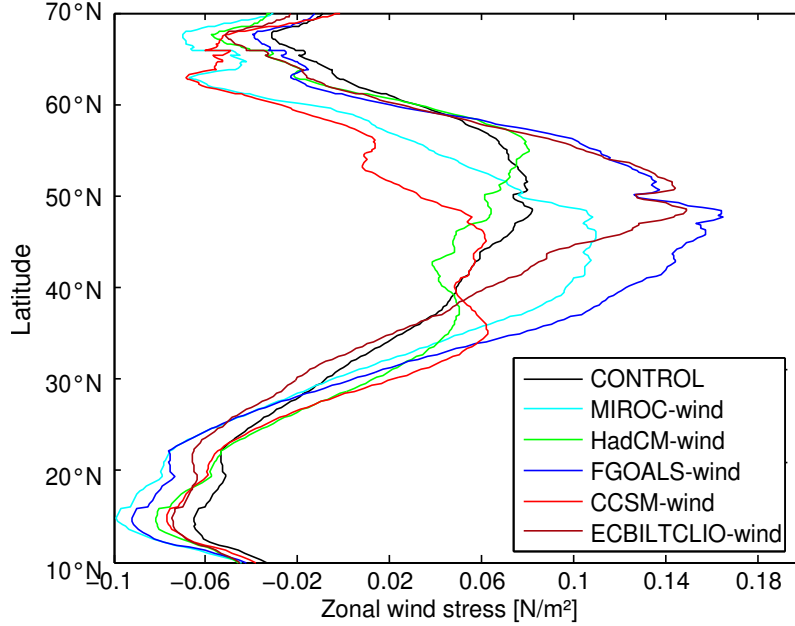


Figure 3.8: Zonal wind stress averaged between 100°W and 20°E in N/m^2 for all model experiments forced with LGM wind (colored lines) and CONTROL (black line).

related to the southward shift of the ITCZ during the LGM. This results in an increase of τ_x between 30°N and 60°N ranging from 20% (MIROC-wind) and 100% (FGOALS-wind), with corresponding effects on the meridional gradient, the wind stress curl and thus, on the Sverdrup transport.

Fig. 3.9 (left column) shows the streamfunction ψ_{Sv} for the Sverdrup transport V calculated from $\beta V = k \times \nabla \cdot \tau$, using the wind stress τ of the LGM-wind experiments (Fig. 3.9c,e,g,l and k) and CONTROL (Fig. 3.9a, while on the right right column the mean streamfunction ψ for the actual depth integrated transport by the individual experiment is shown. Here, β is the meridional gradient of the Coriolis parameter, and V is the vertically integrated meridional mass transport according to the linearized barotropic vorticity equation for steady motion and flat bottom. The streamfunction ψ_{Sv} with $V = \partial\psi_{Sv}/\partial x$ and correspondingly $U = -\partial\psi_{Sv}/\partial y$ was calculated by integrating the meridional Sverdrup transport V from the eastern boundary of the North Atlantic towards the west. For the streamfunction ψ for the depth-averaged flow $\int_{-h}^0 \mathbf{u} dz$ the relation $\int_h^0 u dz = -\partial\psi/\partial y$ and $\int_{-h}^0 v dz = \partial\psi/\partial x$ holds. Fig. 3.9 shows the average of ψ over 5 years at the end of the spin-up to eliminate the strong meso-scale eddy signals which differ between the individual experiments.

Fig. 3.9 shows that in the interior of the ocean, Sverdrup transport ψ_{Sv} and actual simulated transport ψ are rather similar. In particular, a strengthening in transport in

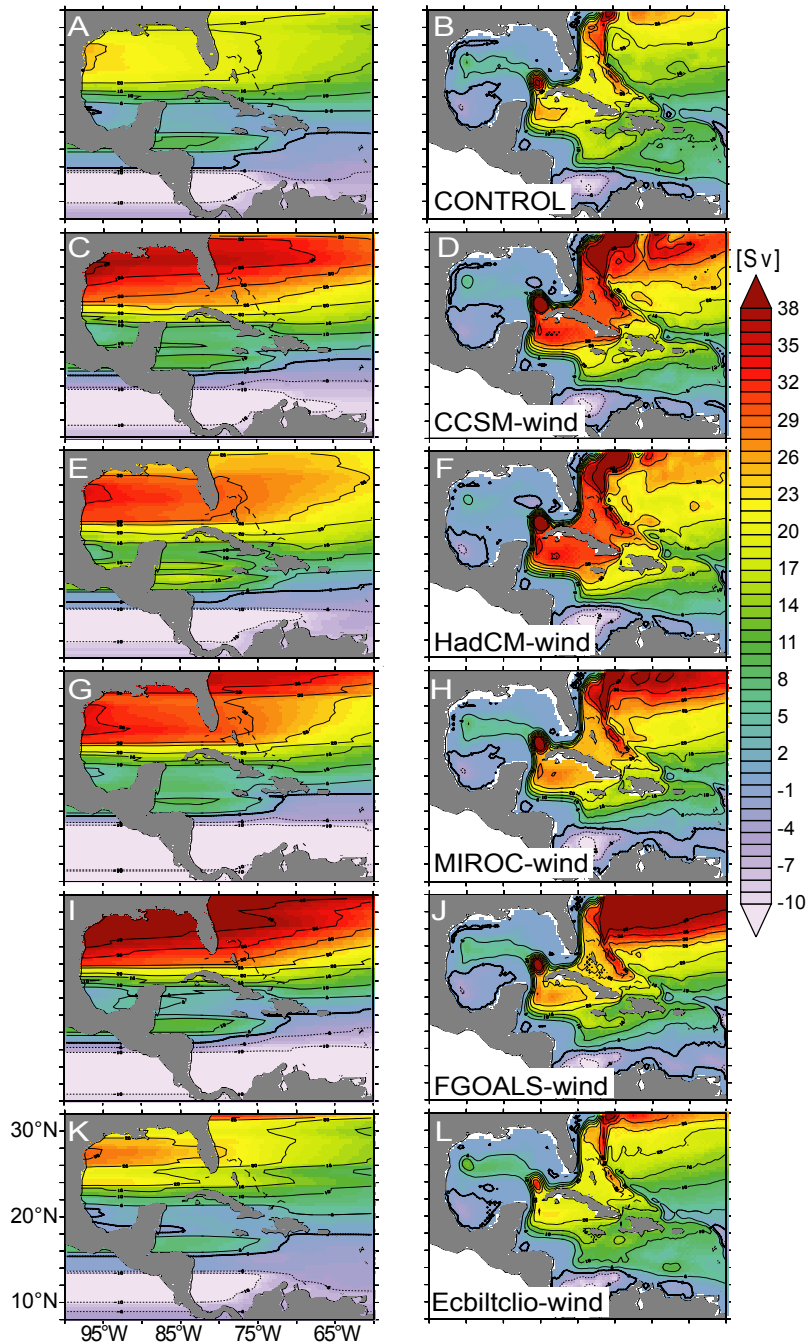


Figure 3.9: Comparison between transport calculated from the Sverdrup relation (after Sverdrup (1947); panels to the left) and from the actual simulated stream function (5-yr mean Sverdrup transport; panels to the right) for CONTROL and the different LGM-wind experiments; CONTROL (A, B), CCSM-wind (C, D), HadCM-wind (E, F), MIROC-wind (G, H), FGOALS-wind (I, J), and Ecbiltc10-wind (K, L). See text for definition of different models applied.

the subtropical gyre can be seen in the LGM-wind experiments, except for ECBILTCIO-wind. The similarity of ψ and ψ_{Sv} does not come as a surprise, since it was shown by Hughes and de Cuevas (2001) and Eden and Olbers (2010) that the depth-averaged vorticity budget is dominated in the interior of the ocean basin by the balance between the planetary vorticity change of a water particle and the torque given by the wind stress forcing, which means that the interior North Atlantic is in Sverdrup balance. According to our model experiments, this also holds during LGM.

In the western boundary layer, on the other hand, the planetary vorticity is balanced to a large extent by a torque related to the pressure variations at the bottom of the ocean and the Sverdrup balance fails (Hughes and de Cuevas, 2001; Eden and Olbers, 2010). However, we can still infer from the increase in the Sverdrup transport an increase in the compensating western boundary currents. We see in ECBILT-wind a reduction in the meridional gradient of τ_x (Fig. 3.8), accordingly a reduction in Sverdrup transport (Fig. 3.9) and also a reduction of 10.7% relative to CONTROL in the YC and FS transport. In all other LGM-wind experiments, we see an increase of the gradient in τ_x (Fig. 3.8), the Sverdrup transport (Fig. 3.9), and YC and FS transport. The largest increase in YC and FS transport can be seen in HadCM-wind and CCSM-wind, by 34.8 and 36.6%, respectively. Note that changes in wind stress do not correspond directly to the changes in FS transport. The strongest increase in the interior Sverdrup transport can be seen in FGOALS-wind, while we see only an increase of 7.6% of the YC and FS transport in FGOALS-wind. It thus appears that it is not the overall strength of the interior Sverdrup transport, which determines the increase in the through-flow of the Caribbean Sea, but rather it appears that the details of the forcing over and east of the Caribbean Sea determines the through-flow. Note that the value of ψ_{Sv} just east of the Caribbean Sea between 10 and $\sim 20^\circ\text{N}$ appears to be largest in the experiments with largest increase in YC and FS transport. It appears that this value determines the through-flow of the Caribbean Sea and the FS and YC transport in our experiments. From the sum of our experiments using the PMIP2 model ensemble we can conclude that the wind stress during the LGM most likely acted to increase the YC and FS transports. This wind driven increase in YC and FS transport during LGM tend to reduce eddy-shedding, thus supporting the impact of the reduced eddy shedding on the LGM cooling of the Gulf.

In the experiments with largest increase in YC and FS transport, HadCM-wind and CCSM-wind, the eddy-shedding stops. While in the experiments with moderate increase in YC and FS transport, FGOALS-wind and MIROC-wind, the eddy-shedding period is similar to CONTROL, the period decreases for the experiment with reduced YC and FS transport in ECBILT-wind. The shedding period in MIROC-wind lies between 13.83 and

23.63 months, in FGOALS-wind between 12.0 and 17.1 and in ECBILT-wind we find very rapid shedding between the 8.2 and the 10.7 months.

While a decreasing FS transport was related to an increase in period and eventual stopping of the eddy-shedding in the experiments with reduced sea level, it thus appears that wind-driven transport increases for today's sea level are not directly related to the eddy-shedding. Only when the transport increases above a certain threshold in HadCM-wind and CCSM-wind, the eddy-shedding stops, while the decreased transport in ECBILT-wind is related to an intensification of eddy-shedding, in contrast to the experiments with reduced sea level. We conclude that it is not the reduced transport but the change in the profile of the YC, which leads to the diminishing eddy-shedding in the experiments with reduced sea level. The wind driven increase in YC and FS transport during LGM tend to reduce eddy-shedding, thus supporting the impact of the reduced eddy shedding on the LGM cooling of the Gulf.

The surface heat flux in the Gulf increases when the period of the eddy shedding is higher than in CONTROL (see Tab. 3.1) and the FS transport is similar compared to CONTROL. When FS transport increases and the eddy shedding ceases, the surface heat flux is almost stationary or even less than in CONTROL. In ECBILT-wind a very low FS transport rate and eddy shedding with an elevated eddy shedding frequency compared to CONTROL permits a slight increase in surface heat flux. As mentioned before, the surface heat flux from the Gulf is not completely balanced by the differences in heat transport between FS and YS but since the model is not in complete balance, parameters show the same qualitative behavior.

3.4.4 Combining lowered sea level and LGM wind stress forcing

Lowering the sea level only (e.g. CONTROL-110) leads to a reduction in FS transport and an extension of the eddy shedding period whereas LGM-wind forcing produces higher transports in FS (except in ECBILT-wind) and with this an increase of the period or a total cease in eddy shedding.

We find the FS and YC transport also to decrease when combining lowered sea level with the LGM wind stress anomalies (ranging from 1.1% with respect to the difference between CCSM-wind/CCSM-wind-110 to 14.6% with respect to the difference between ECBILT-wind/ ECBILT-wind-110). Obviously the changes in topography play a dominant role in these experiments. The eddy shedding is absent in all LGM-wind-110 experiments except in ECBILT-wind-110 where FS transport is rather low compared to the other with LGM

wind and lowered sea level (LGM-wind-110 hereafter) experiments.

However, the combination of sea level and wind stress anomalies does not evolve in a linear way: the difference in transport through FS between CONTROL and CONTROL-110 is much larger (3.16 Sv) than the differences between LGM-wind (all experiments with LGM wind stress forcing) and LGM-wind-110 experiments (e.g. FGOALS-wind and FGOALS-wind-110). We find lower absolute and relative transport changes between all LGM-wind/LGM-wind-110 experiments except between ECBILT-wind/ECBILT-wind-110, where relative transport changes are in the same range as in CONTROL/CONTROL-110.

The diminished eddy shedding in the LGM-wind-110 experiments (except ECBILT-wind-110) seems to be a reasonable consequence given that eddy shedding was highly reduced in CONTROL-110 and also given that the shedding period was elevated or absent in the LGM-wind experiments.

We also find a decrease in surface heat flux from the Gulf in all LGM-wind-110 experiments (Tab. 3.1) and a decrease of absolute heat transport into the Gulf (not shown) when comparing them to our LGM-wind experiments. Note that The reduced heat transport into the Gulf is related to the cease in eddy shedding. Although FS transport is similar to CONTROL in our experiments FGOALS-wind-110 and MIROC-wind-110, eddy shedding stops with the lowered sea level. Only in ECBILT-wind-110, as mentioned before, eddy shedding can still be detected at a very low FS transport leading to the assumption that a very low FS transport allows eddy shedding also when the sea level is lowered.

3.5 Discussion

To unravel the interlinks in the system, it is necessary to study particular scenarios in isolation. Hence, we performed experiments with different sea levels, wind stress anomalies of the LGM combined with present day sea level and finally a combination of wind stress anomalies of the LGM and lowered sea level to test the individual responses.

Many aspects of the present circulation in the Gulf of Mexico in CONTROL are similar to a higher ($1/12^\circ$) resolution version of the same model (HI-ncep) used in Eden (2007) FS transport in CONTROL is 23.32 Sv calculated for the last 20 model years, which is very close to the value in HI-ncep of 22.39 Sv (Mildner et al., 2012). HI-ncep is the same model, using the same forcings and boundary conditions except for a resolution of $1/12^\circ \cos \phi$. Sensitivity experiments with CONTROL and HI-ncep using different topog-

raphy (i.e. changes in depth and width of Windward Passage) and different wind stress products and topography do not show any improvement of the low bias. Although CONTROL reproduces the observations in many cases quite well, a common bias of both models and also others (e.g. Smith et al., 2000) is the low volume transport between Cuba and Florida (compare Tab. 3.1). This low bias is also apparent in more recent global versions of the model by Smith et al. (2000) (A. Griesel, pers. comm), and thus appears to be a common problem of basin-wide eddy-permitting models. Nonetheless, we assume that the low bias in the simulated FC transport does not affect significantly the FC transport variability in the model simulations, which is the focus of the present study. Note that the goal of this study is not to reproduce the absolute transport through the straits but rather to capture the sensitivity of the transport to the different sea level and wind stress conditions during the YD and the LGM

Little is known about the ocean circulation of the inner Gulf of Mexico for the Last Glacial Maximum and what we know are fragments of the whole picture due to limited facilities and uncertainties that can arise from observational dating methods. Slightly more observational and modeling studies involve more recent climatic abrupt events e.g. the Heinrich 1 event, the Younger Dryas or the Bølling Allerød (B/A; ~ 14 kyr BP) focusing mainly on the Caribbean. Observations in marine records from the Gulf of Mexico and the Caribbean show large variations in the SST during the last 21 kyr (Flower et al., 2004; Nürnberg et al., 2008; Schmidt et al., 2004). It is the aim of the present study to relate these differences to changes in the circulation.

We use the PMIP database to reconstruct wind stress forcing. A common signal in all models in the PMIP database is a southward shift of the ITCZ during the LGM. This seems robust, as observations from Cariaco basin allow also this assumption based on alkenones in comparison with Mg/Ca ratios and foraminifera proxy records from sediment cores (Haug et al., 2001; Koutavas et al., 2005; Kuhlemann et al., 2008; Schmidt et al., 2011). Further studies by Lea et al. (2003); Wang et al. (2004) support this assumption. Due to the shift of the ITCZ, a southward shift of the trade winds can be observed in most of our LGM-wind and LGM-wind-110 experiments. As a consequence the wind driven transport into the Caribbean increases and as a result also the transport in YC and FS. The model results also suggest that the lower the sea level, the longer the shedding period of the LC going along with decreased heat and salt transport into the Gulf of Mexico. These results point towards a warming of the GoM across the deglaciation. Also, the interval of the mean shedding period of the LC increases at lower sea levels.

Note that we did not consider salt fluxes. This is due to the salt relaxation surface

conditions in FLAME where we lowered the sea level and where we might miss the influence of the Mississippi freshwater discharge (at the northernmost boundary of the Gulf). Parts of the Mississippi freshwater input into the GoM are not resolved in this case so that the Mississippi freshwater discharge may not be mapped correctly.

The meso-scale anticyclonic eddies shed by the LC are an important component for the heat budget of the Gulf as they transport warm and salty waters into the northern and western part of the Gulf. A high probability of no eddy shedding and reduced heat transport during the full glacial according to our experiments is in good agreement with the observations who suggest a decrease in SST in the Gulf by about 4°C for the LGM based on sediment analyses from De Soto Canyon by Nürnberg et al. (2008) and from Orca Basin Flower et al. (2004). The continuous increase in eddy shedding across the deglaciation found in the model experiments goes also along with a reconstructed continuous 6.5°C SST increase across the deglaciation calculated from marine sediments from De Soto Canyon (Nürnberg et al., 2008). The higher temperatures in the Caribbean found by Schmidt et al. (2004) and the lower SST in the Gulf during the LGM might be related to changes in heat and freshwater transport due to a cease in eddy shedding. Overall the differences in SST records and model results hold information about the eddy shedding behavior during the last 21 kyr.

Observations in this area concerning the FS transport during the LGM contradict each other. Whereas observations of a study by Schönfeld et al. (2005) propose an enhancement in transport through the southern glacial FS by 20% using Sortable Silt estimations as a paleo-flow proxy, observations by Lynch-Stieglitz et al. (1999) propose a reduced FS transport for this period. Lynch-Stieglitz et al. (1999) calculate the glacial FS transport from a density gradient between Florida and the Bahamas using the $\delta^{18}O_{calcite}$ values of foraminifera shells and find glacial FS transports ranging between 15 – 18 Sv. Calculating a horizontal density gradient needs the assumption of a level-of-no-motion at the bottom, which is discussed controversial among others by Wunsch (2010). However, it contradicts our model results regarding the FS transport estimates as they all show a stronger FS transport for the LGM (except ECBILT). The reason for the discrepancy in Lynch-Stieglitz et al. (1999) findings and our results remains unknown.

In our five CONTROL experiments we lowered the sea level according to the relevant sea level reconstructed from observations but with fixed surface forcing. We find a reduced transport in FS and YC the lower the sea level is. This is in agreement with earlier model studies using the Regional Ocean Modeling System by Ionita et al. (2009) who also neglected changes in wind. They lowered the sea level by 120 m and came to similar

results compared to our CONTROL-110 experiment, namely that the transport in FS and YC reduces when the sea level is reduced and present day wind stress is applied. With the present study we have also shown that the wind stress plays an important role with respect to the changes in the circulation.

Note that we did not change the thermohaline forcing and the lateral boundary conditions in our experiments. This is based on the assumption that the overturning has not changed much during the LGM as there is no consensus so far (e.g. Lippold et al, 2012, and references within). Oka et al. (2012) propose in their recent study a thermal threshold for the AMOC, where stadial periods of glacial climate experience a weak AMOC whereas interstadial periods undergo a relatively strong AMOC. However, there are also indications from a model comparison study by Otto-Bliesner et al. (2007) who suggest that the MOC was neither appreciably stronger nor weaker than modern MOC. Note also that the hydrological cycle, and its processes and feedbacks in stabilizing or destabilizing the THC is still largely unknown also for present day ocean circulation. However, concerning the process of the eddy shedding in the Gulf under different forcings we are able to compare the different model results to the observations and draw conclusions based on these results.

3.6 Summary

We used an eddy permitting model to study the dynamics of the Loop Current eddy shedding in the GoM, for different sea levels (late Holocene: 24 m, YD: 67 m, LGM: 110 m and sensitivity experiment: 200 m) and using different wind stress forcings appropriate to LGM conditions (PMIP2 coupled model simulations). The results are summarized in Fig. 10.

- Applying glacial wind stress leads to an equatorward shift of the westerly winds, a stronger meridional gradient of the zonal wind above the Subtropical Gyre and thus to an increase in the wind stress curl and an enhancement of the Sverdrup transport within the Subtropical Gyre. These are the direct results of the intensified wind stress and are common features in the PMIP2 models (Murakami et al., 2008).
- To summarize our findings, Fig. 10a shows the eddy shedding frequency as a function of transport between Cuba and Florida and sea level:
 1. Transport between Cuba and Florida tends to increase when applying glacial wind stress.

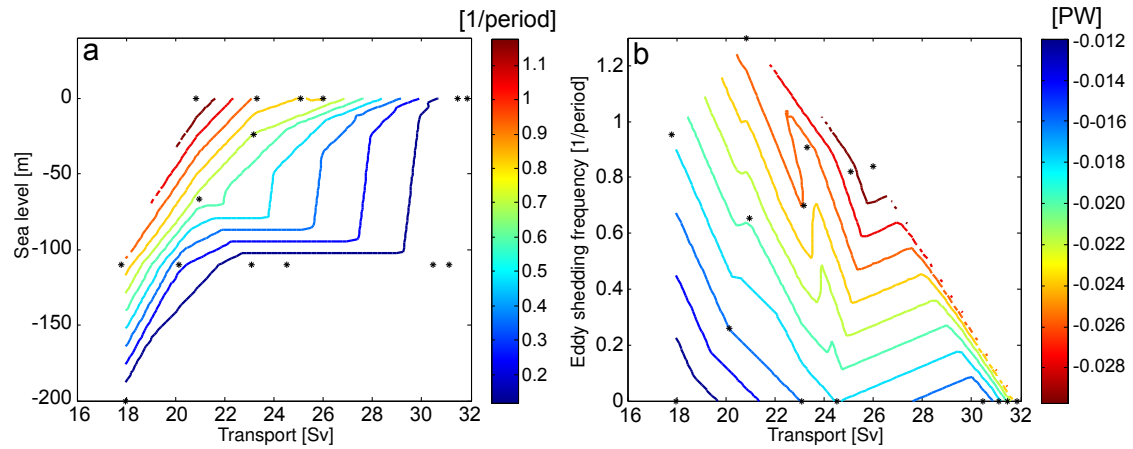


Figure 3.10: **a** shows the eddy shedding frequency as a function of the transport between Cuba and Florida and the sea level. The numbers next to the experiment names reveal the frequency of eddy shedding. **b** shows the surface heat flux [in PW] as a function of FS transport and eddy shedding frequency. Higher negative values denote higher surface heat flux to the atmosphere. The contour lines in both figures show linearly interpolated data.

2. Lowering the sea level leads to a reduction in or to the total absence of eddy shedding.
 3. Increasing transport between Cuba and Florida leads to a decrease in or the total absence of eddy shedding.
- Fig. 10b shows the surface heat flux as a function of transport between Cuba and Florida and eddy shedding frequency, which both determine the heat budget of the Gulf of Mexico:
 1. Increasing eddy shedding frequency increases surface heat loss in the Gulf of Mexico.
 2. The increasing Florida Current and transport between Cuba and Florida also increase surface heat loss from the Gulf of Mexico.

4 The Gulf Stream position during the LGM

T. C. Mildner¹, C. Eden¹ , L. Czeschel¹ and D. Nürnberg²

This chapter is in preparation for submission

¹ KlimaCampus, Institut für Meereskunde, Bundesstr. 53, 20146 Hamburg, Germany.

² GEOMAR Helmholtz Centre for Ocean Research Kiel, Wischhofstr. 1-3, 24148 Kiel, Germany.

4.1 Abstract

In this manuscript, the effect of changes in wind stress and sea level during the Last Glacial Maximum (LGM, ~18-24 ka) for the Gulf Stream position are discussed using a 1/12° ocean general circulation model (OGCM). LGM wind stress is enhanced in the region of the tropical and polar easterlies and the prevailing westerlies are shifted southwards. As a consequence, the line of zero wind stress curl ($\nabla \times \tau = 0$), is also located further south by up to 3° during the LGM compared to present day. The Intertropical Convergence Zone (ITCZ) experiences a latitudinal shift of ~4° to the south. A stronger subpolar gyre and a southward extended northern recirculation gyre lead to a shift of the complete circulation system. The subtropical gyre is less developed and also displaced to the south. The model response suggests a southward shift of the Gulf Stream to the position between 32.5 and 34°N in the experiments (according to the 15°C isotherm in 200 m water depth). Moreover, a more zonal characteristic of the Gulf Stream axis during the LGM was found in our experiments compared to the more meridionally tilted axis of the present Gulf Stream. With a lowered sea level alone sea level did not change the Gulf Stream position, we conclude that the glacial wind plays an important role.

4.2 Introduction

Nowadays the position of the Gulf Stream and its variability are well observed and its importance for the European and the regional climate is known. The Gulf Stream's origin is located in the Gulf of Mexico and it carries the tropical waters from the Florida Straits along the coast as a western boundary current. It leaves the coastline off Cape Hatteras near 35°N, carrying its warm waters over the New England Seamount chain to the northern parts of the North Atlantic. At around 50°W, the Gulf Stream splits into several currents. The most important currents are the North Atlantic Current, the Azores Current, the southern and the northern recirculation gyre (Schmitz et al., 1993; Schmitz, 1996).

Although its pathway is well known from satellite images, modeling of the strong meandering Gulf Stream is still a challenge. Unlike high resolution OGCMs, low resolution ocean models often fail to resolve the separation process correctly (Chassignet et al., 2008). By using finer grids, processes like meso-scale baroclinic instabilities at the scale of the first baroclinic Rossby radius of deformation are better resolved (Smith et al., 2000; Bryan et al., 2007). Increasing the resolution also led to the larger Reynolds numbers due to the possibility of implementing smaller viscosities. It has been shown by different authors that the Reynolds number has to exceed a certain threshold for the separation to occur (Deng

et al., 1996; Munday et al., 2005). For an extensive discussion of the GS separation, we refer to the reviews by Dengg et al. (1996) and Chassignet et al. (2008). Ocean circulation theories predict that the position of the Gulf Stream respectively the North Atlantic current system and the subpolar-subtropical front is set by the line of zero Ekman pumping at which there is no convergence or divergence of water in the directly wind-mixed surface layer of the ocean (Keffer et al., 1988; Gangopadhyay et al., 1992) which is in the area of the observed line of zero wind stress curl. This line was first supposed to mark the position of the Gulf Stream - North Atlantic Current system in ocean general circulation theories by Stommel (1948) and Munk (1950). Considered realistically, this line of zero wind stress curl shows considerable seasonal variation. Taylor et al. (1998) highlight the importance of wind stress and show that stronger westerlies and trade winds lead to a northward shift of the Gulf Stream separation latitude indicating a connection to the North Atlantic Oscillation (NAO) index. Several attempts have been made towards the understanding of the mechanisms of the separation processes but the dynamics controlling the separation of the Gulf Stream remains poorly understood.

Still today, direct observations of the Gulf Stream are hampered due to its large variability resulting in frequent/numerous eddies, filaments and other instabilities. No consistent seasonal cycle was found e.g. in a study by Taylor et al. (1998) who analyzed a 30 year time series of monthly data of the Gulf Stream northern boundary based on surface, aircraft, and satellite observations. Even higher uncertainties arise, if this highly variable system is extrapolated to past ocean circulation conditions. First measurements of the Gulf Stream transport were conducted from hydrographic sections by the US Naval Oceanographic Office since the late 1960s.

The present day Gulf Stream position has also been estimated from geological proxy reconstructions by Matsumoto et al. (2003) using oxygen isotope ratios of deep-dwelling planktonic foraminifera. During the LGM the Gulf Stream was probably shifted further south and did not reach subpolar North Atlantic regions north of $\sim 50^{\circ}\text{N}$ due to the surface melt water layer postulated by Ruddiman et al. (1981). Following a study by Lynch-Stieglitz et al. (1999), who identified a reduction in Florida Current transport and also a reduction of the southern Gulf Stream transport during the LGM, Matsumoto et al. (2003) and LeGrande et al. (2007) reconstructed the latitude of the separation for the LGM and came to the conclusion that the Gulf Stream had almost the same position compared to its modern state. Additionally, they state that the location of the Gulf Streams' intermediate depth density gradient was the same during the last ice age as today. The increase in wind strength in the North Atlantic, as assumed by the PMIP community for the LGM, would lead to an increase in circulation strength, is questioned by Huybers et al. (2010). Model

studies by Hewitt et al. (2001) suggest a stronger subtropical gyre during the LGM and (also) a southward shift of the Gulf Stream, which is not consistent with the line of zero Ekman pumping in their results. The most difficult part when comparing numerical model results to geological records is that sediments are often scarce for the LGM Gulf Stream because of the strong prevailing currents. Characteristic for the North Atlantic are slumps and turbidity currents on the continental margin hindering the recovery of undisturbed and adequate sediment material.

In this paper, we evaluate Gulf Stream position during the Last Glacial Maximum based on a high resolution ocean circulation model study. The advantage of a high resolution ocean general circulation model is the resolution of the first Rossby radius of deformation hence providing a good representation of baroclinic instability processes such as meso-scale eddies. We analyze our model results to assess whether the position of the Gulf Stream has changed during the Last Glacial Maximum.

4.3 Experimental design

We use an eddy-permitting ocean general circulation model of the Atlantic Ocean (FLAME, <http://www.ifm.zmaw.de/mitarbeiter/prof-dr-carsten-eden/numerical-models>) to assess the impact of sea level change and glacial wind stress on the dynamics of the North Atlantic upper ocean circulation as well as the Gulf Stream separation latitude. The model is based on a revised version of Geophysical Fluid Dynamics Laboratory (GFDL) Modular Ocean Model 2 (MOM2; (Pacanowski, 1995)) and has been used to address various topics (e.g. Dengler et al., 2004; Eden et al., 2004). To resolve meso-scale processes such as eddies in the Gulf Stream the model version used in the present study is based on a configuration for the Atlantic Ocean from 20°S to 70°N and 16°E to 100°W with 45 vertical levels (10 m thick at the surface increasing to 250 m starting from 2,300 m below sea level to the maximum depth of 5,500 m/bottom) and with a spatial resolution of $1/12^\circ \cos \phi$. All model experiments are forced using a Haney-type heat flux condition as given by Barnier et al. (1995). Atmospheric forcing is taken identical to the present day reference simulation also given by Barnier et al. (1995) and a restoring boundary condition for sea surface salinity, using the Antonov et al. (1998) climatology, which serves also as initial condition. Northern and southern margins of the domain are formulated as open boundaries after Stevens (1991). The temperature and salinity climatology are taken from Levitus and Boyer (1998).

In a first set of experiments, we reconfigure our CONTROL experiment of the FLAME

model with glacial sea level corresponding to the cold-glacial period of the LGM. For the period of the LGM the sea level was lowered by 110 m (CONTROL-110), according to observational estimates from Barbados, the North Atlantic and New Jersey by (e.g. Fairbanks, 1989; Waelbroeck et al., 2002; Wright et al., 2009) (see also Tab. 4.3).

Model-experiment	forcing: sea level -110 m	forcing: LGM wind anomalies	Florida Straits transport	Antilles Current	Deep Western Boundary Current	Vertical eddy bouancy [TW]	EKE [Joule]
CONTROL	-	-	20.7	12.9	-17	0.0063	8.4×10^{16}
CONTROL-110	✓	-	14.8	14.0	-11.3	0.0034	5.8×10^{16}
HadCM-wind-110	✓	✓	19.0	14.2	-12.8	0.0040	6.5×10^{16}
CCSM-wind-110	✓	✓	19.0	17.6	-10.4	-	-

Table 4.1: List of experiments and forcings applied and the calculated Florida Straits transports. The Florida Straits fluxes given in Sverdrup were calculated for the area 26°N between 79.1° and 81.1°W (between the Bahamas and Florida), Antilles Current in the area 26°N and between 76.1° and 71.6°W over the top 1000 m. Vertical eddy buoyancy was calculated between 32°N and 42°N, and between 50°W and 75°W and averaged over the top 500 m. All values are averaged over 5 model years.

In addition, we have reduced the sea level in the model by eliminating the first 9 levels of the original vertical grid of 45 levels of the model. We allow for a dynamical quasi-steady equilibrium of the basin-wide circulation, which the model reaches after approximately 10 model years. Note that due to the restricted length of the integrations, the simulations are not in equilibrium with the thermohaline surface forcing and the water mass characteristics prescribed at the open boundaries. Further, we did not change the thermohaline forcing in the model, i.e. it represents current climate. Therefore we do not aim to realistically simulate the response of the thermohaline circulation in our model simulation, but to focus on the response of the wind-driven, quasi-geostrophically balanced regional circulation in/of the Gulf Stream to the changes in sea level and wind stress.

Our model experiment are forced by LGM wind stress anomalies calculated from model results of the PMIP2 community (LGM-wind experiments) and combined the wind stress anomalies with lowered sea level due to glacial conditions. Available to us are results from the HadCM (HadCM3M2) (Gordon et al., 2000) and from the CCSM (the National Center for Atmospheric Research CCSM3 model) (Otto-Bliesner et al., 2006) model. All models in PMIP2 use the same boundary conditions namely ICE-5G (ice sheet) and topography described in L  n   et al. (2009) and which are online accessible from <http://www.pmip2.lsce.ipsl.fr>. They provide large continental ice sheets over North America and northern Eurasia. Forcings for PMIP2 models differ from present day insolation due to a difference in the Earth's orbit. Derived from the Greenland and Antarctic ice core records they included the changes in atmospheric carbon dioxide (185 ppmv - parts per million by volume) concentration, methane (350 ppbv - parts per billion by volume) and nitrous oxide (200 ppbv). Also these models are fully coupled atmosphere-ocean-ice models. We calculated anomalies of monthly mean wind stress from steady state model solutions for 21 kyr simulations minus present day control simulations of each PMIP model mentioned above and added this anomaly to our monthly varying forcing of CONTROL to create a new forcing for each experiment (altogether two with LGM-wind and lowered sea level). These experiments are listed in Tab. 4.3 and named HadCM-wind-110 and CCSM-wind-110.

4.4 Results

The Gulf Stream position in the model agreed quite well with the observations, although it had a slight overshoot to the north at its observed separation point off Cape Hatteras (Frankignoul et al., 2001). While observations found the long-term mean separation point at $\sim 36.5^\circ\text{N}$, it occurred about $1.5\text{-}2^\circ$ further north in the model. The split of the Gulf

Stream into several different currents e.g. the North Atlantic Current and the Azores Current at about 50°W (Fuglister et al., 1951) was therefore nicely reproduced by FLAME. The Azores Current could be clearly seen in the mean SSH field and the North Atlantic Current could be seen in the mean velocity field (not shown). The analyses revealed a width of the Gulf Stream in CONTROL of ~ 130 km which is in good agreement with observations by Johns et al. (1995) from a mooring array at 68°W. Note that although the Gulf Stream had this slight overshoot to the north, we assume here that this well known model bias did not affect significantly the results. The bias might be a result of the choice of the lateral boundary conditions applied (Chassignet et al., 2008).

4.4.1 Influence of sea level and glacial wind stress forcing

As criteria for the separation latitude of the Gulf Stream, Hansen (1970) suggested the depth of the 15°C isotherm at 200 m water depth which indeed agreed well with the model results (see Fig. 4.3). Further, the line of zero wind stress curl marking the boundary between the subtropical and the subpolar gyres as separation criteria suggested by Keffer et al. (1988) was found in the model, where the thermoclines rose towards the Gulf Stream and was located a little further to the south (Fig. 4.1a+b). Nevertheless that shelf areas were reduced during the LGM and therefore also in CONTROL-110 without the glacial wind forcing, only a slight shift in the position of the Gulf Stream was found compared to CONTROL. However, in both experiments the slight overshoot to the north existed. The Gulf Stream itself was located as in CONTROL close to the western boundary. However, the strength of the current flow was reduced by $\sim 30\%$. This was further supported by the Eady growth rate (after (Eady, 1949)) and the mean eddy kinetic energy (EKE, see Fig. 4.2).

$$EKE_{z=0:500} = \frac{1}{2} * (\overline{u'^2} + \overline{v'^2}) \quad (4.1)$$

The EKE is a measure for the ocean dynamics and turbulence, where u is a long term mean with $u = u' + \bar{u}$ and is strongly reduced (averaged over the top 500 m) in the experiment with lowered sea level.

$$\sigma_{\text{Eady}} = \frac{1}{\sqrt{Ri f}} \quad (4.2)$$

The Eady growth rate comprises the Richardson number which is defined as $\frac{N^2}{S^2}$, where N is the buoyancy frequency and S is the vertical shear of the geostrophic horizontal velocities

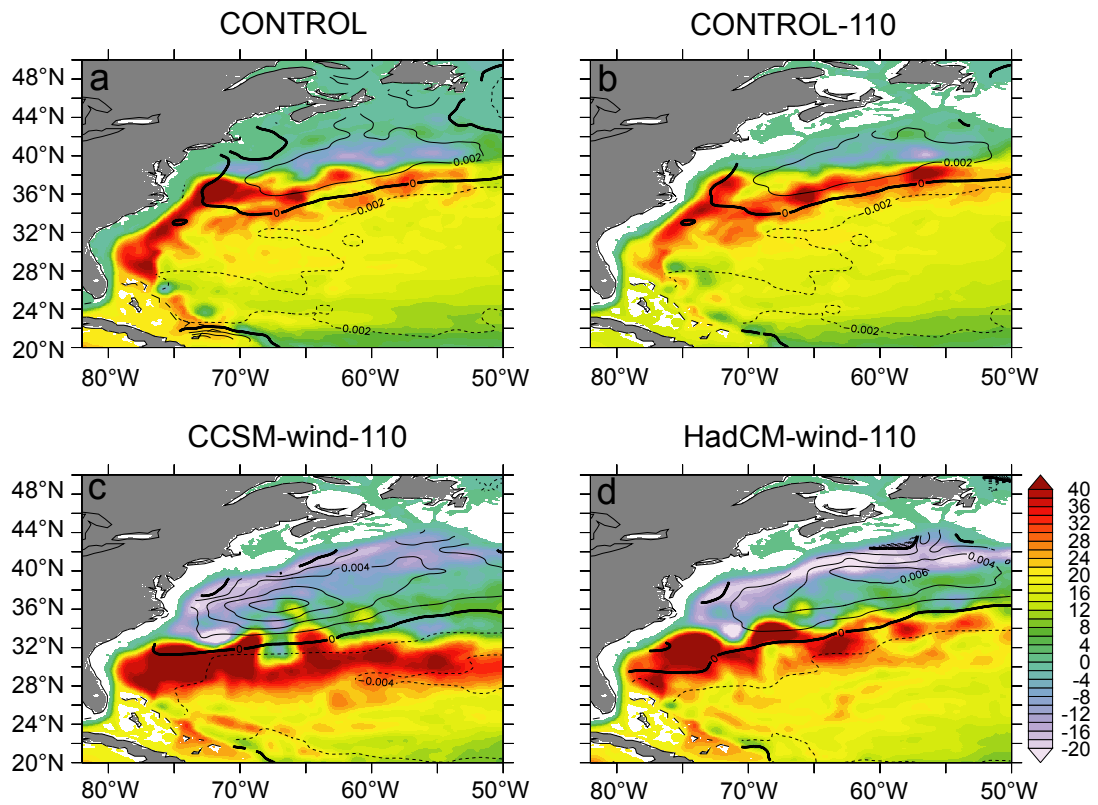


Figure 4.1: Colors display the simulated barotropic streamfunction (in Sverdrup) averaged over 5 years. In contour lines overlain the curl τ (in N/m^2) calculated from the climatological wind stress is shown whereas positive wind stress curl causes divergence in the Ekman layer and upward Ekman pumping, while negative wind stress curl causes convergence and hence Ekman suction. Curl τ was smoothed using a Hanning window.

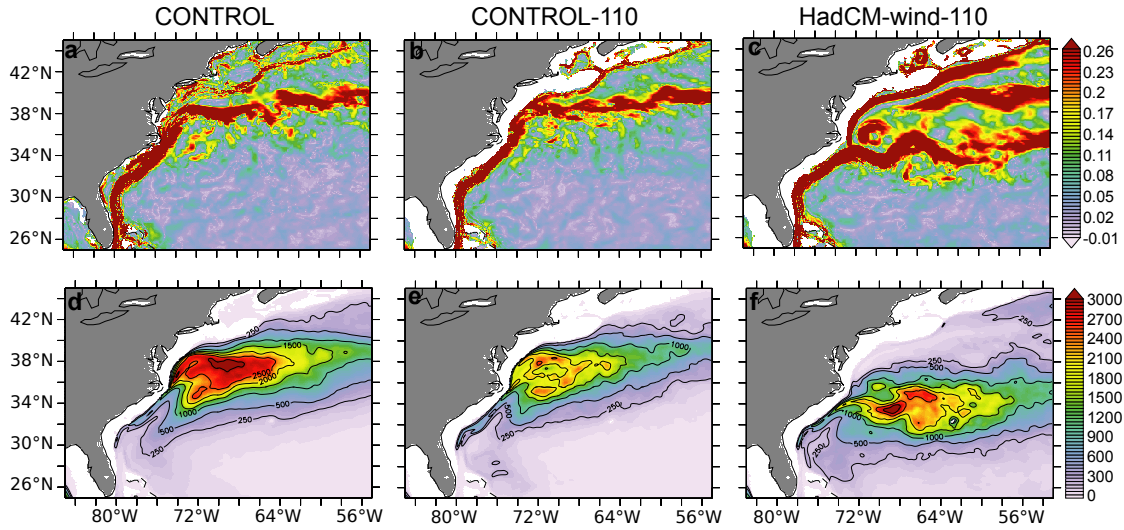


Figure 4.2: a)-c) the eddy growth rate in 1/day; d)-f) the eddy kinetic energy in cm^2/s^2 . Both parameters are averaged over the top 500 m and over 5 years.

and the Coriolis parameter f . It assesses baroclinic instability through the vertical gradient in horizontal wind speed and is therefore a measure of baroclinic stability. Fig. 4.2 b shows a slight reduction but also a slight northward shift. A calculation of the vertical eddy buoyancy gradient in the entire Gulf Stream region provided further evidence of the assumption that baroclinic instabilities were reduced in CONTROL-110 revealing a total reduction of 46%. Although these two parameters were strongly reduced (see also Tab. 4.3) their extent was almost the same as compared to CONTROL.

The present northward heat transport in the Atlantic was in good agreement to what observations suggest (Garzoli et al., 2007). The LGM Atlantic ocean transported less heat northward than in CONTROL especially in the tropics and mid-latitudes. Beyond 57°N the differences became less extensive. The decreased heat transport in the mid-latitudes and in the tropics was a consequence of the weaker meridional overturning circulation (not shown). In the north, a stronger subpolar gyre evolved with an extended northern recirculation gyre between 38°N and 55°N . The gyre heat transport in this area was increased in HadCM-wind-110 and CCSM-wind-110 expressed in elevated temperatures in the top 500 m. However, the decreased overturning during the LGM was accompanied by a decrease in the amount of heat and salt transported northwards in the tropical and mid-latitude Atlantic and possibly also influences the separation latitude of the Gulf Stream. These findings could be consolidated by a reduced Deep Western Boundary Current (DWBC), an increased Antilles Current (see Tab. 4.3) and also the reduced heat, gyre, salt and overturning transport.

The line of zero wind stress curl appeared more as a boundary between the northern

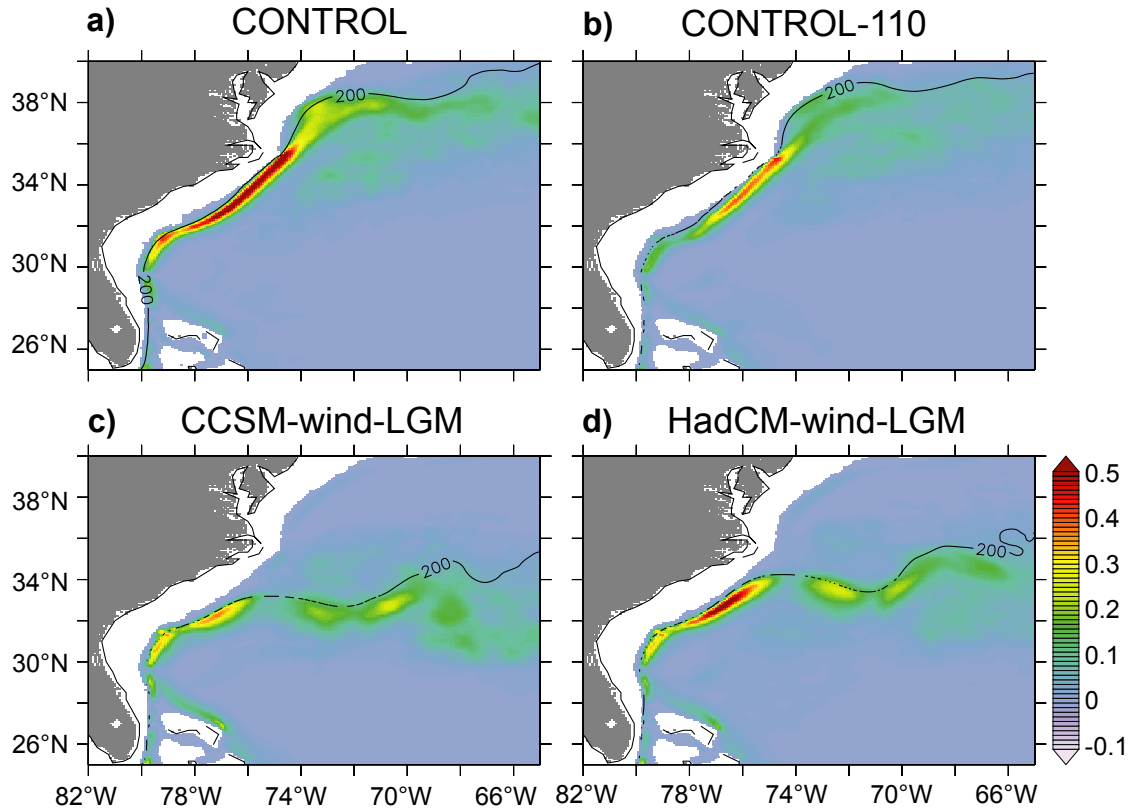


Figure 4.3: Displayed is the current speed in at 200 m water depth in m/s. The contour line show the location of the 15°C isotherm at 200 m water depth.

recirculation and the subtropical gyre in the model results (Fig. 4.1). This line of zero Ekman pumping where no convergence or divergence of water in the directly wind-forced layer occurred, coincides with the sloping of the thermoclines that became strongest in the Gulf Stream. The line of the 15°C isotherm in 200 m water depth (Fig. 4.3) matched again quite well as separation criteria. Although the separation in CONTROL occurred a little to far in the north, a striking shift in the separation latitude during the LGM could be distinguished. The separation latitude in experiment CCSM-wind-110 and HadCM-wind-110 shifted to $\sim 32^\circ\text{N}$ (Fig. 4.3). This made a latitudinal shift of the Gulf Stream towards the south by $\sim 6^\circ$ compared to CONTROL. The horizontal extent of the Gulf Stream during the glacial was also enhanced and can be seen in the barotropic streamfunction in Fig. 4.1.

The zonally averaged wind stress in CONTROL and in CONTROL-110 only deviated between 45°N and 60°N (Fig. 4.4).

The most prominent changes could be analyzed in CCSM-wind-110, where a strong southward shift of the westerly winds occurred combined with an increase in the polar easterlies and the northeast trades at tropical and mid latitudes. Stronger westerlies in

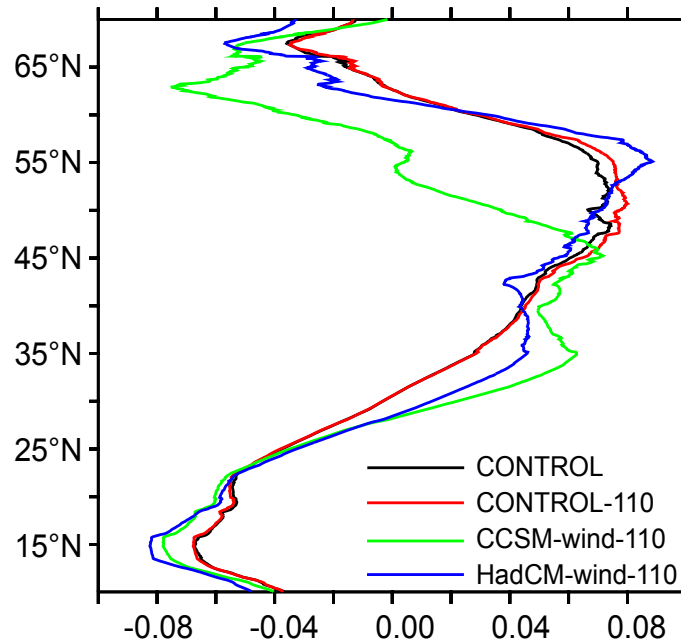


Figure 4.4: Zonally averaged wind stress for the model experiments between 10°N and 70°N in N/m^2 .

HadCM-wind-110 occurred between 48°N and 63°N and also stronger NE trades between 10°N and 25°N. In the mid latitudes a southward shift in the easterly and westerly winds could be observed, whereas in CCSM-wind-110 a more pronounced southward shift occurred.

Further, the eddy growth rate shifted towards the glacial Gulf Stream position but became also enhanced within the northern recirculation gyre (Fig. 4.2). A calculation of the vertical eddy buoyancy gradient in the entire Gulf Stream region showed a reduction by 36%. The mean EKE was also strongest in the 'new' Gulf Stream area but slightly reduced compared to CONTROL.

In addition the character after separation changed. The LGM-wind experiments displayed a more zonal Gulf Stream compared to the modern, more meridional character. This feature was more distinct in CCSM-wind-LGM than in HadCM-wind-110.

4.5 Summary and conclusions

The details of external forcings such as a reduced sea level or glacial wind and glacial sea level on the dynamics of the ocean circulation in the North Atlantic were investigated using a high resolution ocean general circulation model.

Northward heat transport decreased strongest in the tropics and mid latitudes owing to a reduced overturning and processes initiated by the LGM wind which was supported by several studies who found a reduction in SST at Blake Ridge of $\sim 3-4^{\circ}\text{C}$ (Carlson et al., 2008; Schmidt et al., 2011). This involves, that subpolar surface waters were cooler and that deep-water production was reduced as already described by Ruddiman (1977). The importance of wind stress was previously analyzed e.g. by Taylor et al. (1998), who proposed a connection between the NAO and the Gulf Stream separation latitude also showing the possible influence of stronger westerlies and trade winds during high index NAO phases. Due to the absence of glacial ice sheets in the northern hemisphere in their study they found the Gulf Stream shifting towards the north two years after phases of a high NAO index, whereas our experiments during the last ice age were influenced by the large continental ice sheets and associated stronger winds. Furthermore, the formation of a stronger northern recirculation gyre in our LGM experiments lead to a southward displacement of the Gulf Stream separation latitude. A former study by Keffer et al. (1988) supports our assumption. They also suggest that the ice sheet modified the field of Ekman pumping and a shallower overturning rate existed during the LGM also found by Vidal et al. (1997).

A southward shift of the Gulf Stream was also analyzed in a model study by Zhang (2010) during times when an anomalous cyclonic gyre propagates to the south of the Grand Banks, strengthening also the DWBC. Nevertheless, in the LGM model experiments with a similar increase in the northern recirculation gyre and an associated southward shift of the Gulf Stream we found a reduced DWBC, but therefore recirculating water masses rejoin the Antilles Current increasing its transport. Transports in Florida Straits were similar in magnitude to the present although a weaker overturning was assessed in the model experiments. However, there is no consensus about Atlantic meridional overturning circulation strength during the LGM (Lippold et al, 2012).

It is proposed that during the LGM the atmospheric circulation system was probably stronger due to the ice covered land masses. With a strengthened wind-system, the total transport was likely to be larger than today, rather than smaller (Wunsch, 2003). But Huybers et al. (2010) question also lately the conclusion that an increase in wind strength would lead to an increase in circulation strength.

The higher available potential energy in the northern recirculation gyre was shifted to the south due to the shift in the Ekman pumping derived from the wind stress curl which is positive in the northern recirculation gyre and negative in the subtropical gyre. In CCSM-wind-110 and HadCM-wind-110 higher Ekman pumping rates and therefore

higher upwelling in the northern recirculation gyre occur. The available potential energy is degraded through baroclinic instabilities which were highest in these areas and became visible in the strong eddy growth rate. The shear rate increased with the evolution of the baroclinic instabilities and build up EKE in the main Gulf Stream area. This supports the assumption that the mean EKE in the experiments was mostly influenced by the glacial wind and to a lesser extent by the lowered sea level

Previous studies have suggested that the reason for the reorientation of the Gulf Stream axis is related to atmospheric forcing, but the exact mechanism remain unclear. This study supports the assumption that winds play a crucial role for the Gulf Stream separation. The implication of these findings is that especially changes in the wind stress and to a lesser extent the changes in ocean bathymetry due to sea level drop changed the overall circulation pattern of the western North Atlantic under LGM conditions compared to the present day.

5 Conclusions and outlook

The Loop Current plays an important role transporting mass, heat, salt and other tracers into the Gulf of Mexico on one side via the YC with its irregular anticyclonic eddy shedding in the GoM and on the other side via the FC into the North Atlantic circulation. This circulation system is of major importance for the past and present climate because of its warm water transport into the northern hemisphere. Using a number of different model experiments and various observations, the dynamics of the Loop Current and adjacent seas are examined in this study. The aim of this thesis was therefore to improve the present understanding of the Loop Current and the Gulf Stream system in the past and in the present. Using a combined approach of model experiments and observations from satellites, an undersea telephone cable, and oceanographic and climatic proxy data from marine sediment cores enabled to contribute to improve the understanding of the ocean dynamics in the western subtropical North Atlantic. The role of the eddy shedding period and the decadal to interannual variability in Yucatan Channel on the Florida Straits transport and the Gulf Stream position during the LGM were investigated using an eddy-permitting OGCM at two resolutions ($1/3^\circ$ and $1/12^\circ$). The higher resolution version of the numerical model was used to better resolve the small-scale processes and also to verify the model results from the lower horizontal resolution model simulations.

In **Chapter 2**, the transport changes in the Florida Current and their relation to the ocean dynamics, especially the variability of the Loop Current and its eddy shedding into the Gulf of Mexico were discussed. The experiments were compared to the long term daily mean transport of the Florida Current inferred from voltage measurements of a deep sea telephone cable located at 27°N between Florida and the Bahamas and to sea surface height satellite data.

The main result of **Chapter 2** is that the observed low-frequency variability in the Florida Current is mostly driven by the internal dynamics related to the Loop Current eddies in the Yucatan Channel. The results of this study suggest a strong influence by the eddy shedding and to a lesser extent by the wind forcing on the Florida Straits transport, in contrast to what has been hypothesized in the past. Nevertheless, additional mechanisms might also support the eddy shedding process. Transport changes in Florida

Straits have a significant influence on the transport variability on monthly to decadal time scales. Differences (and changes) between the ring shedding period (~ 9 month) and the seasonal cycle of the Florida Straits transport (~ 12 month) lead to an interannual to decadal beat frequency, which explains large parts of the variability of the Florida Current transport in the model simulations, even exceeding atmospheric forcing variability on the considered time scales. Whenever an eddy is stationary north of the Yucatan Strait, it blocks the outflow to the North Atlantic in the model simulations and water masses recirculate into the Caribbean and are therefore reduced in the Florida Straits. A blocking mechanism is assumed to explain large parts of this variability in Florida Straits transport. A release of the blocking occurs once the eddy separates from the Loop Current or when it intrudes further northwards into the Gulf. As a consequence this process is accompanied by an increase in the Florida Straits transport. A combined comparison from observations including sea surface height data and transport estimates from the undersea telephone cable confirm the hypothesis that the Florida Straits transport can be strongly influenced by this blocking mechanism.

Although the variability of the Florida Straits transport seems to be influenced by the Loop Current eddy position, the processes that induce the separation of an eddy needs further investigations to resolve the mechanisms. The short period of lowered heat transport due to the short duration of the blocking mechanism under present day climatic conditions would only have a minor impact on the North Atlantic. Nevertheless, assuming that under different climatic conditions the blocking would occur permanently in the Yucatan Strait, the Florida Current transport would be permanently reduced transporting less heat towards Europe. An associated cooling in the North Atlantic would thus have consequences for the atmospheric and oceanic circulation system. Further research could imply extended model studies for past climates to investigate under what climatic conditions a permanent blocking was conceivable.

Chapter 3 discusses the influence of changes in wind stress forcings and sea level on the ocean dynamics according to different climatic events in the past 25 kyr. The influence of sea level changes on the heat and salt budget of the Gulf of Mexico and the associated influence of the Loop Current eddy shedding during the last glacial-interglacial cycle were investigated.

The results of this study suggest that a reduced sea level compared to the present has an important influence on the Loop Current eddy shedding. The Florida Straits and Yucatan Channel transport decreased with a decrease in sea level. Moreover, under these conditions eddy shedding was attenuated while the eddy shedding interval increased. As

a consequence, the heat and the salt transport into the Gulf of Mexico were reduced.

In other experiments with LGM wind stress, the eddy shedding was absent while Florida Straits transport increased by >80% and the heat transport into the Gulf of Mexico was accordingly reduced. It was also absent in most of the experiments with glacial wind stress and lowered sea level. Although the different wind stress products of the PMIP2 models use the same boundary conditions, applying the wind stress anomalies to our climatological forcing did not lead to a linear response. Nevertheless, if transport in Florida Straits and Yucatan Channel increases or decreases, the heat transport is very low in all experiments suggesting the absence of eddy shedding during the LGM.

Our experiments revealed a complex relationship between Yucatan Channel and Florida Straits transport, sea levels, eddy shedding, salt and surface heat fluxes. A main finding in **Chapter 3** is the proposed absence of eddy shedding during the LGM. Stronger westerlies caused an enhanced Sverdrup transport within the Subtropical Gyre leading to an increase in Florida Straits and Yucatan Strait transport with a decrease in eddy shedding with increasing transport. The heat and salt transport into the Gulf was reduced when eddy shedding was less frequent or absent. This study supports observations in the Gulf that revealing a temperature increase across the deglaciation which in turn could be related to an enhancement of the eddy shedding into the Gulf of Mexico approaching present day conditions.

The atmospheric and oceanic circulation changes during the LGM are reflected in the oxygen isotopic composition of Greenland ice cores. Recent results from corals and pollen records indicate a global $\sim 4\text{-}6^\circ\text{C}$ cooling which is also consistent with the cooler surface temperatures of the same range estimated for the northern Gulf of Mexico during the LGM. These fresher and cooler conditions in the Gulf, most likely resulted from higher fluvial discharge from the Mississippi river and less or no eddy shedding from the Loop Current. This is consistent with observations in the Gulf of Mexico which suggest an increase in SST across the deglaciation in the northern Gulf. Although little is known about the glacial atmosphere, massive wind stress changes are assumed for the LGM with a shift in the ITCZ position towards the south. This can be analyzed to a good extent from sedimental isotope records combined with Mg/Ca analysis revealing the past rainfall intensity. The elevated increase in Florida Straits and Yucatan Channel transport can be related to the wind forcing and is a common signal in all PMIP2 LGM model simulations where westerly winds are shifted equator-ward and the trade winds strengthen over the North Atlantic ocean. Further studies with a coupled model similar to PMIP2 and an idealized LGM atmospheric model resembled similar results, in which the response was

related to an equator-ward shrinking of the Hadley circulation as a response to the reduced tropical convection. The equator-ward shift in wind stress is assumed to lead to a stronger meridional gradient of the zonal wind above the subtropical gyre and thus, to an increase in the Sverdrup transport of the subtropical gyre in the North Atlantic. Since the subtropical gyre has to be in Sverdrup balance, the enhancement was also observed in the simulated depth integrated volume transport of the models used in this study.

Paleoceanographic proxy records are ambiguous concerning the LGM Florida Straits transport. While a consistent increase in the sortable silt fraction from Holocene to Glacial would support the model results, other studies assume a weaker Florida Straits transport. Nevertheless, with a strengthened atmospheric circulation system a stronger transport in the Florida Straits is more conceivable.

In **Chapter 4**, the Gulf Stream position was analyzed for the present day situation and during the LGM. The model simulations were evaluated with regard to the glacial circulation patterns in the western part of the North Atlantic and compared to paleo-proxy observations focusing on the Gulf Stream position under different atmospheric conditions and sea level.

The results of this study show a southward shift of the complete current system in the North Atlantic during the LGM. This shift is accompanied by a southward shift in the isotherms, of the line in zero wind stress curl, of the EKE and the Eady growth rate maxima. As a consequence, the Gulf Stream is also deflected towards the equator. This leads on the other hand to a change in the upwelling intensity of the northern recirculation gyre. The northern recirculation gyre is reduced in all experiments but has almost the same position compared to the present if only implementing a lowered sea level. For continuity reasons also the experiments with the lower resolution models were analyzed (not shown in manuscript 3). The same models that revealed the displacement in the high resolution simulations, indicated the southward shift in the low resolution simulation. However, the Gulf Stream shift did not occur in three of the low resolution simulations neither did the shift of the line in zero wind stress curl. This supports the hypothesis that the wind is the major driving force for the southward displacement of the Gulf Stream circulation system.

Previous studies already emphasized that wind stress plays an important role for the changes in the North Atlantic circulation system especially with regard to the position of the Gulf Stream. If the Iceland low pressure system strengthens, the Gulf Stream becomes weaker and hence the northern Atlantic cools down. Consequently the westerly winds strengthen. The cooling of the northern hemisphere and the changes in the wind system are assumed to be accompanied by a southward shift of the polar front during the

LGM that retained its modern position around ~ 6000 years BP with less pronounced re-advances afterwards. A southward shift of the currents in the North Atlantic due to this shift has been found in the paleo-records.

However, observations from paleoceanographic proxy records are scarce for the Gulf Stream axis due to the highly variable and strong current regime. The observations that exist for the glacial position of the Gulf Stream are not consistent though. Further sediment cores from the Atlantic interior between 32°N and 36°N could support our present study to estimate the latitudinal changes in the mixing zone between southern and northern source waters and therefore the past Gulf Stream position. Locations with less or preferentially undisturbed sedimentation rates are crucial for the investigations and should be drilled offshore around 65°W in the open Atlantic. To verify the stronger upwelling associated within the strengthened northern recirculation gyre one would expect higher concentration of nutrients and an abundance of certain species. This could be analyzed by drilling sediment cores north of 34°N . Further investigations are also needed to study if the wind induces a cooling in the northern recirculation gyre and therefore shifts the isotherms.

This study comprises integrated numerical ocean model results with paleoceanographic proxy data during the last 25 kyr. In summary, future work motivated by this thesis should address combined high resolution studies of observations and models in the Florida Straits and in the North Atlantic to tackle the unanswered questions and improve the understanding of ocean dynamics in the past and in the present. The conflicting observations concerning the Florida Straits transport during the LGM or the position of the Gulf Stream should be investigated carefully. A better knowledge of the general ocean circulation and mixing processes is needed to verify model results. Meso-scale and small-scale parameterization can then be applied and tested over a range of model resolutions to improve the models for future simulations.

6 Appendix

6.1 The model

The model used in this study is the FLAME (Family of Linked Atlantic Model Experiments) model and has been developed by the FLAME group (Dengg et al., 1999) and was further refined by C. Eden (see also https://ifm.zmaw.de/fileadmin/files/theoretical_oceanography/Modelldaten_CE/spflame.pdf). It is an ocean general circulation model based on the Princeton GFDL (Geophysical Fluid Dynamics Laboratory) MOM (Modular Ocean Model) code (version 2.1) (Pacanowski, 1995) and can be run on parallel high performance vector computational systems. It is discretized on an Arakawa-B-grid.

The model is a regional model of the North Atlantic spanning from 20°S to 70°N and 100°W to 16°W. It has three different spatial resolutions. The coarsest resolution is 4/3° in longitude, 4/3° $\cos(\phi)$ in latitude. The next higher spatial resolution is 1/3° resulting in a mesh size of 37 km at the equator decreasing to 26 km at the subpolar boundaries. The highest spatial resolution is 1/12° resolving 8.4 km at 25°N. The vertical is discretized in 45 non-equidistance levels in all models, with a spacing of 10 m in the uppermost level and a smooth increase to 250 m at 2500 m depth. Below 2500 m the vertical grid box thickness is a constant 250 m up to a maximum depth of 5500 m. The model topography is realistic (shown in Fig. 6.1) and is taken from ETOPO5 [NOAA, National Geophysical Data Center, Boulder, Colorado, 1988] dataset.

The lateral boundary conditions are closed with the no-slip boundary condition. The parcels that are in direct contact with the boundary have to be at rest. This leads to a gradual removal of energy. Northern and southern margins of the domain are formulated as open boundaries after Stevens (1991). The initial conditions for the northern and the southern boundaries prescribing temperature and salinity are taken from Levitus and Boyer (1998). Wind stress and heat flux of a monthly climatology were implemented, using a three year analysis performed at ECMWF by Barnier et al. (1995) to obtain a quasi dynamical equilibrium of the model. The heat flux forcing that builds the surface boundary conditions is formulated after Haney (1971):

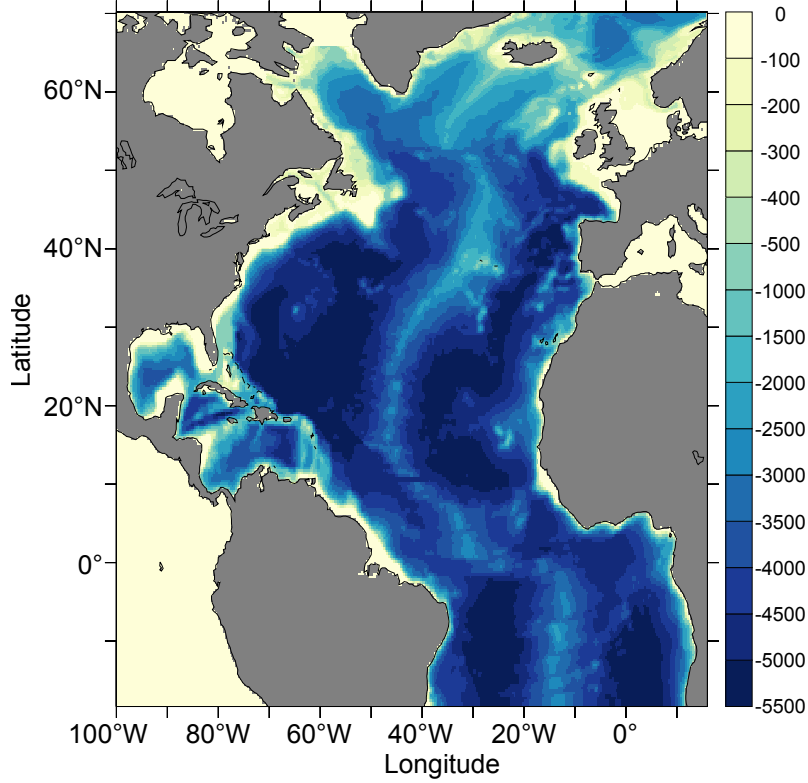


Figure 6.1: Model domain. Ocean bathymetry in m of the $1/3^\circ$ model of the Atlantic.

$$Q = Q_0 + Q_1(SST_{model} - SST_{clim}) \quad \text{with} \quad Q_1 = \left. \frac{\partial Q}{\partial SST} \right|_{SST_{clim}} \quad (6.1)$$

To the prescribed heat flux Q_0 a flux correction term is added composed of a climatological SST (SST_{clim}) that is temporally and spatially varying. The relaxation that evolves from equation 6.1 restores the model SST to a temperature T^* as follows:

$$Q = Q_1(SST_{model} - T^*) \quad \text{where} \quad T^* = SST_{clim} - Q_0/Q_1 \quad (6.2)$$

It is necessary to implement such a surface boundary condition because a relaxation of the modeled SST to a climatological SST with a fixed time scale would lead to a vanishing of surface heat flux for a realistically modeled SST.

In order to avoid the severe limitation on the time step due to the fast gravity waves a rigid lid formulation on the ocean is used as this affects the large-scale motions only slightly. Of course, wind stress and heat flux can penetrate through this 'lid'. Another advantage of using the rigid lid formulation is that a barotropic streamfunction can be

calculated. The bottom friction is parameterized as a quadratic function.

Vertical mixing (diapycnal mixing) via small scale processes like the breaking of internal waves is implemented into the model by a turbulent kinetic energy (TKE) scheme of Gaspar et al. (1990). The friction is implemented as biharmonic friction in both versions to reduce damping on scales larger than the model grid. The $1/3^\circ$ and $1/12^\circ$ models permit meso-scale eddy activity, except for an additional simulation at $1/3^\circ \cos \phi$ resolution in which we inhibit this variability by adding eddy-driven velocities to the tracer advection following Gent and McWilliams (1990) with an isopycnal thickness diffusivity of $2000 \text{ m}^2/\text{s}$ and harmonic instead of biharmonic friction. The Gent and McWilliams parameterization is also used in the non-eddy-resolving $4/3^\circ$ model version, which is, however, not discussed in this study.

6.2 Model configuration for paleoclimate experiments

A set of time slice experiments is set up changing certain boundary conditions to test the model response to different forcings. In a first set of experiments the sea level is lowered due to different climatic events in the past.

6.2.1 Sea level experiments

In a first step the sea level is reduced by eliminating the first 2, 6, 9 and 13 levels of the original vertical grid of 45 levels of the model, respectively (see also Fig. 6.2).

In all experiments we allow for a dynamical quasi-steady equilibrium of the basin-wide circulation, which the model reaches after approximately 30 model years. Due to the restricted length of the integrations, the simulations are not in equilibrium with the thermohaline surface forcing and the water mass characteristics prescribed at the open boundaries. Further, we do not have changed the thermohaline forcing in the model, i.e. it represents current climate. Therefore we do not aim to realistically simulate the response of the thermohaline circulation in our model simulation, but to focus on the response of the wind-driven, quasi-geostrophically balanced regional circulation in the Gulf of Mexico to the changes in sea level and wind stress.

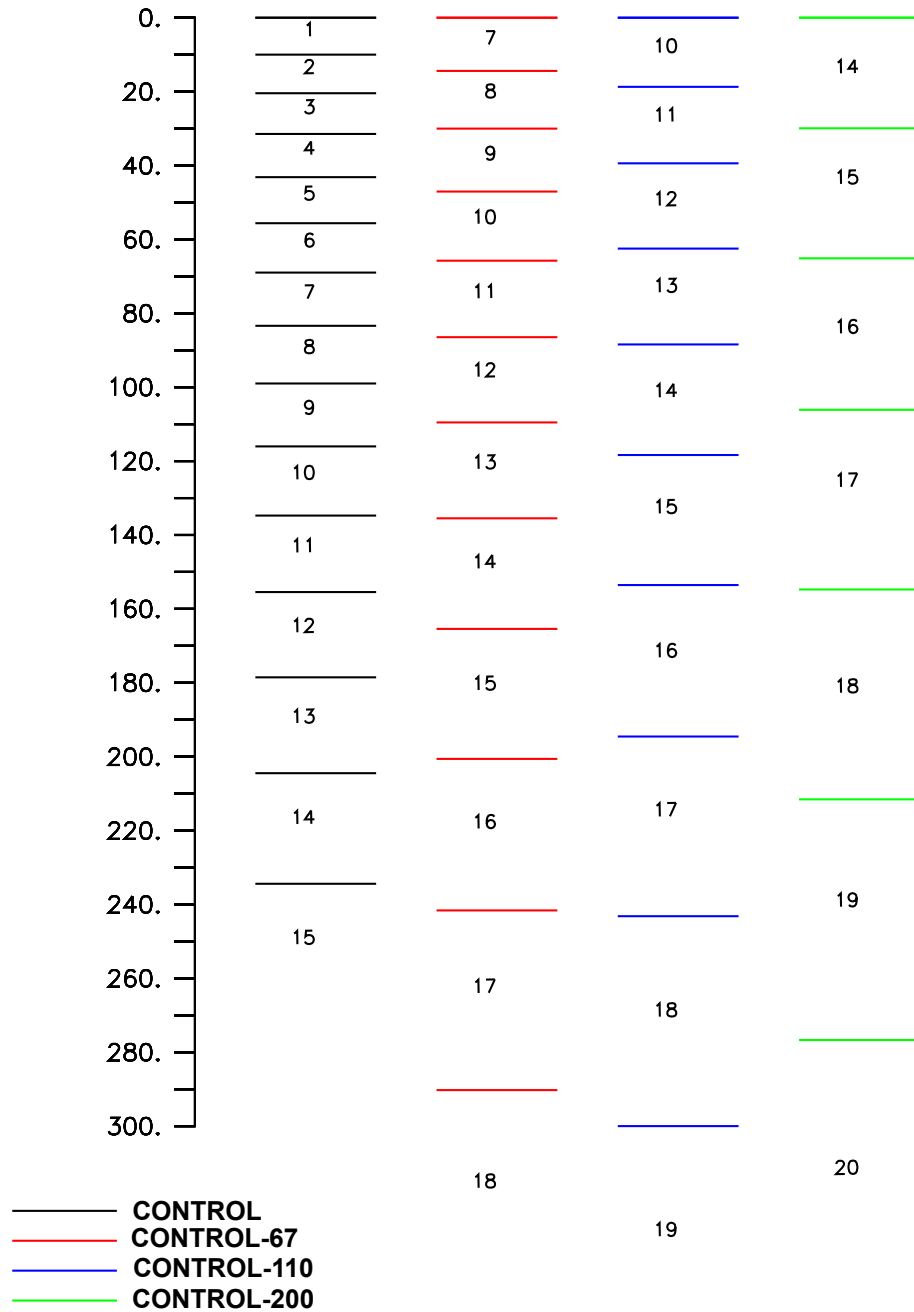


Figure 6.2: Shown is the upper rough section of the vertical model grid used in four experiments. Numerical labels of the different levels denote the k -th element of the vector $z_t()$. The levels itself represent the elements of the vector $z_w()$ (Pacanowski, 1995).

6.2.2 Wind stress experiments

In a second step an anomaly of glacial wind stress was added upon our climatological wind stress of ECMWF. To perform these experiments, data from the PMIP 2 database is used. All models are global fully coupled atmosphere-ocean-ice models. The anomalies are calculated and added to the climatological wind stress of Barnier et al. (1995).

$$LGM_{wind} = \Delta\tau = \tau_{preindustrial} - \tau_{LGM} \quad (6.3)$$

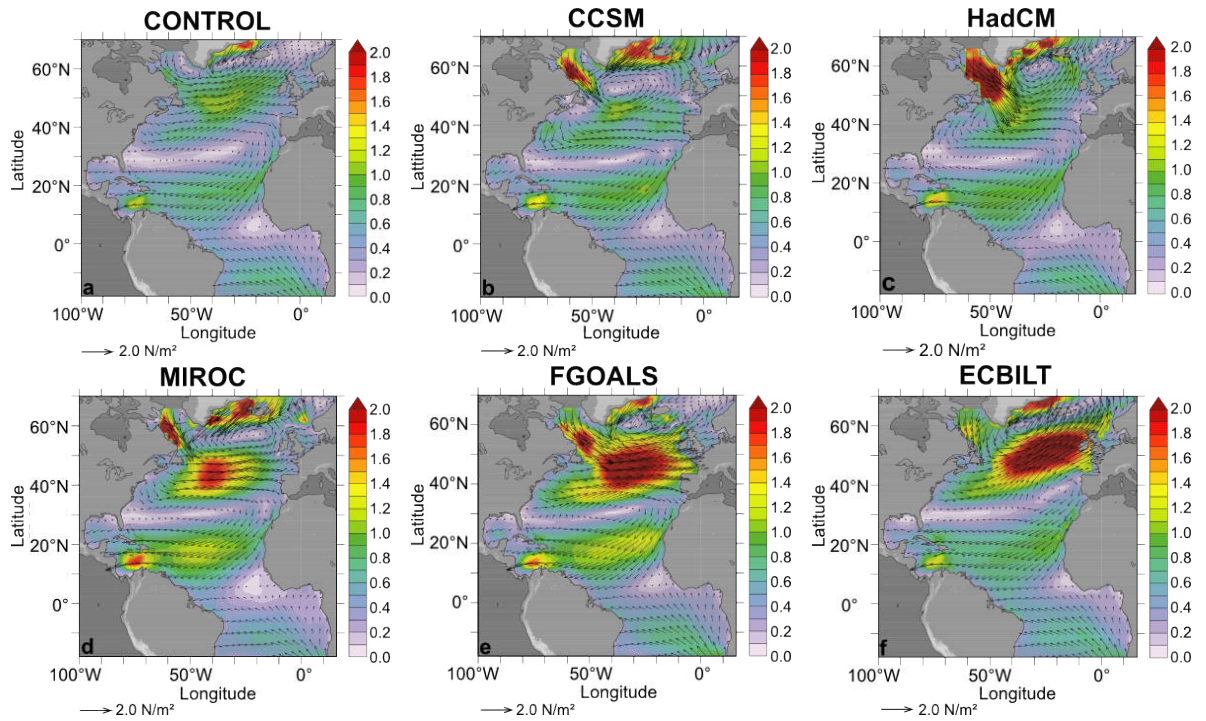


Figure 6.3: Wind stress of CONTROL (a) and the LGM wind stress anomaly that was added upon the climatological wind stress of CONTROL (i.e. the forcing) of each PMIP 2 model used in this study (b-f) in N/m^2 overlain by the wind stress vectors also displayed in N/m^2 .

The Pre-Industrial wind stress products between the individual models that take part in the PMIP project differ slightly. The LGM_{wind} is therefore the difference of each PMIP 2 product (see also Fig 6.3) between LGM (21 kyr) and the Pre-Industrial (0 kyr) to be able to directly compare the model results after adding these to our climatological wind stress. Available to us are results from the CCSM3 model (the National Center for Atmospheric Research, (Otto-Bliesner et al., 2006)), the HadCM3M2 model (Gordon et al., 2000), FGOALS-1.0g model (Yu et al., 1996), ECBilt/Louvain-la-Neuve CLIO intermedi-

ate complexity model (de Vries and Weber, 2005) and the MIROC3.2.2 (medres) model (Hasumi and Emori, 2004). The PMIP models all have the same boundary conditions. First, they all use the ICE-5G (ice sheet) and topography described in L ain e et al. (2009). This provides large continental ice sheets over North America and northern Eurasia. Second, the PMIP models all differ from present day insolation due to the differences in the Earth’s orbit during the LGM. Furthermore, the atmospheric composition measured in Greenland and Antarctic ice core records revealed a different atmospheric composition of methane and nitrous oxide for the LGM. These were also implemented into the 21 kyr forcing of the PMIP 2 models.

The model integrations of this study were performed on a NEC-SX9 at the University Kiel and on a IBM Power6 at the Deutsches Klimarechenzentrum (DKRZ), Hamburg.

List of Figures

1.1	Schematic diagram of the global meridional overturning circulation. Re-circulation loops are implemented by Lumpkin (2007). Shown are shallow surface currents (red), deep bottom currents (blue) and currents between surface and the deep ocean which are displayed by a gradient from red to blue. The Loop Current in the Gulf of Mexico belongs to the strongest surface currents feeding the Gulf Stream. Adapted from Richardson (2008).	2
1.2	Map of the Caribbean Sea and the main passages between the Atlantic Ocean and the Caribbean Sea. Displayed in blue and simplified are the main surface currents including the Florida Current, the LC = Loop Current, the YC = Yucatan Current, the Caribbean Current, the North Equatorial Current, the Guiana Current and the Antilles Current. Figure modified after (Johns et al., 2002).	3
1.3	Snapshot of barotropic streamfunction in the Gulf of Mexico in Sv (colors) from the 1/12° model (from June). The positive values indicate transports that can be associated with elevated SSH. Negative values show the cyclonic eddies and are associated with depressions. The velocity/current speed is displayed by the vectors (in cm/s).	4
1.4	Variations in climate over the last 800 kyr BP (before present). Fig. 1.4 a) shows a compilation of benthic foraminiferal $\delta^{18}\text{O}$ records revealing changes in continental glaciations and deep ocean temperature, 1.4 b) atmospheric CO_2 reconstructed from Antarctic ice cores. In 1.4 c) the Antarctic air temperature derived from the deuterium content of an Antarctic ice core is displayed and in 1.4 d) the sediment reflectance of the Antarctic sediment core ODP 1094 revealing the export of biogenic material out of the upper ocean layers. Grey shaded are warm intervals (interglacials). Figure from Sigman et al. (2010).	9

-
- 1.5 SST reconstruction from Greenland ice and from ocean sediments. The green line displays the proxy data from the Atlantic (Sachs et al., 1999), the blue line displays data from GISP2 (Greenland). Several Dansgaard-Oeschger events are indicated with numbers, Heinrich events are indicated by red squares. The thin lines displays intervals of 1470 kyr pointing to a tendency of periodic re-occurrence of the Dansgaard-Oeschger events. Figure from Rahmstorf (2002). 11
- 1.6 Surface circulation scheme of the North Atlantic Ocean from Talley et al. (2011). 12
- 1.7 Mean position of the recent ITCZ (Robinson et al., 1999) shown for July (left) and January (right). During boreal summer the ITCZ is in its northernmost position while in austral summer it is shifted to its southernmost position below 10°S. 14
- 1.8 Sea level history estimates from Barbados coral records (blue symbols), prediction with ICE-5G(VM2) model and values from Lambeck et al. (2002) (cyan) for Barbados, Bonaparte Gulf (orange), Huon Peninsula (grey), Tahiti (purple) for the Sunda Shelf (black). Light green transparent bars mark the LGM at 26 kyr, the H1 event at ~16 kyr and the YD at ~12 kyr. Small figure shows the sea level reconstruction (black line) and its error (grey surrounding) by Waelbroeck et al. (2002) for the last 120 kyr derived from oxygen isotope measurements, red line displays the prediction by the ICE-5G model. Figure modified after (Peltier et al., 2006). 16
- 1.9 Locations of relative sea-level records and the northern hemisphere continental ice sheets at the Last Glacial Maximum from Peltier et al. (2006) . . 17
- 1.10 Map of total area covered by Lake Agassiz during its 5 kyr history (Leverington et al., 2003). Arrows and letters show the main routes of overflow; NW=northwestern outlet, S=southern outlet to the Gulf of Mexico via the Minnesota and Mississippi river valleys, K=eastern outlets through Thunder Bay area, E=eastern outlets through Nipigon basin, KIN=Kinojvis outlet, HB=Hudson Bay route of final drainage. Colors are sea surface temperatures from Levitus (red = warm, blue = cold). 18
- 1.11 Major currents in the westernmost North Atlantic from Schmitz (1996). Displayed is the DWBC (Deep Western Boundary Current) in blue, the Gulf Stream in red and typical features accompanying the GS like warm core rings (WCR) and cold core rings (CCR). 21

- 2.1 Time series of volume transport between Florida and the Bahamas (79.2°W at 25.5°N) from observations (Cable) and model simulations (HI, HI-ncep, LOW, LOW-ncep, LOW-noeddy-ncep). Blue lines denote annual averages, black lines monthly averages. Note that except for Cable, arbitrary mean transports have been added to the time series in order to shift them vertically. The dashed black lines denote zero means for each experiment, respectively. Mean transports in the model simulations are listed in Table 2.1. 29
- 2.2 Lagged (negative) correlation of observed monthly mean SSH and FC transport anomalies (1992-2010). Note that negative correlation coefficients are shown to indicate the relation between positive SSH anomalies and FC transport minima. Correlations are shaded only when they are significantly different from zero with a likelihood of 95%. Also shown is the mean SSH taken from Niiler et al. (2003) as thin lines (contour distance of 10 cm) and the coastlines as thick lines. 32
- 2.3 a) Transport between Florida and Bahamas at 25.5°N in HI (in Sv). b) Monthly mean volume transport (in Sv) in HI at 24°N in the Gulf of Mexico. c)-j) Composites of monthly mean streamfunction (in Sv) and FC transport minima as indicated in a) and b) by solid dashed lines in HI for lags -3 to 0 (c-f) and lags 1 to 4 months (g-j, FC leads). In the 8 year long time series, we found 9 minima of FC transport and corresponding ring shedding. Contour interval is 5 Sv. 33
- 2.4 Two stages of LC ring shedding cycle. (a) shows a blocking situation in Yucatan Strait. (b) release of blocking together with ring shedding 35
- 2.5 a) Maxima (red circles) and minima (blue circles) in Florida Straits cable derived transport in Sv, b) a composite of SSH (in cm) derived from AVISO satellite data for all the marked minima minus maxima in Florida Straits cable derived transport, c) composite of all minima in the cable transport (blocking situation shortly before a ring is shed), and d) composite of all maxima in the cable transport (after or during a ring detachment). . . . 36

3.1	Sea surface temperatures reconstructed from marine sediment core MD02-2575 (blue) from De Soto Canyon (Nürnberg et al., 2008), EN32-PC6 (red) from Orca Basin (Flower et al., 2004) and from ODP-999 (green) from Columbia Basin (Schmidt et al., 2004) (see also Fig. 3.2 for core locations) overlain by the relative sea level curve after Waelbroeck et al. (2002) for the last 80 kyr. Grey shaded are the even marine isotope stages (MIS) representing cold glacial periods and in dark grey the Younger Dryas (YD) and the Last Glacial Maximum (LGM).	42
3.2	Wind stress for CONTROL (arrows, in N/m^2) and Ekman transport in m/year (see legend). Positive values denote Ekman suction, while negative values denote Ekman pumping. Note that the Ekman transport cannot be calculated within $\sim 5^\circ$ of the equator. Also shown are the marine sediment core locations mentioned in Fig. 3.1. The white square marks the area considered for the velocity calculations shown in Fig. 3.5.	43
3.3	Topography changes for different sea level experiments compared to CONTROL (landmasses in black). The blue line marks the coastline for a lowered sea level by 200 m (CONTROL-200). The red line is for lowered sea level by 110 m (CONTROL-110). The CONTROL-67 scenario (green) implies a lowered sea level by 67 m. CONTROL-24 has the same coast line as CONTROL.	46
3.4	Eddy separation process in CONTROL shown by sea surface elevation depicted as composite from 20 years simulation (18 events in total) in meters; contour lines are 0.8 – 1.2 meters with 10 cm interval.	49
3.5	Transect of velocities averaged between 22°N and 24°N and between 87°W and 84°W (see white square in Fig. 3.2) in m/s through Yucatan Channel for 20 model years at 200 m water depth. Shown are the experiments for lowered sea level and CONTROL (description of the experiments can be found in the text). Note the increase in eddy shedding across the deglaciation derived from these experiments. \bar{T}_{shed} is the shedding period of the LC from one eddy detachment until the next.	51
3.6	a presents a time series of speed (m/s) calculated from 10 years of daily averages at 100 m water depth averaged between 23° - 27°N ; b reveals two time series of heat transport in PW across section A-B (black line) and C (red line) calculated for the same time period; both figures show data of CONTROL.	52
3.7	Annual mean surface heat flux in W/m^2 calculated from 10 years of daily averages from CONTROL.	52

-
- 3.8 Zonal wind stress averaged between 100°W and 20°E in N/m^2 for all model experiments forced with LGM wind (colored lines) and CONTROL (black line). 55
- 3.9 Comparison between transport calculated from the Sverdrup relation (after Sverdrup (1947); panels to the left) and from the actual simulated stream function (5-yr mean Sverdrup transport; panels to the right) for CONTROL and the different LGM-wind experiments; CONTROL (A, B), CCSM-wind (C, D), HadCM-wind (E, F), MIROC-wind (G, H), FGOALS-wind (I, J), and ECBILT-wind (K, L). See text for definition of different models applied. 56
- 3.10 **a** shows the eddy shedding frequency as a function of the transport between Cuba and Florida and the sea level. The numbers next to the experiment names reveal the frequency of eddy shedding. **b** shows the surface heat flux [in PW] as a function of FS transport and eddy shedding frequency. Higher negative values denote higher surface heat flux to the atmosphere. The contour lines in both figures show linearly interpolated data. 63
- 4.1 Colors display the simulated barotropic streamfunction (in Sverdrup) averaged over 5 years. In contour lines overlain the curl τ (in N/m^2) calculated from the climatological wind stress is shown whereas positive wind stress curl causes divergence in the Ekman layer and upward Ekman pumping, while negative wind stress curl causes convergence and hence Ekman suction. Curl τ was smoothed using a Hanning window. 72
- 4.2 a)-c) the eady growth rate in 1/day; d)-f) the eddy kinetic energy in cm^2/s^2 . Both parameters are averaged over the top 500 m and over 5 years. 73
- 4.3 Displayed is the current speed in at 200 m water depth in m/s. The contour line show the location of the 15°C isotherm at 200 m water depth. 74
- 4.4 Zonally averaged wind stress for the model experiments between 10°N and 70°N in N/m^2 75
- 6.1 Model domain. Ocean bathymetry in m of the 1/3° model of the Atlantic. . 86
- 6.2 Shown is the upper rough section of the vertical model grid used in four experiments. Numerical labels of the different levels denote the k-th element of the vector $z_t()$. The levels itself represent the elements of the vector $z_w()$ (Pacanowski, 1995). 88
- 6.3 Wind stress of CONTROL (a) and the LGM wind stress anomaly that was added upon the climatological wind stress of CONTROL (i.e. the forcing) of each PMIP 2 model used in this study (b-f) in N/m^2 overlain by the wind stress vectors also displayed in N/m^2 89

List of Tables

- 2.1 Mean volume transports between Florida and the Bahamas (79.2°W ; 25.5°N) in the observations and the model experiments and standard deviations of the monthly and annual means. All values are given in Sv. 28
- 3.1 List of experiments and forcings applied and the calculated eddy shedding periods, and Florida and Yucatan Channel water mass, heat and salt transports. The Florida Straits fluxes were calculated for the area 23.17° and 24.39°N at 81.83°W (between Cuba and Florida) whereas Yucatan Channel fluxes were calculated between 87.17° and 84.5°W at 21.94°N in CONTROL. For the experiments at lowered sea level, the transports were calculated considering new coastlines due to the exposed shelf areas (see Fig. 3.3). The values are mean transports for 20 model years (1930 – 1950). The surface heat flux is calculated from 3 years of daily averages and reveals the amount of heat being delivered to the atmosphere. Higher negative values denote a higher amount of heat delivered to the atmosphere. 48
- 4.1 List of experiments and forcings applied and the calculated Florida Straits transports. The Florida Straits fluxes given in Sverdrup were calculated for the area 26°N between 79.1° and 81.1°W (between the Bahamas and Florida), Antilles Current in the area 26°N and between 76.1° and 71.6°W over the top 1000 m. Vertical eddy buoyancy was calculated between 32°N and 42°N , and between 50°W and 75°W and averaged over the top 500 m. All values are averaged over 5 model years. 69

Bibliography

- Aharon, P., 2003: Meltwater flooding events in the Gulf of Mexico revisited: Implications for rapid climate changes during the last deglaciation. *Paleoceanography*, 18, 4, doi:10.1029/2002PA000840.
- Anand, P., H. Elderfield and M. H. Conte, 2003: Calibration of Mg/Ca thermometry in planktonic foraminifera from a sediment trap time series. *Paleoceanography*, 18, 2, 1050, doi:10.1029/2002PA000846.
- Andersen, K. K., N. Azuma, J.-M. Barnola, M. Bigler, P. Biscaye, N. Caillon, J. Chappellaz, H. B. Clausen, D. Dahl-Jensen, H. Fischer and others, 2004: High-resolution record of Northern Hemisphere climate extending into the last interglacial period. *Nature*, 431, 7005, 147–151, doi:10.1038/nature02805.
- Antonov, J., S. Levitus, T. Boyer, M. Conkright, T. O'Brien, and C. Stephens, 1998: World Ocean Atlas 1998 Vol. 1: Temperature of the Atlantic Ocean. NOAA Atlas NESDIS, 27, 166.
- Atkinson, L. P., T. Berger, P. Hamilton, E. Waddell, K. Leaman, and T. N. Lee, 1995: Current meter observations in the Old Bahama Channel. *Journal of Geophys. Research*, 100, 8555–8560, doi:10.1029/95JC00586.
- Atkinson, C. P., H. L. Bryden, J. Hirschi, and T. Kanzow, 2010: On the seasonal cycles and variability of Florida Straits, Ekman and Sverdrup transports at 26°N in the Atlantic Ocean. *Ocean Science*, 6 (4), 837–859, doi:10.5194/os-6-837-2010.
- Bard, E., F. Rostek, J.-L. Turon and S. Gendreau, 2000: Hydrological impact of Heinrich Events in the Subtropical Northeast Atlantic. *Science*, 289, 1321–1323, doi:10.1126/science.289.5483.1321.
- Baringer, M., and J. Larsen, 2001: Sixteen Years of Florida Current Transport at 27° N. *Geophysical Research Letters*, 28(16), 3179–3182, doi:10.1029/2001GL013246.
- Barker, S., P. Diz, M. J. Vautravers, J. Pike, G. Knorr, I. R. Hall and W. S. Broecker, 2009: Interhemispheric Atlantic seesaw response during the last deglaciation. *Nature*, 457, 7233, 1097–1102, doi:10.1038/nature07770.

- Barnier, B., L. Siefridt, and P. Marchesiello, 1995: Thermal forcing for a global ocean circulation model using a three-year climatology of ECMWF analyses. *Journal of Marine Systems*, 6, (4), 363–380, doi:10.1016/0924-7963(94)00034-9.
- Bay, R. C., N. E. Bramall, P. B. Price, G. D. Clow, R. L. Hawley, R. Udisti and E. Castellano, 2006: Globally synchronous ice core volcanic tracers and abrupt cooling during the last glacial period. *Journal of Geophysical Research*, 111, D11, D11108, doi:10.1029/2005JD006306.
- Berger, A. L., 1978: Long-term variations of caloric insolation resulting from the Earth's orbital elements. *Quaternary Research*, 9, 2, 139–167, doi:10.1175/1520-0469(1978)035<2362:LTVODI>2.0.CO;2.
- Bindoff, N.L., J. Willebrand, V. Artale, A. Cazenave, J. Gregory, S. Gulev, K. Hanawa, C. Le Qur, S. Levitus, Y. Nojiri, C.K. Shum, L.D. Talley and A. Unnikrishnan, 2007: Observations: Oceanic Climate Change and Sea Level. *in: Climate Change 2007: The Physical Science Basis*, Contribution of Working Group I to the Fourth Assessment Report of the Intergovernmental Panel on Climate Change, [Solomon, S., D. Qin, M. Manning, Z. Chen, M. Marquis, K.B. Averyt, M. Tignor and H.L. Miller (eds.)], Cambridge University Press, Cambridge, United Kingdom and New York, NY, USA.
- Berger, A., 2009: Encyclopedia of paleoclimatology and ancient environments. *New York Springer, Encyclopedia of Earth Sciences Series*, Gornitz, V..
- Bond, G., W. Broecker, S. Johnsen, J. McManus, L. Labeyrie, J. Jouzel, G. Bonani, et al., 1993: Correlations between climate records from North Atlantic sediments and Greenland ice. *Nature*, 365(6442), 143–147, doi:10.1038/365143a0.
- Bouttes, N., D. Paillard, D. M. Roche, V. Brovkin and L. Bopp, 2011: Last Glacial Maximum CO₂ and $\delta^{13}\text{C}$ successfully reconciled. *Geophysical Research Letters*, 38, 2, doi:10.1029/2010GL044499.
- Braconnot, P., B. Otto-Bliesner, S. Harrison, S. Joussaume, J. Y. Peterschmitt, A. Abe-Ouchi, M. Crucifix, E. Driesschaert, T. Fichefet, C. Hewitt, et al., 2007a: Results of PMIP2 coupled simulations of the Mid-Holocene and Last Glacial Maximum—Part 1: experiments and large-scale features. *Climate of the Past*, 3(2), 261–277, doi:10.5194/cp-3-261-2007.
- Braconnot, P., B. Otto-Bliesner, S. Harrison, S. Joussaume, J. Y. Peterschmitt, A. Abe-Ouchi, M. Crucifix, E. Driesschaert, T. Fichefet, C. Hewitt, et al., 2007b: Results of PMIP2 coupled simulations of the Mid-Holocene and Last Glacial Maximum—Part 2:

- feedbacks with emphasis on the location of the ITCZ and mid-and high latitudes heat budget. *Climate of the Past*, 3(2), 279–296, doi:10.5194/cp-3-279-2007.
- Broccoli, A., K. Dahl, and R. Stouffer, 2006: Response of the ITCZ to Northern Hemisphere cooling. *Geophysical Research Letters*, 33, 1, doi:10.1029/2005GL024546.
- Broecker, W. S., D. M. Peteet and D. Rind, 1985: Does the ocean-atmosphere system have more than one stable mode of operation?. *Nature*, 315, 6014, 21–26, doi:10.1038/315021a0.
- Broecker, W., G. Bond, M. Klas, E. Clark and J. McManus, 1991: Origin of the northern Atlantic's Heinrich events. *Climate Dynamics*, 6, 3-4, 265–273, doi:10.1007/BF00193540.
- Broecker, W. S., 2006: Was the Younger Dryas triggered by a flood?. *Science*, 312, 1146 – 1148, doi:10.1126/science.1123253.
- Brohan, P., J. J. Kennedy, I. Harris, S. F. B. Tett and P. D. Jones, 2006: Uncertainty estimates in regional and global observed temperature changes: A new data set from 1850. *Journal of Geophysical Research*, 111, D12, D12106, doi:10.1029/2005JD006548.
- Bryan, F. O., M. W. Hecht and R.D. Smith, 2007: Resolution convergence and sensitivity studies with North Atlantic circulation models. Part I: The western boundary current system. *Ocean Modelling*, 16, 3, 141–159, doi:10.1016/j.ocemod.2006.08.005.
- Bunch, T. E., R. E. Hermes, A. M. T. Moore, D. J. Kennett, J. C. Weaver, J. H. Wittke, P. S. DeCarli, J. L. Bischoff, G. C. Hillman, G. A. Howard and others, 2012: Very high-temperature impact melt products as evidence for cosmic airbursts and impacts 12,900 years ago. *Proceedings of the National Academy of Sciences*, 109, 28, E1903–E1912, doi:10.1073/pnas.1204453109 .
- Bunge, L., J. Ochoa, A. Badan, J. Candela, and J. Sheinbaum, 2002: Deep flows in the Yucatan Channel and their relation to changes in the Loop Current extension. *Journal of Geophysical Research*, 107(10.1029), doi:10.1029/2001JC001256.
- Candela, J., J. Sheinbaum, J. Ochoa, A. Badan and R. Leben: The potential vorticity flux through the Yucatan Channel and the Loop Current in the Gulf of Mexico. *Geophys. Res. Lett.*, 29 (22), 2059, doi:10.1029/2002GL015587.
- Candela, J., S. Tanahara, M. Crepon, B. Barnier, J. Sheinbaum and others, 2003: Yucatan Channel flow: Observations versus CLIPPER ATL6 and MERCATOR PAM models. *J. Geophys. Research*, 108, 3385, 24 pp., doi:10.1029/2003JC001961.

- Carlson, A. E., P. U. Clark, B. A. Haley, G. P. Klinkhammer, K. Simmons, E. J. Brook and K. J. Meissner, 2007: Geochemical proxies of North American freshwater routing during the Younger Dryas cold event. *Proceedings of the National Academy of Sciences*, 104, 16, 6556–6561, doi:10.1073/pnas.0611313104.
- Carlson, A. E., D. W. Oppo, R. E. Came, A. N. LeGrande, L. D. Keigwin and W. B. Curry, 2008: Subtropical Atlantic salinity variability and Atlantic meridional circulation during the last deglaciation. *Geology*, 36, 12, 991–994, doi:10.1130/G25080A.1.
- Carlson, A. E., 2010: What Caused the Younger Dryas Cold Event?. *Geology*, 38, 4, 383–384, doi:10.1130/focus042010.1.
- Chang, Y. L. and L. Y. Oey, 2010: Why can wind delay the shedding of Loop Current eddies?. *J. Phys. Oceanogr.*, 40 (11), 2481–2495, doi:10.1175/2010JPO4460.1.
- Chang, Y.-L. and L.-Y. Oey, 2012: Why does the Loop Current tend to shed more eddies in summer and winter?. *Geophysical Research Letters*, 39, doi:10.1029/2011GL050773.
- Chang, Y.-L. and L.-Y. Oey, 2013: Loop Current Growth and Eddy Shedding Using Models and Observations: Numerical Process Experiments and Satellite Altimetry Data. *J. Phys. Oceanogr.*, 43, 669689, doi:10.1175/JPO-D-12-0139.1.
- Chassignet, Eric P and Garraffo, Zulema D, 2001: Viscosity parameterization and the Gulf Stream separation. in *From Stirring to Mixing in a Stratified Ocean*, Proceedings Aha Hulikoa Hawaiian Winter Workshop January 1519, 2001, edited by P. Muller and D. Henderson, pp. 3741, University of Hawaii.
- Chassignet, E. P. and D. P. Marshall, 2008: Gulf Stream separation in numerical ocean models. *Geophysical Monograph Series*, 177, 39–61, doi:10.1029/177GM05.
- Chérubin, L., Y. Morel, and E. Chassignet, 2006: Loop Current ring shedding: The formation of cyclones and the effect of topography. *J. Phys. Oceanogr.*, 36(4), 569–591, doi:10.1175/JPO2871.1.
- Chiang, J. C. H. and C. M. Bitz, 2005: Influence of high latitude ice cover on the marine Intertropical Convergence Zone. *Climate Dynamics*, 25, 5, 477–496, doi:10.1007/s00382-005-0040-5.
- Clark, P. U., R. B. Alley and D. Pollard, 1999: Northern Hemisphere ice-sheet influences on global climate change. *Science*, 286, 5442, 1104–1111, doi:10.1126/science.286.5442.1104.

- Clark, P. U., S. J. Marshall, G. K. C. Clarke, S. W. Hostetler, J. M. Licciardi J. T. Teller, 2001: Freshwater forcing of abrupt climate change during the last glaciation. *Science*, 293, 5528, 283–287, doi:10.1126/science.1062517.
- Clark, P. U., N. G. Pisias, T. F. Stocker and A. J. Weaver, 2002: The role of the thermohaline circulation in abrupt climate change. *Nature*, 415, 6874, 863–869, doi:10.1038/415863a.
- Clark, P. U., A. S. Dyke, J. D. Shakun, A. E. Carlson, J. Clark, B. Wohlfarth, J. X. Mitrovica, S. W. Hostetler and A. M. McCabe, 2009: The last glacial maximum. *Science*, 325, 5941, 710–714, doi:10.1126/science.1172873.
- Coats, D. A., 1992: The Loop Current. *Physical oceanography of the U.S. Atlantic and Eastern Gulf of Mexico*, U.S. dept of the Interior, Mineral Management Service, Atlantic OCS Region, Herndon, Va. Chapter 6.
- Cochrane, J. D., 1972: Separation of an anticyclone and subsequent developments in the Loop Current. *Contributions on the Physical Oceanography of the Gulf of Mexico*, L. R. A. Capurro and J. L. Reid, Eds., Vol. II, Gulf Publishing Co., 2, 91–106.
- Colling, A., 2001: Ocean circulation. *Open University*, Butterworth Heinemann, Walton Hall, Milton Keynes, MK7 6AA, UK.
- Cunningham, S., M. Baringer, B. Johns, J. Toole, S. Osterhaus, J. Fischer, A. Piola, E. McDonagah, S. Lozier, U. Send and others, 2010: The present and future system for measuring the Atlantic meridional overturning circulation and heat transport. *OceanObs'09*.
- Curry, R. G. and M. S. McCartney, 2001: Ocean gyre circulation changes associated with the North Atlantic Oscillation. *J. Phys. Oceanogr.*, 31, 12, 3374–3400, doi:10.1175/1520-0485(2001)031<3374:OGCCAW>2.0.CO;2.
- Czeschel, L., C. Eden, and R. Greatbatch, 2011: On the driving mechanism of the annual cycle of the Florida Current transport. *J. Phys. Oceanogr.*, 42, 824–839, doi:10.1175/JPO-D-11-0109.1.
- Dengg, J., 1993: The problem of Gulf Stream separation: A barotropic approach. *Journal of Physical Oceanography*, 23, 10, 2182–2200, doi:10.1175/1520-0485(1993)023<2182:TPOGSS>2.0.CO;2.
- Dengg, J., A. Beckmann, R. Gerdes and others, 1996: The gulf stream separation problem. *In: The Warmwatersphere of the North Atlantic Ocean*, 253–290, Gebr. Borntraeger.

- Dengg, J., C. W. Böning, U. Ernst, R. Redler and A. Beckmann, 1999: Effects of an improved model representation of overflow water on the subpolar North Atlantic, *International WOCE Newsletter*, 37, 10–15.
- Dengler, M., F. Schott, C. Eden, P. Brandt, J. Fischer, and R. Zantopp, 2004: Break-up of the Atlantic deep western boundary current into eddies at 8 S. *Nature*, 432(7020), 1018–1020, doi:10.1038/nature03134.
- de Vries, P. and S. L. Weber, 2005: The Atlantic freshwater budget as a diagnostic for the existence of a stable shut down of the meridional overturning circulation. *Geophys. Res. Letters*, 32, doi:10.1029/2004GL021450.
- DiNezio, P. N., L. J. Gramer, W. E. Johns, C. S. Meinen, and M. O. Baringer, 2009: Observed interannual variability of the Florida Current: Wind forcing and the North Atlantic Oscillation. *Journal of Physical Oceanography*, 39, 3, 721–736, doi:10.1175/2008JPO4001.1.
- Döös, K., 1995: Interocean exchange of water masses. *Journal of Geophysical Research*, 100, C7, 13499–13514, doi:10.1029/95JC00337.
- Eady, E. T., 1949: Long waves and cyclone waves. *Tellus*, 1, 3, 33–52, doi:10.1111/j.2153-3490.1949.tb01265.x.
- Eden, C. and C. Böning, 2002: Sources of eddy kinetic energy in the Labrador Sea. *J. Phys. Oceanogr.*, 32 (12), 3346–3363, doi:10.1175/1520-0485(2002)032<3346:SOEKEI>2.0.CO;2.
- Eden, C. and H. Dietze, 2009: Effects of mesoscale eddy/wind interactions on biological new production and eddy kinetic energy. *J. Geophys. Res.-Oceans*, 114, C5, 23, DOI:10.1029/2008JC005129.
- Eden, C., and D. Olbers, 2010: Why western boundary currents are diffusive: A link between bottom pressure torque and bolus velocity. *Ocean Modeling*, 32(1-2), 14–24, doi:10.1016/j.ocemod.2009.07.003.
- Eden, C., R. Greatbatch, and Böning, C.W., 2004: Adiabatically correcting an eddy-permitting model using large-scale hydrographic data: Application to the Gulf Stream and the North Atlantic Current. *J. Phys. Oceanogr.*, 34(4), 701–719, doi:10.1175/1520-0485(2004)034<0701:ACAEMU>2.0.CO;2.
- Eden, C., 2007: Eddy length scales in the North Atlantic Ocean. *Journal of Geophysical Research*, 112, C6, DOI:10.1029/2006JC003901.

- Edwards, R. L., J. W. Beck, G. S. Burr, D. J. Donahue, J. M. A. Chappell, A. L. Bloom, E. R. M. Druffel and F. W. Taylor, 1993: A Large Drop in Atmospheric $^{14}\text{C}/^{12}\text{C}$ and Reduced Melting in the Younger Dryas, Documented with ^{230}Th Ages of Corals. *Science*, 260, 962–962, doi: 10.1126/science.260.5110.962.
- Elliott, B., 1982: Anticyclonic rings in the Gulf of Mexico. *J. Phys. Oceanogr*, 12(11), 1292–1309, doi:10.1175/1520-0485(1982)012<1292:ARITGO>2.0.CO;2.
- Ezer, T., L.-Y. Oey, H.-C. Lee and W. Sturges, 2003: The variability of currents in the Yucatan Channel: Analysis of results from a numerical ocean model. *Journal of Geophysical Research*, 108, C1, 3012, doi:10.1029/2002JC001509.
- Fairbanks, R.G., 1989: A 17,000-year glacio-eustatic sea level record: influence of glacial melting rates on the Younger Dryas event and deep-ocean circulation. *Nature*, 342, 6250, 637–642, doi:10.1038/342637a0.
- Firestone, R. B., A. West, J. P. Kennett, L. Becker, T. E. Bunch, Z. S. Revay, P. H. Schultz, T. Belgya, D. J. Kennett, J. M. Erlandson and others, 2007: Evidence for an extraterrestrial impact 12,900 years ago that contributed to the megafaunal extinctions and the Younger Dryas cooling. *Proceedings of the National Academy of Sciences*, 104, 41, 16016–16021, doi:10.1073/pnas.0706977104.
- Flower, B.P., D. W. Hastings, H. W. Hill and T. M. Quinn, 2004: Phasing of deglacial warming and Laurentide Ice Sheet meltwater in the Gulf of Mexico. *Geology*, 32, 7, doi:10.1130/G20604.1.
- Franke, J., A. Paul and M. Schulz, 2008: Modeling variations of marine reservoir ages during the last 45 000 years. *Climate of the Past Discussions*, 4, 1, 81–110, doi:10.5194/cpd-4-81-2008.
- Frankignoul, C., G. de Coëtlogon, T. M. Joyce and S. Dong, 2001: Gulf Stream Variability and Ocean-Atmosphere Interactions*. *Journal of physical Oceanography*, 31, 12, 3516–3529, doi:10.1175/1520-0485(2002)031<3516:GSVAOA>2.0.CO;2.
- Fratantoni, P. S., T. N. Lee, G. P. Podesta and F. Muller-Karger, 1998: The influence of Loop Current perturbations on the formation and evolution of Tortugas eddies in the southern Straits of Florida. *Journal of Geophysical Research*, 103, C11, doi:10.1029/98JC02147.
- Fuglister, F. C. and Worthington, L. V., 1951: Some Results of a Multiple Ship Survey of the Gulf Stream*. *Tellus*, 3, 1, 1–14, doi:10.1111/j.2153-3490.1951.tb00771.x.

- Gangopadhyay, A., P. Cornillon and D. R. Watts, 1992: A test of the Parsons-Veronis hypothesis on the separation of the Gulf Stream. *Journal of Physical Oceanography*, 22, 1286–1286, doi:10.1175/1520-0485(1992)022<1286:ATOTPH>2.0.CO;2.
- Garzoli, S. L. and M. O. Baringer, 2007: Meridional heat transport determined with expandable bathythermographs Part II: South Atlantic transport. *Deep Sea Research Part I: Oceanographic Research Papers*, 54, 8, 1402–1420, doi:10.1016/j.dsr.2007.03.011.
- Gaspar, P., Y. Grégoris, and J. M. Lefevre, 1990: A simple eddy kinetic energy model for simulations of the oceanic vertical mixing: Tests at station Papa and long-term upper ocean study site. *J. Geophys. Res.*, 95 (C9), 16179–16193, doi:10.1029/JC095iC09p16179.
- Gent, P. R. and J. C. McWilliams, 1990: Isopycnal mixing in ocean circulation models. *J. Phys. Oceanogr.*, 20 (1), 150–155, doi:10.1175/1520-0485(1990)020<0150:IMIOCM>2.0.CO;2.
- Gordon, A. L., 1986: Interocean exchange of thermocline water. *Journal of Geophysical Research: Oceans (1978–2012)*, 91, C4, 5037–5046, doi:10.1029/JC091iC04p05037.
- Gordon, C., C. Cooper, C. A. Senior, H. Banks, J. M. Gregory, T. C. Johns, J. F. B. Mitchell and R.A. Wood, 2000: The simulation of SST, sea ice extents and ocean heat transports in a version of the Hadley Centre coupled model without flux adjustments. *Climate Dynamics*, 16(2/3), 147–168, doi:10.1007/s003820050010.
- Grootes, P. M., M. Stuiver, J. W. C. White, S. Johnsen and J. Jouzel, 1993: Comparison of oxygen isotope records from the GISP2 and GRIP Greenland ice cores. *Nature*, 366, 552554, doi:10.1038/366552a0.
- Grousset, F. E., M. Parra, A. Bory, P. H. Martinez, P. H. Bertrand, G. Shimmield and R. M. Ellam, 1998: Saharan wind regimes traced by the Sr–Nd isotopic composition of subtropical Atlantic sediments: last glacial maximum vs today. *Quaternary Science Reviews*, 17, 4-5, 395–409, doi:10.1016/S0277-3791(97)00048-6.
- Grousset, F. E., C. Pujol, L. Labeyrie, G. Auffret and A. Boelaert, 2000: Were the North Atlantic Heinrich events triggered by the behavior of the European ice sheets?. *Geology*, 28, 2, 123–126, doi: 10.1130/0091-7613(2000).
- Haidvogel, D. B., J. C. McWilliams and P. R. Gent, 1992: Boundary current separation in a quasigeostrophic, eddy-resolving ocean circulation model. *Journal of Physical Oceanography*, 22, 8, 882–902, doi:10.1175/1520-0485(1992)022<0882:BCSIAQ>2.0.CO;2.

- Hamilton, P., T. J. Berger, and W. Johnson, 2002: On the structure and motions of cyclones in the northern Gulf of Mexico. *J. Geophys. Res.*, 107, (C12), 3208, doi:10.1029/1999JC000270.
- Hamilton, P. and T. N. Lee, 2005: Eddies and jets over the slope of the northeast Gulf of Mexico. *Geophysical Monograph-American Geophysical Union*, 161, 123–142, doi:10.1029/161GM010.
- Haney, Robert L., 1971: Surface thermal boundary condition for ocean circulation models. *Journal of Physical Oceanography*, 1, 4, 241–248 doi: 10.1175/1520-0485(1971)001<0241:STBCFO>2.0.CO;2.
- Hansen, D. V., 1970: Gulf Stream meanders between Cape Hatteras and the Grand Banks. *newblockDeep Sea Research and Oceanographic Abstracts*, 17, 3, 495–511, doi:10.1016/0011-7471(70)90064-1.
- Hasumi, H. and S. Emori, 2004: K-1 coupled GCM (MIROC) description. *K-1 Tech. Report 1*, Centre for Climate Syst. Research, University of Tokyo, 1–34.
- Haug, G., K. Hughen, D. Sigman, L. Peterson, and U. Rohl, 2001: Southward migration of the intertropical convergence zone through the Holocene. *Science*, 293(5533), 1304–1308, doi:10.1126/science.1059725.
- Hays, James D and Imbrie, John and Shackleton, Nicolas J and others, 1976: Variations in the Earth's orbit: Pacemaker of the ice ages. *American Association for the Advancement of Science*1976.
- Heinrich, H., 1988: Origin and consequences of cyclic ice rafting in the northeast Atlantic Ocean during the past 130,000 years. *Quaternary research*, 29, 2, 142–152, doi:10.1016/0033-5894(88)90057-9.
- Hewitt, C. D., A. J. Broccoli, J. F. B. Mitchell and R. J. Stouffer, 2001: title=A coupled model study of the last glacial maximum: Was part of the North Atlantic relatively warm?. *Geophysical Research Letters*, 28, 8, 1571–1574, doi: 10.1029/2000GL012575.
- Hill, H.W. and B.P. Flower, T.M. Quinn, D.J. Hollander and T.P. Guilderson, 2006: Laurentide Ice Sheet meltwater and abrupt climate change during the last glaciation. *Paleoceanography*, 21(1), doi:10.1029/2005PA001186.
- Hughen, K. A., J. T. Overpeck, S. J. Lehman, M. Kashgarian, J. Southon, L. C. Peterson, R. Alley and D. M. Sigman, 1998: Deglacial changes in ocean circulation from an extended radiocarbon calibration. *Nature*, 391, 6662, 65–68, doi:10.1038/34150.

- Hughes, C., and B. de Cuevas, 2001: Why western boundary currents in realistic oceans are inviscid: A link between form stress and bottom pressure torques. *J. Phys. Oceanogr.*, 31(10), 2871–2885, doi:10.1175/1520-0485(2001)031<2871:WWBCIR>2.0.CO;2.
- Hurlburt, H., and J. Thompson, 1980: A numerical study of Loop Current intrusions and eddy shedding. *Journal of Physical Oceanography*, 10(10), 1611–1651, doi: http://dx.doi.org/10.1175/1520-0485(1980)010<1611:ANSOLC>2.0.CO;2.
- Huybers, P., and C. Wunsch, 2010: Paleophysical Oceanography with an Emphasis on Transport Rates. *Annual Review of Marine Science*, 2, 1–34, doi:10.1146/annurev-marine-120308-081056.
- Ionita, D. A., E. Di Lorenzo and J. Lynch-Stieglitz, 2009: Effect of lower sea level on geostrophic transport through the Florida Straits during the Last Glacial Maximum. *Paleoceanography*, 24, doi:10.1029/2009PA001820.
- Johns, W. E., T. J. Shay, J. M. Bane and D. R. Watts, 1995: Gulf Stream structure, transport, and recirculation near 68 W. *Journal of Geophysical Research: Oceans (1978–2012)*, 100, C1, 817–838, doi:10.1029/94JC02497.
- Johns, W. E., T. L. Townsend, D. M. Fratantoni and W. D. Wilson, 2002: On the Atlantic inflow to the Caribbean Sea. *Deep Sea Research Part I: Oceanographic Research Papers*, 49, 2, 211–243, doi:10.1016/S0967-0637(01)00041-3.
- Kalnay, E., et al., 1996: The NCEP/NCAR 40-Year Reanalysis Project. *Bull. Amer. Meteor. Soc.*, 77, 437–471, doi:10.1175/1520-0477(1996)077<0437:TNYRP>2.0.CO;2.
- Kanzow, T., S. Cunningham, D. Rayner, J. Hirschi, W. Johns, M. Baringer, H. Bryden, L. Beal, C. Meinen, and J. Marotzke, 2007: Observed Flow Compensation Associated with the MOC at 26.5° N in the Atlantic. *Science*, 317(5840), 938, doi:10.1175/2009JPO4185.1.
- Kanzow, T., H. L. Johnson, D. P. Marshall, S. A. Cunningham, J. J. M. Hirschi, OI: 10.1175/2009JPO4185.1 A. Mujahid, H. L. Bryden, and W. E. Johns, 2009: Basinwide integrated volume transports in an eddy-filled ocean. *J. Phys. Oceanogr.*, 39 (12), 3091–3110, doi:10.1175/2009JPO4185.1.
- Keeling, C. D., R. B. Bacastow, A. F. Carter, S. C. Piper, T. P. Whorf, M. Heimann, W. G. Mook and H. Roeloffzen, 1989: A three-dimensional model of atmospheric CO₂ transport based on observed winds: 1. Analysis of observational data. *Aspects of Climate Variability in the Pacific and the Western Americas, Geophys. Monogr. Ser.*, 55, 165–236.

- Keffer, T., D. G. Martinson and B. H. Corliss, 1988: The position of the Gulf Stream during Quaternary glaciations. *Science*, 241, 4864, 440–442, doi: 10.1126/science.241.4864.440.
- Kim, S.-J., G. Flato, G. Boer and N. McFarlane, 2002: A coupled climate model simulation of the Last Glacial Maximum, Part 1: transient multi-decadal response. *Climate Dynamics*, 19, 5-6, 515–537, doi:10.1007/s00382-002-0243-y.
- Koutavas, A. and J. Lynch-Stieglitz, 2005: Variability of the marine ITCZ over the eastern Pacific during the past 30,000 years: Regional perspective and global context. *The Hadley Circulation: Present Past and Future*, Chapter 12, 347–369, doi:10.1007/978-1-4020-2944-8_12.
- Kuhlbrodt, T., A. Griesel, M. Montoya, A. Levermann, M. Hofmann, and S. Rahmstorf, 2007: On the driving processes of the Atlantic meridional overturning circulation, *Reviews of Geophysics*, 45.
- Kraus, E. B. and J. S. Turner, 1967: A one-dimensional model of the seasonal thermocline II. The general theory and its consequences. *Tellus*, 19 (1), 98–106, doi:10.1111/j.2153-3490.1967.tb01462.x.
- Kuhlemann, J., E. J. Rohling, I. Krumrei, P. Kubik, S. Ivy-Ochs and M. Kucera, 2008: Regional synthesis of Mediterranean atmospheric circulation during the last glacial maximum. *Science*, 321, 5894, 1338–1340, doi: 10.1126/science.1157638.
- Kujau, A., D. Nürnberg, C. Zielhofer, A. Bahr and U. Röhl, 2010: Mississippi River discharge over the last ~560,000 years—Indications from X-ray fluorescence core-scanning. *Palaeogeography, Palaeoclimatology, Palaeoecology*, 298(3-4), 311–318, doi:10.1016/j.palaeo.2010.10.005.
- Jansen, E., J. Overpeck, K. R. Briffa, J.-C. Duplessy, F. Joos, V. Masson-Delmotte, D. Olago, B. Otto-Bliesner, W. R. Peltier, S. Rahmstorf, R. Ramesh, D. Raynaud, D. Rind, O. Solomina, R. Villalba and D. Zhang, 2007: Palaeoclimate. In: *Climate Change 2007: The Physical Science Basis.. Contribution of Working Group I to the Fourth Assessment Report of the Intergovernmental Panel on Climate Change*, Solomon, S., D. Qin, M. Manning, Z. Chen, M. Marquis, K.B. Averyt, M. Tignor and H.L. Miller (eds.), Cambridge University Press, Cambridge, United Kingdom and New York, NY, USA.
- Laîné, A., M. Kageyama, D. Salas-Mélia, A. Voldoire, G. Rivière, G. Ramstein, S. Planton, S. Tyteca, and J. Peterschmitt, 2009: Northern hemisphere storm tracks during the last glacial maximum in the PMIP2 ocean-atmosphere coupled models: energetic study,

- seasonal cycle, precipitation. *Climate Dynamics*, 32(5), 593–614, doi: 10.1007/s00382-008-0391-9.
- Lambeck, K., Y. Yokoyama and T. Purcell, 2002: Into and out of the Last Glacial Maximum: sea-level change during Oxygen Isotope Stages 3 and 2. *Quaternary Science Reviews*, 21, 1, 343–360, doi:10.1016/S0277-3791(01)00071-3.
- Larsen, J., and T. Sanford, 1985: Florida Current volume transports from voltage measurements. *Science*, 227(4684), 302, doi:10.1126/science.227.4684.302.
- Larsen, J. C., 1992: Transport and heat flux of the Florida current at 27 degrees N derived from cross-stream voltages and profiling data: Theory and observations. *Philosophical Transactions: Physical Sciences and Engineering*, 338, 169–236, doi:10.1098/rsta.1992.0007.
- Lea, D. W., D. K. Pak and H. J. Spero, 2000: Climate impact of late Quaternary equatorial Pacific sea surface temperature variations. *Science*, 289, 5485, 1719–1724, doi:10.1126/science.289.5485.1719.
- Lea, D. W., D. K. Pak, L. C. Peterson and K. A. Hughen, 2003: Synchronicity of tropical and high-latitude Atlantic temperatures over the last glacial termination. *Science*, 301, 1361–1364, doi:10.1126/science.1088470.
- Leaman, K. D., P. S. Vertes, L. P. Atkinson, T. N. Lee, P. Hamilton and E. Waddell, 1995: Transport, potential vorticity, and current/temperature structure across Northwest Providence and Santaren Channels and the Florida Current off Cay Sal Bank. *Journal of Geophysical Research*, 100, C5, 8561–8569, doi:10.1029/94JC01436.
- Leben, R. R., 2005: Altimeter-derived loop current metrics. *Geophysical Monograph*, 161, 181–202, doi:10.1029/161GM15.
- LeGrand, P. and C. Wunsch, 1995: Constraints from paleotracer data on the North Atlantic circulation during the last glacial maximum. *Paleoceanography*, 10, 6, 1011–1045, doi:10.1029/95PA01455.
- LeGrande, A. N. and J. Lynch-Stieglitz, 2007: Surface currents in the western North Atlantic during the Last Glacial Maximum. *Geochemistry Geophysics Geosystems*, 8, 1, doi:10.1029/2006GC001371.
- Leverington, D. W. and J. T. Teller, 2003: Paleotopographic reconstructions of the eastern outlets of glacial Lake Agassiz. *Canadian Journal of Earth Sciences*, 40, 9, 1259–1278, doi:10.1139/e03-043.

- Levitus, S., and T. Boyer, 1998: *World Ocean Database 1998*, 1.
- Li, C. and D. S. Battisti, 2008: Reduced Atlantic storminess during Last Glacial Maximum: Evidence from a coupled climate model. *Journal of Climate*, 21, 14, 3561–3579, doi:10.1175/2007JCLI2166.1.
- Lin, Y., R. J. Greatbatch, and J. Sheng, 2009: A model study of the vertically integrated transport variability through the Yucatan Channel: Role of Loop Current evolution and flow compensation around Cuba. *J. Geophys. Res. -Oceans*, 114, C08003, doi:10.1029/2008JC005199.
- Lin, Y., R. J. Greatbatch, and J. Sheng, 2010: The influence of Gulf of Mexico Loop Current intrusion on the transport of the Florida Current. *Ocean Dynamics*, pp. 1–10, doi:10.1007/s10236-010-0308-0.
- Lippold, J., Y. Luo, R. Francois, S. E. Allen, J. Gherardi, S. Pichat, B. Hickey, and H. Schulz, 2012: Strength and geometry of the glacial Atlantic Meridional Overturning Circulation. *Nature Geoscience*, 1–4, doi:10.1038/ngeo1608.
- Lynch-Stieglitz, J., W. Curry, and N. Slowey, 1999: Weaker Gulf Stream in the Florida Straits during the last glacial maximum. *Nature*, 402, 644–648, doi:10.1038/45204.
- Lynch-Stieglitz, J., M. W. Schmidt and W. B. Curry, 2011: Evidence from the Florida Straits for Younger Dryas ocean circulation changes. *Paleoceanography*, 26, doi:10.1029/2010PA002032.
- Marotzke, J., 2000: Abrupt climate change and thermohaline circulation: Mechanisms and predictability. *Proceedings of the National Academy of Sciences*, 97, 4, 1347, doi:10.1073/pnas.97.4.1347.
- Matsumoto, K., and J. Lynch-Stieglitz, 2003: Persistence of Gulf Stream separation during the Last Glacial Period: Implications for current separation theories. *J. Geophys. Res.*, 108(C6), 3174, doi:10.1029/2001JC000861.
- Mayewski, P. A., L. D. Meeker, S. Whitlow, M. S. Twickler, M. C. Morrison, R. B. Alley, P. Bloomfield, K. Taylor and others, 1993: The atmosphere during the Younger Dryas. *Science*, 261, 5118, 195, doi:10.1126/science.261.5118.195.
- McManus, J. F., R. Francois, J. M. Gherardi, L. D. Keigwin and S. Brown-Leger, 2004: Collapse and rapid resumption of Atlantic meridional circulation linked to deglacial climate changes. *Nature*, 428, 6985, 834–837, doi:10.1038/nature02494.

- Meinen, C. S., M. O. Baringer, and R. F. Garcia, 2010: Florida Current transport variability: An analysis of annual and longer-period signals. *Deep Sea Res. Part I: Oceanographic Research Papers*, 57 (7), 835–846, doi: 10.1016/j.dsr.2010.04.001.
- Mildner, T. C., C. Eden and L. Czeschel, 2012: Florida Straits transport variability driven by internal ocean dynamics. paper presented at *16th Ocean Science Meeting*, February 20th - 24th, Salt Palace Convention Center, Salt Lake City, Utah, USA.
- Minobe, S., A. Kuwano-Yoshida, N. Komori, S.-P. Xie and R. J. Small, 2008: Influence of the Gulf Stream on the troposphere. *Nature*, 452, 7184, 206–209, doi:10.1038/nature06690.
- Molinari, R. L., G. A. Maul, F. Chew, W. D. Wilson, M. Bushnell, D. Mayer, K. Leaman, F. Schott, T. Lee, R. Zantopp and others, 1985: Subtropical Atlantic climate studies - Introduction. *Science*, 227, 4684, 292–295, doi:10.1126/science.227.4684.292.
- Monnin, E., A. Indermühle, A. Dällenbach, J. Flückiger, B. Stauffer, T. F. Stocker, D. Raynaud and J.-M. Barnola, Jean-Marc, 2001: Atmospheric CO₂ concentrations over the last glacial termination. *Science*, 291, 5501, 112–114, doi:10.1126/science.291.5501.112.
- Moore, J. K., M. R. Abbott and J. G. Richman, 1999: Location and dynamics of the Antarctic Polar Front from satellite sea surface temperature data. *Journal of Geophysical Research: Oceans (1978–2012)*, 104, C2, 3059–3073, doi:10.1029/1998JC900032.
- Morey, S. L., P. J. Martin, J. J. O'Brien, A. A. Wallcraft and J. Zavala-Hidalgo, 2003: Export pathways for river discharged fresh water in the northern Gulf of Mexico. *Journal of Geophysical Research: Oceans*, 108, C10, doi:10.1029/2002JC001674.
- Munday, David R and Marshall, David P., 2005: On the separation of a barotropic western boundary current from a cape. *Journal of Physical Oceanography*, 35, 10, 1726–1743, doi:10.1175/JPO2783.1.
- Munk, W. H., 1950: On the wind-driven ocean circulation. *J. Meteor.*, 7, 2, 79–93, doi:10.1175/1520-0469(1950)007<0080:OTWDOC>2.0.CO;2.
- Munk, W. and C. Wunsch, 1998: Abyssal recipes II: energetics of tidal and wind mixing. *Deep-Sea Research Part I*, 45, 12, 1977–2010, doi:10.1016/S0967-0637(98)00070-3.
- Murakami, S., R. Ohgaito, A. Abe-Ouchi, M. Crucifix, and B. Otto-Bliesner, 2008: Global-Scale Energy and Freshwater Balance in Glacial Climate: A Comparison of Three PMIP2 LGM Simulations. *Journal of Climate*, 21, 5008–5033, doi:10.1175/2008JCLI2104.1.

- Niiler, P. P. and W. S. Richardson, 1973: Seasonal variability of the Florida Current. *Journal of Mar. Research*, 31, 3, 144–167, doi:10.1029/2003GL018628.
- Niiler, P. P., N. Maximenko and J. C. McWilliams, 2003: Dynamically balanced absolute sea level of the global ocean derived from near-surface velocity observations. *Geophysical Research Letters*, 30, 22, doi:10.1029/2003GL018628.
- Nof, D., and T. Pichevin, 2001: The ballooning of outflows. *J. Phys. Oceanogr*, 31(10), 3045–3058, doi:10.1175/1520-0485(2001)031<3045:TBOO>2.0.CO;2.
- Nürnberg, D., M. Ziegler, C. Karas, R. Tiedemann, and M. Schmidt, 2008: Interacting Loop Current variability and Mississippi River discharge over the past 400 kyr. *Earth and Planetary Science Letters*, 272,1-2, 278–289, doi:10.1016/j.epsl.2008.04.051.
- Ochoa, J., J. Sheinbaum, A. Badan, J. Candela and D. Wilson, 2001: Geostrophy via potential vorticity inversion in the Yucatan Channel. *Journal of Marine Research*, 59(5), 725–747, doi:10.1357/002224001762674917.
- Oey, L., T. Ezer and H. Lee, 2005: Loop Current, rings and related circulation in the Gulf of Mexico: A review of numerical models and future challenges. *in Geophysical Monograph Series, American Geophysical Union*, 161, doi:10.1029/161GM04.
- Oey, L. Y. and Y.-L. Cheng, 2011: Loop Current Cycle and trigger mechanism for Loop Current ring separations. *Proc. BOEMRE Info. Transfer Meeting, New Orleans, LA*.
- Oka, A., H. Hasumi and A. Abe-Ouchi, 2012: The thermal threshold of the Atlantic meridional overturning circulation and its control by wind stress forcing during glacial climate. *Geophys. Res. Letters*, 39, 9, L09709, doi:10.1029/2012GL051421.
- Oppo, D. W. and S. J. Lehman, 1993: Mid-depth circulation of the subpolar North Atlantic during the last glacial maximum. *Science*, 259, 5098, 1148–1152, doi:10.1126/science.259.5098.1148.
- Otto-Bliesner, B., E. Brady, G. Clauzet, R. Tomas, S. Levis, and Z. Kothavala, 2006: Last glacial maximum and Holocene climate in CCSM3. *Journal of Climate*, 19(11), 2526–2544, doi:10.1175/JCLI3748.1.
- Otto-Bliesner, B. L., C. D. Hewitt, T. M. Marchitto, E. Brady, A. Abe-Ouchi, M. Crucifix, S. Murakami and S. L. Weber, 2007: Last Glacial Maximum ocean thermohaline circulation: PMIP2 model intercomparisons and data constraints. *Geophys. Res. Lett.*, 34, 12, (L12706), doi:10.1029/2007GL029475.

- Pacanowski, R., 1995: MOM 2 documentation user's guide and reference manual, version 1.0. *GFDL Ocean Group Tech. Rep*, Princeton University, 3, 232.
- Peltier, W. R., 1994: Ice age paleotopography. *Science*, 265, 195–201, doi:10.1126/science.265.5169.195 .
- Peltier, W. R. and R. G. Fairbanks, 2006: Global glacial ice volume and Last Glacial Maximum duration from an extended Barbados sea level record. *Quaternary Science Reviews*, 25, 23, 3322–3337, doi:10.1016/j.quascirev.2006.04.010.
- Peng, G., Z. Garraffo, G. R. Halliwell, O. M. Smedstad, C. S. Meinen, V. Kourafalou, and P. Hogan, 2009: Temporal Variability of the Florida Current Transport at 27°N. *Ocean Circulation: The New Research*, 119–137.
- Peterson, L. C., G. H. Haug, K. A. Hughen, and U. Röhl, 2000: Rapid changes in the hydrologic cycle of the tropical Atlantic during the last glacial, *Science*, 290(5498), 1947–1951, doi:10.1126/science.290.5498.1947.
- Peterson, L. C. and G. H. Haug, 2006: Variability in the mean latitude of the Atlantic Intertropical Convergence Zone as recorded by riverine input of sediments to the Cariaco Basin (Venezuela). *Palaeogeography, Palaeoclimatology, Palaeoecology*, 234, 1, 97–113, doi:10.1016/j.palaeo.2005.10.021.
- Petit, J.-R., J. Jouzel, D. Raynaud, N. I. Barkov, J.-M. Barnola, I. Basile, M. Bender, J. Chappellaz, M. Davis, G. Delaygue and others, 1999: Climate and atmospheric history of the past 420,000 years from the Vostok ice core, Antarctica. *Nature*, 399, 6735, 429–436, doi:10.1038/20859.
- Pichevin, T. and D. Nof, 1997: The momentum imbalance paradox. *Tellus A*, 49, 2, 298–319, doi:10.1034/j.1600-0870.1997.t01-1-00009.x.
- Poore, R. Z., T. M. Quinn and S. Verardo, 2004: Century-scale movement of the Atlantic Intertropical Convergence Zone linked to solar variability. *Geophysical Research Letters*, 31, 12, doi:10.1029/2004GL019940.
- Quadfasel, D., 2005: Oceanography: The Atlantic heat conveyor slows. *Nature*, 438, 7068, 565–566, doi:10.1038/438565a.
- Rahmstorf, S., 2002: Ocean circulation and climate during the past 120,000 years. *Nature*, 419, 6903, 207–214, doi:10.1038/nature01090.

- Rahmstorf, S., 2006: Thermohaline Ocean CThermohaline Ocean Circulationirculation. In:*Encyclopedia of Quaternary Sciences*, Edited by S. A. Elias. Elsevier, Amsterdam 2006.
- Rasmussen, T. L. and E. Thomsen, 2012: Changes in planktic foraminiferal faunas, temperature and salinity in the Gulf Stream during the last 30,000 years: influence of meltwater via the Mississippi River. *Quaternary Science Reviews*, 33, 42–54, doi:10.1016/j.quascirev.2011.11.019.
- Regenberg, M., S. Steph, D. Nürnberg, R. Tiedemann and D. Garbe-Schönberg, 2009: Calibrating Mg/Ca ratios of multiple planktonic foraminiferal species with $\delta^{18}\text{O}$ -calcification temperatures: Paleothermometry for the upper water column. *Earth and Planetary Science Letters*, 278, 3, 324–336, doi:10.1016/j.epsl.2008.12.019.
- Richardson, P. L., 2008: On the history of meridional overturning circulation schematic diagrams. *Progress in Oceanography*, 76, 4, 466–486, doi:10.1016/j.pocean.2008.01.005.
- Ritz, S. P., T. F. Stocker and S. A. Müller, 2008: Modeling the effect of abrupt ocean circulation change on marine reservoir age. *Earth and Planetary Science Letters*, 268, 1, 202–211, doi:10.1016/j.epsl.2008.01.024.
- Robinson, P. and A. Henderson-Sellers, 1999: Contemporary Climatology. *Pearson Education Limited*, London, ISBN-13: 978-0582276314.
- Romanou, A., E. P. Chassignet and W. Sturges, 2004: Gulf of Mexico circulation within a high-resolution numerical simulation of the North Atlantic Ocean. *Journal of Geophysical Research*, 109, C1, C01003, doi:10.1029/2003JC001770.
- Rousset, C., and L. Beal, 2010: Observations of the Florida and Yucatan Currents from a Caribbean cruise ship. *Journal of Physical Oceanography*, 40, doi:10.1175/2010JPO4447.1.
- Ruddiman, W. F., 1977: Late Quaternary deposition of ice-rafted sand in the subpolar North Atlantic (lat 40 to 65 N). *Geological Society of America Bulletin*, 88, 12, 1813–1827, doi:10.1130/0016-7606(1977)88<1813:LQDOIS>2.0.CO;2.
- Ruddiman, W. F. and A. McIntyre, 1981: The mode and mechanism of the last deglaciation: oceanic evidence. *Quaternary Research*, 16, 2, 125–134, doi:10.1016/0033-5894(81)90040-5.
- Ruddiman, W. F., J. E. Kutzbach and S. J. Vavrus, 2011: Can natural or anthropogenic explanations of late-Holocene CO₂ and CH₄ increases be falsified?. *The Holocene*, 21, 5, 865–8879, doi:10.1177/0959683610387172.

- Rühlemann, C., S. Mulitza, P. J. Müller, G. Wefer and R. Zahn, 1999: Warming of the tropical Atlantic Ocean and slowdown of thermohaline circulation during the last deglaciation. *Nature*, 402, 6761, 511–514, doi:10.1038/990069.
- Sachs, J. P. and S. J. Lehman, 1999: Subtropical North Atlantic temperatures 60,000 to 30,000 years ago. *Science*, 286, 5440, 756–759, doi: 10.1126/science.286.5440.756.
- Schmidt, M.W., H. J. Spero and D. W. Lea, 2004: Links between salinity variation in the Caribbean and North Atlantic thermohaline circulation. *Nature*, 428, 6979, 160–163, doi:10.1038/nature02346.
- Schmidt, M. W. and H. J. Spero, 2011: Meridional shifts in the marine ITCZ and the tropical hydrologic cycle over the last three glacial cycles. *Paleoceanography*, 26, 1, doi:10.1029/2010PA001976.
- Schmidt, M. W. and Lynch-Stieglitz, J., 2011: Florida Straits deglacial temperature and salinity change: Implications for tropical hydrologic cycle variability during the Younger Dryas. *Paleoceanography*, 26, 4, doi: 10.1029/2011PA002157.
- Schmitz Jr, W. J. and W. S. Richardson, 1968: On the transport of the Florida Current. *Deep Sea Research and Oceanographic Abstracts*, 15, 6, 679–693, doi:10.1016/0011-7471(68)90081-8.
- Schmitz Jr, W. J. and P. L. Richardson, 1991: On the sources of the Florida Current. *Deep Sea Research Part A. Oceanographic Research Papers*, 38, S379–S409, doi:10.1016/S0198-0149(12)80018-5.
- Schmitz, W. J. and M. S. McCartney, 1993: On the north Atlantic circulation. *Reviews of Geophysics*, 31, 1, 29–49, doi:10.1029/92RG02583.
- Schmitz Jr, W. J., 1996: On the World Ocean Circulation. Volume 1. Some Global Features/North Atlantic Circulation.. *Technical Report. WHOI-96-03*, Woods Hole Oceanographic Institution, Woods Hole, Mass.
- Schmitz Jr, W. J., 2005: Cyclones and westward propagation in the shedding of anticyclonic rings from the Loop Current. in *Circulation in the Gulf of Mexico: Observations and Models, Geophys. Monogr. Ser.*, 161, edited by W. Sturges and A. Lugo-Fernandez, pp. 241–261, AGU, Washington, D. C, doi:10.1029/161GM18.
- Schmitz Jr, W., and W. Richardson, 1968: On the transport of the Florida Current. *Deep Sea Research*, 15, 6, 679–693, doi:10.1016/0011-7471(68)90081-8.

- Schönfeld, J., Dullo, W.-C., Kuhnt, W., Lezius, J., Lynch-Stieglitz, J., Nürnberg, D. and J. Steinlchner, 2005: Late Quaternary Variability of the Florida Current linked to North Atlantic thermohaline circulation. *International Conference on Palaeoceanography, Bordeaux, France (ICP)*.
- Schott, F., T. Lee, and R. Zantopp, 1988: Variability of structure and transport of the Florida Current in the period range of days to seasonal. *J. Phys. Oceanogr*, 18(9), 1209–1230, doi:10.1175/1520-0485(1988)018<1209:VOSATO>2.0.CO;2.
- Seidov, D. and M. Maslin, 2001: Atlantic ocean heat piracy and the bipolar climate seesaw during Heinrich and Dansgaard–Oeschger events. *Journal of Quaternary Science*, 16, 4, 321–328, doi: 10.1002/jqs.595.
- Sheinbaum, J., J. Candela, A. Badan, and J. Ochoa, 2002: Flow structure and transport in the Yucatan Channel. *Geophysical Research Letters*, 29(3), 10–1, doi:10.1029/2001GL013990.
- Siddall, M., E. J. Rohling, A. Almogi-Labin, C. Hemleben, D. Meischner, I. Schmelzer, D. A. Smeed and others, 2003: Sea-level fluctuations during the last glacial cycle. *Nature*, 423, 6942, 853–858, doi:10.1038/nature01690.
- Sigman, D. M., M. P. Hain and G. H. Haug, 2010: The polar ocean and glacial cycles in atmospheric CO₂ concentration. *Nature*, 466, 7302, 47–55, doi:10.1038/nature09149.
- Slowey, N. C. and T. J. Crowley, 1995: Interdecadal variability of Northern Hemisphere circulation recorded by Gulf of Mexico corals. *Geophysical Research Letters*, 22, 17, 2345–2348, doi:10.1029/95GL02236.
- Smith, R., M. Maltrud, F. Bryan and M. Hecht, 2000: Numerical simulation of the north atlantic ocean at 1/10°. *Journal of Physical Oceanography*, 30(7), 1532–1561, doi:10.1175/1520-0485(2000)030<3C1532:NSOTNA>3E2.0.CO;2.
- Stevens, D., 1991: The open boundary condition in the United Kingdom fine-resolution Antarctic model. *J. Phys. Oceanogr*, 21, 1494–1499, doi:10.1175/1520-0485(1991)021<1494:TOBCIT>2.0.CO;2.
- Stocker, T. F., 1998: The seesaw effect. *Science*, 282, 5386, 61–62, doi:10.1126/science.282.5386.61.
- Stommel, H., 1948: The westward intensification of wind-driven ocean currents. *Trans. Amer. Geophys. Union*, 29, 2, 202–206.

- Sturges, W., 1992: The spectrum of Loop Current variability from gappy data. *J. Phys. Oceanogr.*, 22(11), 1245–1256, doi:10.1175/1520-0485(1992)022<1245:TSOLCV>2.0.CO;2.
- Sturges, W. and R. Leben, 2000: Frequency of Ring Separations from the Loop Current in the Gulf of Mexico: A Revised Estimate. *J. Phys. Oceanography*, 30, 1814–1819, doi:10.1175/1520-0485(2000)030<1814:FORSFT>2.0.CO;2.
- Sturges, W., A. Lugo-Fernandez and M. D. Shargel, 2005: Circulation in the Gulf of Mexico: Observations and Models. *Geophys. Monograph Series, American Geophysical Union*, 161, 1–10, doi:10.1029/GM161.
- Sturges, W., N. G. Hoffmann, and R. R. Leben, 2010: A Trigger Mechanism for Loop Current Ring Separations. *J. Phys. Oceanogr.*, 40, 900–913, doi:10.1175/2009JPO4245.1.
- Sverdrup, H. U., 1947: Wind-driven currents in a baroclinic ocean; with application to the equatorial currents of the eastern Pacific. *Proceedings of the National Academy of Sciences of the United States of America*, 33, 11, PMID: PMC1079064.
- Talley, L. D., G. L. Pickard, W. J. Emery, and J. H. Swift, 2011: Descriptive physical oceanography: an introduction. *Academic Press is an imprint of Elsevier, 32 Jamestown Road, London NW1 7BY, UK*, 2011.
- Tarasov, L. and W. R. Peltier, 2005: Arctic freshwater forcing of the Younger Dryas cold reversal. *Nature*, 435, 7042, 662–665, doi:10.1038/nature03617.
- Taylor, A. H. and J. A. Stephens, 1998: The North Atlantic oscillation and the latitude of the Gulf Stream. *Tellus A*, 50, 1, 134–142, doi:10.1034/j.1600-0870.1998.00010.x.
- Teller, J. T., M. Boyd, Z. Yang, P. S. G. Kor and F. A. Mokhtari, 2005: Alternative routing of Lake Agassiz overflow during the Younger Dryas: New dates, paleotopography, and a re-evaluation. *Quaternary Science Reviews*, 24, 16, 1890–1905, doi.org/10.1016/j.quascirev.2005.01.008.
- Vidal, L., L. Labeyrie, E. Cortijo, M. Arnold, J. C. Duplessy, E. Michel, S. Becque and T. C. E. Van Weering 1997: Evidence for changes in the North Atlantic Deep Water linked to meltwater surges during the Heinrich events. *Earth and Planetary Science Letters*, 146, 1, 13–27, doi:10.1016/S0012-821X(96)00192-6.
- Vukovich, F., and G. Maul, 1985: Cyclonic eddies in the eastern Gulf of Mexico. *J. Phys. Oceanogr.*, 15(1), 105–117, doi:10.1175/1520-0485(1985)015<0105:CEITEG>2.0.CO;2.

- , Vukovich, F. M., 1995: An updated evaluation of the Loop Current's eddy-shedding frequency. *J. of Geophys. Research*, 100, C5, 8655–8659, doi:10.1029/95JC00141.
- Waelbroeck, C., L. Labeyrie, E. Michel, J. C. Duplessy, J. F. McManus, K. Lambeck, E. Balbon and M. Labracherie, 2002: Sea-level and deep water temperature changes derived from benthic foraminifera isotopic records. *Quaternary Science Reviews*, 21(1-3), 295–305, doi:10.1016/S0277-3791(01)00101-9.
- Wang, X., A. S. Auler, R. L. Edwards, H. Cheng, P. S. Cristalli, P. L. Smart, D. A. Richards and C. C. Shen, 2004: Wet periods in northeastern Brazil over the past 210 kyr linked to distant climate anomalies. *Nature*, 432, 740–743, doi:10.1038/nature03067.
- Webb, R. S., D. H. Rind, S. J. Lehman, R. J. Healy and D. Sigman, 1997: Influence of ocean heat transport on the climate of the Last Glacial Maximum. *Nature*, 385, 6618, 695–699, doi:10.1038/385695a0.
- Williams, G. P. and K. Bryan, 2006: Ice age winds: an aquaplanet model. *Journal of climate*, 19, 9 1706–1715, doi:10.1175/JCLI3766.1.
- Wiseman Jr, W. J. and S. P. Dinnel, 1988: Shelf currents near the mouth of the Mississippi River. *Journal of Physical Oceanography*, 18, 9, 1287–1291, doi:10.1175/1520-0485(1988)018<1287:SCNTMO>2.0.CO;2.
- Wright, J. D., R. E. Sheridan, K. G. Miller, J. Uptegrove, B. S. Cramer and J. V. Browning, 2009: Late Pleistocene sea level on the New Jersey Margin: implications to eustasy and deep-sea temperature. *Global and Planetary Change*, 66, 1, 93–99, <http://dx.doi.org/10.1016/j.gloplacha.2008.03.013>.
- Wunsch, C., 2003: Determining paleoceanographic circulations, with emphasis on the Last Glacial Maximum. *Quaternary Science Reviews*, 22, 2, 371–385, doi:10.1016/S0277-3791(02)00177-4.
- Wunsch, C., 2010: Towards understanding the Paleoocean. *Quaternary Science Reviews*, 29, 17, 1960–1967, doi:10.1016/j.quascirev.2010.05.020.
- Xu, X., W. J. Schmitz, H. E. Hurlburt, and P. J. Hogan, 2012: Mean Atlantic meridional overturning circulation across 26.5N from eddy-resolving simulations compared to observations. *J. Geophys. Res.*, 117 (C3), C03042, doi: 10.1029/2011JC007586.
- Yu, E.-F., R. Francois and M. P. Bacon, 1996: Similar rates of modern and last-glacial ocean thermohaline circulation inferred from radiochemical data. *Nature*, 379, 689694, doi:10.1038/379689a0.

-
- Yongqiang, Y., Y. Rucong, Z. Xuehong and L. Hailong, 2002: A flexible coupled ocean-atmosphere general circulation model. *Advances in Atmospheric Sciences*, 19(1), 169–190, doi:10.1007/s00376-002-0042-8.
- Zhang, R., 2010: Latitudinal dependence of Atlantic meridional overturning circulation (AMOC) variations. *Geophys. Reserach Letters*, 37, L16703, doi:10.1029/2010GL044474.

Acknowledgements

First and foremost, I would like to thank Prof. Carsten Eden for his help and encouragement, advice, guidance, seemingly eternal patience. I am very grateful for his supervision, for his ever open door, that I could enter whenever I wished and for providing the financial support until the end of my PhD thesis. Further I really appreciate that he established the contact to Axel Timmermann at IPRC, Hawaii for work collaboration including a research stay for me on O’ahu.

I would also like to thank Prof. Dirk Nürnberg for his support and co-supervision, for providing me paleodata from marine sediment cores, for discussions and also for giving me the opportunity to take part in the research cruise M94 in March 2013.

Joachim Schönfeld and Sascha Flögel answered emails within hours and I really appreciate their comments and discussions on conference posters and their explanation of proxy interpretation and uncertainties.

Many thanks to my great office colleagues Franziska Schwarzkopf, Nils Brüggemann, and Joke Lübbecke for answering the never ending questions that came up whenever I was stuck in Ferret and Matlab codes or just getting some really good and helpful personal introduction for \LaTeX . Lars Czeschel, Mirjam Glessmer and Markus Scheinert were also of great help whenever questions arose. I would also like to thank Nora Kemmler and Friderike Powe for all the coffee and lunch breaks on the roof of GEOMAR cheering me up when FLAME didn’t do what I wanted it to do.

Funding through DFG-SPP-1266 (INTERDYNAMIK, Project LOOP) is gratefully acknowledged.

Erklärung

Hiermit erkläre ich, dass ich die vorliegende Dissertation - abgesehen von der Beratung durch meine akademischen Lehrer - selbstständig verfasst und keine weiteren Quellen und Hilfsmittel als die im Text angegebenen verwendet habe. Diese Arbeit hat weder ganz, noch in Teilen, bereits an anderer Stelle einer Promotionskommission zur Erlangung des Doktorgrades vorgelegen. Ich erkläre, dass die vorliegende Arbeit gemäß den Grundsätzen zur Sicherung guter wissenschaftlicher Praxis der Deutschen Forschungsgemeinschaft erstellt wurde.

Hamburg, den 17.09.2013